On the Interaction of Cationic Compounds with ABC-Transporters and Lipid Membranes

INAUGURALDISSERTATION

zur

Erlangung der Würde eines Doktors der Philosophie

vorgelegt der

Philosophischen-Naturwissenschaftlichen Fakultät

der Universität Basel

von

Andreas Beck

aus

Rohrbachgraben, Bern

Basel 2012

Namensnennung-Keine kommerzielle Nutzung-Keine Bearbeitung 2.5 Schweiz

Sie dürfen:

das Werk vervielfältigen, verbreiten und öffentlich zugänglich machen

Zu den folgenden Bedingungen:

Namensnennung. Sie müssen den Namen des Autors/Rechteinhabers in der von ihm festgelegten Weise nennen (wodurch aber nicht der Eindruck entstehen darf, Sie oder die Nutzung des Werkes durch Sie würden entlohnt).

Keine kommerzielle Nutzung. Dieses Werk darf nicht für kommerzielle Zwecke verwendet werden.

Keine Bearbeitung. Dieses Werk darf nicht bearbeitet oder in anderer Weise verändert werden.

- Im Falle einer Verbreitung müssen Sie anderen die Lizenzbedingungen, unter welche dieses Werk fällt, mitteilen. Am Einfachsten ist es, einen Link auf diese Seite einzubinden.
- Jede der vorgenannten Bedingungen kann aufgehoben werden, sofern Sie die Einwilligung des Rechteinhabers dazu erhalten.
- Diese Lizenz lässt die Urheberpersönlichkeitsrechte unberührt.

Quelle: http://creativecommons.org/licenses/by-nc-nd/2.5/ch/ Datum: 3.4.2009

Genehmigt von der Philosophisch-Naturwissenschaftlichen Fakultaet
auf Antrag von

Prof. Dr. Anna Seelig
Prof. Dr. Joachim Seelig
Prof. Dr. Dagmar Klostermeier

Basel, den 22. Juni. 2010

Prof. Dr. Eberrhard Parlow

Table of Contents

1 Introduction

1.1 Integral Membrane Proteins

Integral Membrane proteins (IMPs) are permanently attached to biological membranes and are simultaneously in contact with two distinct aqueous compartments (Gohon and Popot 2003). IMPs are amphipatic and requiere therefore the lipid bilayer and the water phase for stabilization (von Heijne 2006). IMPs can be divided into many different classes such as transporters, channels, receptors, enzymes, structural membrane-anchoring domains, proteins involved in accumulation and transduction of energy, and proteins responsible for cell adhesion. The main function of all IMPs is the translocation of various substances or signals through the membrane. This can be achieved either by active (transporters) or passive (channels/pores) transport or translocation, respectively.

In order to study IMPs in terms of structure and activity they have to be purified. For purification purposes detergents are used to disintegrate the lipid membrane to get access to the IMP (Rigaud and others 1997). However the stabilization of IMPs by detergents or detergents mixtures is still a semi-empirical task. Compared to soluble proteins the amphipaticity of IMPs makes them difficult to study. The database shows that in March 2010 only 234 unique structures of membrane proteins have been solved. However the structures of more than 30’000 soluble proteins have already been solved.

Since most of the commercially available drugs target IMPs the interest in this research area has increased in the past years (Overington and others 2006). In the next chapter one of the largest superfamiliy of IMPs, the so called ATP binding cassette-transporters are discussed. Further, the focus will concentrate on the two structurally related, specific ABC-transporters of which one is of eukaryotic (P-glycoprotein) and the other of prokaryotic (Sav1866) origin, respectively. The two transporters will be compared in terms of structure and function.

1.2 ABC-Transporters

ATP-**b**inding **c**assette transporters (**ABC**-transporters) are integral membrane proteins and are found in every organism from archae to man (Holland 2003). A common feature of all ABC-transporters is the energy dependent transport of substances across cell membranes that is driven by ATP hydrolysis (Holland and Blight 1999; Schneider and Hunke 1998). ABC-transporters are structurally related but can transport structurally unrelated substances. The maltose transporter from *E.coli* transports maltose (Davidson and others 1996) from one aqueos compartement to the other. On the other hand P-glycoprotein (P-gp) transports various amphipathic substances from one membrane leaflet to the other (Seelig 1998). Transported substances are referred to as allocrites or substrates. However the word substrate has to be taken with care as in a strict nomenclature ATP is the proper substrate.

ABC-transporters consist of two **t**rans**m**embrane **d**omains (TMDs) to which the substrate binds and two **n**ucleotide **b**inding **d**omains (NBDs) where ATP is hydrolyzed. The energy from the NBDs is transferred over the coupling helices to the TMDs (Dawson and Locher 2006). The NBDs are highly conserved among different ABC-transporters as the energy source is ATP. On the other hand the TMDs are less conseved as they are responsible for the transport of the various structurally unrelated substrates.

In both eukaryotes and prokaryotes the ABC-transporters are responsible for import as well as export of substances. In bacteria ABC-transporters export drugs and antibiotics, whereas ABC-importers mediate the uptake of nutrients. The third class of ABC-transporters are involved in mRNA translation and DNA repair (Davidson and others 2008). Bacterial ABC-transporters usually are organized as separate subunits or half transporters and assemble at/in the membrane to become fully active. Eukaryotic transporters in contrast are generally expressed as fully functional transporters (Lage 2003).

In man ABC-transporters belong to a class of IMPs which are often involved in clinical severe problems. Mutations in almost half of the 48 human ABC-transporters cause a severe disease in humans (Dean and Annilo 2005). Two of the best studied ABC-transporters in human are P-glycoprotein (P-gp, MDR1, ABCB1) and the **c**ystic **f**ibrosis **t**ransduction **r**egulator (CFTR) as both contribute to significant clinical problems.

Because P-gp (MDR1, ABCB1) contributes to multi-drug resistance (MDR) of human cancer cells they are important in clinics and thus probably the best studied ABC-transporters in eukaryotes (Gottesman and Ambudkar 2001). The term MDR is used for a cross-resistance phenotype against unrelated drugs and has to be destinguished from single-drug resistance (SDR). P-gp is over-expressed in cancer cells which make drug treatment very difficult. The applied drugs remain ineffective since they are exported out of the membrane therefore not reaching the cytosol (Ling 1997; Nervi and others). A close description of the substrate pathway can be found in chapter 1.4.

The other example of a clinically relevant ABC-transporter is the human **c**ystic **f**ibrosis **t**ransduction **r**egulator (CFTR) (Sheppard and Welsh 1999). Only one point mutation in the CFTR protein causes a miss-folding and destroys the protein function which causes the disease called cystic fibrosis. As CFTR is involved in chloride transport, which is coupled with H_20 transport, the CFTR patients suffer under thick mucus especially in the lung.

Clinically relevant ABC-transporters in prokaryotes are involved in MDR of bacteria (Van Bambeke and others 2000). The first evidence that antibiotic resistances is caused by active efflux of drugs was found in 1980 (McMurry and others 1980). Most prokaryotic drug transporter belong to the class of secondary active drug transporters. However several ABC-transporters are involved in multiple drug export. Such efflux systems are thought to have an important role in bacterial MDR (Li and others 2004; Lomovskaya and Totrov 2005; Poole 2005).

1.3 P-glycoprotein, a Human ABC-Transporter

P-gp is the best studied ABC-transporter. P-gp is able to transport a variety of different substances across the lipid bilayer and is therefore involved in many different tasks. Moreover human P-glycoprotein (P-gp, ABCB1, MDR1) accounts for significant clinical problems (for review (Ambudkar and others 1999; Litman and others 2001)).

Since P-gp is also involed in **m**ulti **d**rug **r**esistance (MDR) of cancer cells and cancer is the second most common death cause in first world, there is great interest in this protein (Bronchud MH 2000). The phenomenon of MDR was first described in the scientific

literature in 1970 (Biedler and Riehm 1970). The classical MDR phenotype is characterized by cross resistance patterns against a variety of drugs. P-gp, however, was originally isolated from Chinese hamster ovary (CHO) cells in 1976 (Juliano and Ling 1976). In 1979 P-gp was purified (Riordan and Ling 1979) and its encoding gene was identified as MDR1 or ABCB1 (Shen and others 1986), and also found to be over-expressed in multidrug-resistant human and mammalian cell lines (Kartner and others 1983); (Kartner and others 1985).

The main functions of P-gp are (i) the protection of various tissues against environmental toxins (Schinkel 1997) or (ii) the absorption of molecules in the intestinal barrier. For toxin protection, P-gp is expressed at the apical surface of endothelial cells in tissues like the blood-brain barrier, blood testis barrier, blood nerve or fetal maternal barrier (Ceckova-Novotna and others 2006; Cordon-Cardo and others 1990; Holash and others 1993; Schinkel and others 1996; Tanaka and others 1994; Tatsuta and others 1992; Thiebaut and others 1987; Thiebaut and others 1989). For substrate uptake it is expressed at the intestinal barrier.

P-gp has as most of the ABC-transporters two times six transmembrane helices in the TMDs and the two NBDs where ATP binds to. Like other ABC-transporters P-gp has typical conseved sequence motifes in the NBDs, which are listed: The Walker A (GXSGCGKST) and Walker B (ILLLDEA) motifs, the signature region (LSGGQ), and the A, D, H and Q structural loops (Gottesman and others 1996). These conserved residues play important role in positioning the MgATP, in the activation of the catalytic water molecule and in the signal transduction between the NBDs and the TMDs (Carrier and others 2007).

P-gp can transport a wide variety of substrates and the question how the individual substrates are recognized is still matter of debate. In general there are three different approaches used to get insight into the substrate recognition. If a crystal structure is available computer models can predict what the possible recognition sites are. Further mutational studies of the binding region can give insight where the specific substrate binds to. Probably the most successful approach is the close investigation of the transported substrates in order to find the possible recognition patterns. The mechanism proposed in 1998 by Seelig based on this approach is well accepted (Seelig 1998). The

investigation of 100 different substrates in terms of structures led to the conclusion that the substrate recognition has to be via hydrogen-bonding. All the substrates investigated had specific H-bond acceptor patterns. This modular recognition theory can explain the wide variety of transported substrates.

Probably one of the most difficult parts in P-gp research field is the fact that the substrates are amphipatic. The substrate first incorporates into the membrane and is then flipped to the other site of the lipid bilayer by the transporter under ATP hydrolisis. The measurement of a drug concentration in the membrane is hardly feasible. Binding constants are measured of a substrate from water to the membrane. The binding constant of a substance to the membrane can be measured by various techniques, probably most sophisticated is the use of isothermal titration calorimetry as this technique does not need labelling of the substance. However it should be mentioned at this point that incorporation of a charged substrate into a charged membrane has to be evaluated carefully as the incorporation behavior is governed by hydrophobic and electrostatic contributions. The topic is explained in more detail in chapter 6 (DTAC).

1.4 Sav1866, a Bacterial ABC-transporter

Most prokaryotic drug transporters belong to the class of secondary active transporters particular drug-proton exchange systems (Paulsen and others 1996). However several drug transporting systems utilize the energy of ATP hydrolysis to drive drug efflux (Lage 2003). The high-resolution structure of SAV1866 is the first reported for an ABC exporter (Dawson and Locher 2006; Dawson and Locher 2007). Sav1866 is a close homolog of the multidrug ABC transporter P-glycoprotein (see previous chapter). Therefore the structure raised great interest since at the time the structure of SAV1866 was solved there was no high resolution structure of P-gp available. Sav1866 provided the basis for structural models for P-glycoprotein (O'Mara and Tieleman 2007). However nowadays the high resolution structure of P-glycoprotein is solved (Aller and others 2009). Figure 1 shows the structure of Sav1866 in a ADP bound outward facing conformation. The approximate location of the lipid bilayer and the substrate pathway are depicted.

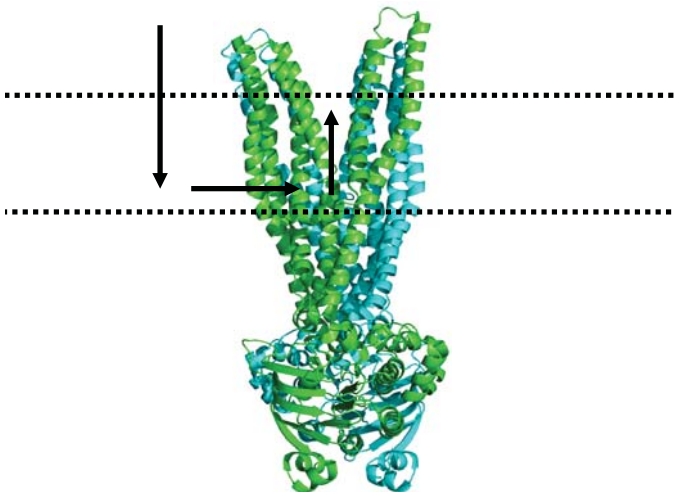

Figure 1. *High resolution structure of the bacterial ABC-transporter Sav1866.* The structure of Sav1866 was solved to a 3 Å resolution in detergents micelles (C12E8) in the year 2006. The two sbdomains are depicted in green and blue. The dotted line depicts the approximate location of the lipid bilayer.

Sav1866 originates from *Staphylococcus aureus* a gram positive bacterium invloved in multidrug resistance (Huet and others 2008). Sav1866 can transport structurally unrelated substrates similar to P-glycoprotein (Velamakanni and others 2008). Therefore it is thougth to be invloved in multidrug-resistance of *Staphylococcus aureus* which makes it clinically relevant. Generally, *Staphylococcus aureus* is involved in severe antibiotic resistance in hospitals. Very well known is for example the MRSA strain, which was called in previous times **m**ethicillin-**r**esistant **s**taphylococcus **a**ureus strain, nowaday called **m**ulti-**r**esistant **s**taphylococcus **a**ureus strain, as it is resistent against all kind of beta-lactam-antibiotics. However the mechanism is very well known and originates from a modified penicillin binding protein. Sav1866 is not involved.

For crystallisation purposes the ABC transporter was overexpressed in *E.coli* and solubilized in a detergent mixture (Dawson and Locher 2006). The crystallization step was performed in $C_{12}E_8$. The crystal showed a very good diffraction pattern and the structure was solved to a 3 Å resolution. The structural motifs of Sav1866 are typical for ABC-transporters. The Sav1866 dimer consits of 2 transmembrane domains (TMDs) containing 6 α-helices each for drug translocation and 2 nucleotidbinding domains (NBDs) as P-gp. Usually ABC-importers contain a short coupling helix that contacts a

single NBD. Sav1866, as an ABC exporter, has two intracellular coupling helices, one contacting the NBDs of both subunits and the other interacting with the opposite subunit (Rees and others 2009). A major improvement was the mode of action the autors propose. In earlier times it was believed that the transporter opens and closes in a book-like manner and therefore undergoes large structural changes. However Dawson and Locher predicted that it is more a twisting like mechanism. The structural movement upon drug transport are suggested to be rather small.

The substrate pathway is disscussed at this point. Upon addition of an amphipatic substrate to the water phase it will incorporate into the outer layer of the lipid membrane. Neutral molecules flip fast to the inner leaflet of the bilayer and if no transporter is present, they will partition to the water phase of the inner compartement (into the cell or bacterium). Charged molecules do not flip as fast as the uncharged molecules since only the uncharged fraction flips (the size of the molecule plays also an important role). In the inner leaflet the substances are caught by the transporter and flipped to the outer leaflet. Therefore the ABC-transporters prevent the molecules from enetring the cell. On the outer water phase the substances are constantly flushed away or digested by enzymes.

In summary the multi-drug related ABC-transporters change the partition equilibrium of a substrate therefore preventing molecules to enter the cell or the bacterium. However in the ATPase assay desribed in chapter 4 and 5 the molecules reach the transporter directly from the inner leaflet (from the NBD site) as the transporter in reconstituted inside-out (all NBDs which bind ATP are outside of the proteoliposomes).

1.5 Comparison of SAV1866 with P-glycoprotein

Despite the different origin of the two ABC-transporters, Sav1866 from bacteria (*Staph. aureus*) and P-gp from eukaryotes (man), respectively, they share a lot of similarities. The sequence similarity in the NBDs is high as expected for conserved ABC-transporters (80.4 and 77.8%, *vs.* identity 48.4% and 44.6%). The TMDs share a similarity of 56 and 52.8%, respectively (identity 15.8 and 12.9%). Figure 2 shows the TMDs of P-gp (left) and of Sav1866 (right). The two straight dotted lines show the approximate lipid/water interface. It becomes obviously from the structure that SAV1866 carries more charged

amino acids in the drug translocation pocket than P-gp what different substrate specificities implies. P-gp has no anionic charges in the TMD binding region but on the other hand three cationic charges. Sav1866 has 4 cationic and 6 anionic charges in the TMDs.

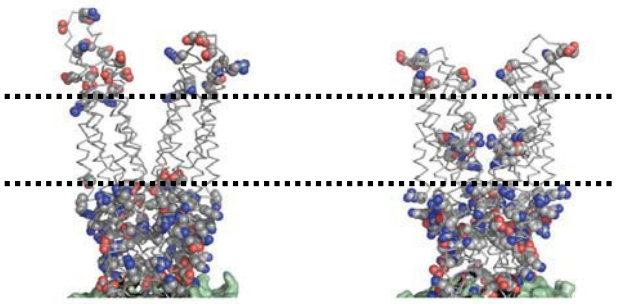

Figure 2. *Transmembrane domains of P-glycoprotein and Sav1866.* Left molecule depicts the modelled P-glycoprotein structure from the crystal structure of Sav1866 (right) each consisting of 12 transmembrane helices. Cationic amino acids are depicted in blue whereas anionic amino acids are depicted in red. The black dotted lines show the approximate location of the lipid/water interface. Obviously from the structures is the fact that Sav1866 (right) contains much charged amino acids in the binding pocket (in the bilayer).

P-gp is a full transporter with a MW of 170 kDa whereas Sav1866 is expressed as half-transporter, what is typical for bacterial transporters, with a molecular weight of 130.8 kDa. Smaller differences are for example that Pgp is glycosylated whereas Sav1866 is not.

As discussed above P-glycoprotein can transport a wide variety of different structurally unrelated compaounds. It was recently shown that also Sav1866 can trasnport different substrates among them Hoechst33342 and verapamil (Velamakanni and others 2008). Verapamil is the model substarte of P-gp. However it is not clear how Sav1866 recognizes its substartes. One may speculate that the recognition patterns are similar to P-gp.

1.6 Detergents in Membrane Protein Research

Detergents are able to solubilize membranes and therefore widely used in membrane protein research fields. In this chapter the general model of membrane solubilization is

discussed in detail. Moreover non-ionic and ionic detergents will be discussed separately as they are used in fundamentally different applications.

The famous "three-stage model" proposed by Helenius and Simons (1975) (Helenius and Simons 1975) to described membrane solubilization by detergents is simple and very well accepted. If we consider a mixture of lipids, detergent and water the three stage model predicts the following. At low detergents concentration the detergent will incorporate into the membrane, what is called stage I, "detergent binding" (see figure 3 bil+mon). The detergents incorporate according to its amphipaticity and its charge to a certain extend into the bilayer described by the binding constant. At that stage the mixed lipid bilyer coexists with the detergent monomer in suspension. At higher detergents concentration the vesicles begin to solubilize and the first micelles begin to coexist with lamellar phase, called stage II, the lamellar-micellar phase transition (see Figure 3 bil+mon+mic). The detergents stabilize the edges of the bilayer. At higher detergents concentration all lamellar structures are solubilized and only micelles exits, called satge III, the purely micellar phase (see Figure 3 mic+mon).

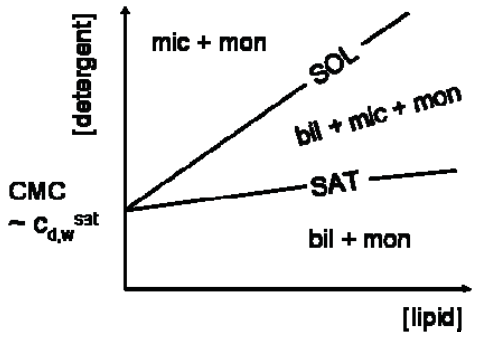

Figure 3. *Surfactant lipid phase diagram adapted from* (Heerklotz 2008). Figure 2 shows the typical phase diagram containing one surfactant and one lipid species.

Nonionic Detergents

Nonionic detergents and mixtures of them are used to isolate membrane proteins in order to study them structurally or in terms of activity. However isolation of membrane proteins is a very complex task and only empirically optimised solutions are found for very specific systems (Heerklotz 2008). Solubilization of native membrane proteins often

requires more than one detergent species and is therefore extremely difficult as the combination of detergents is extremely large, considering 60 commercially available detergents. For example the solubilization buffer of neurotensin (Grisshammer and others 2005) and cannabinoid receptors (Yeliseev and others 2005) contains at least three different detergents and additional cosolvents. An attempt to quantifiy the solubilization behaviour of two detergents on a model membrane has been made (Beck and others 2008).

After solubilization of the membrane protein, it has to be reconstituted into model membranes in order to study the activity, since a micellar environment is distinctly different than a bilayer environment, e.g. in terms of packing properties. An often used technique nowadays is removing the detergent with help of Bio-Beads SM2. Since most detergents are not spectroscopically detectable the quantification of detergents in proteoliposomes is difficult. Chapter 3 deals with the problem and shows a way to quantify the residual amount of detergent upon reconstitution by means of isothermal titration calorimetry.

Ionic Detergents

Ionic detergents are not used in isolation of membrane proteins as they denature proteins. The most famous example is SDS used in gel-electrophoresis. The protein is unfolded in SDS, ran according to its size and quantified by comparing with standarts. This technique is probably the world's most widely used biochemical method (1983). Ionic detergents have therfore became much less important than nonionic in terms of membrane protein research. They are used as bacteriocides or in cosmetic industry.

In contrast to non-ionic detergent there is much less biophysical data available for ionic detergents in terms of membrane incorporation and solubilization due to its complicated incorporation and solubilization behaviour. The membrane partitioning has to be corrected for electrostatic contribution and the solubilization is extremely slow at room temperature. Here we have focussed on a quaternary ammonium compound, dodecyltrimethylammoinum chloride (DTAC), where no partition and solubilization data is available (Chapter 6). We discuss the thermodynamic parameters of DTAC by comparing with its negatively charged counterpart SDS (Tan and others 2002).

1.7 Literature

http://blanco.biomol.uci.edu/Membrane_Proteins_xtal.html.
http://www.tcdb.org/tcdb/.

1983. Electrophoresis: A survey of techniques and applications. Part B: Applications : Edited by , Elsevier Scientific, Amsterdam/New York, 1983, 462 pp. $104.00. Analytical Biochemistry 131(1):284.

Aller SG, Yu J, Ward A, Weng Y, Chittaboina S, Zhuo R, Harrell PM, Trinh YT, Zhang Q, Urbatsch IL and others. 2009. Structure of P-Glycoprotein Reveals a Molecular Basis for Poly-Specific Drug Binding 10.1126/science.1168750. Science 323(5922):1718-1722.

Ambudkar SV, Dey S, Hrycyna CA, Ramachandra M, Pastan I, Gottesman MM. 1999. Biochemical, cellular, and pharmacological aspects of the multidrug transporter. Annu Rev Pharmacol Toxicol 39:361-98.

Beck A, Tsamaloukas AD, Jurcevic P, Heerklotz H. 2008. Additive action of two or more solutes on lipid membranes. Langmuir 24(16):8833-40.

Biedler JL, Riehm H. 1970. Cellular resistance to actinomycin D in Chinese hamster cells in vitro: cross-resistance, radioautographic, and cytogenetic studies. Cancer Res 30(4):1174-84.

Bronchud MH PW. 2000. Selecting the right targets for cancer therapy. Humana press Inc. Principles of molecular oncology(3):127.

Carrier I, Urbatsch IL, Senior AE, Gros P. 2007. Mutational analysis of conserved aromatic residues in the A-loop of the ABC transporter ABCB1A (mouse Mdr3). FEBS Lett 581(2):301-8.

Ceckova-Novotna M, Pavek P, Staud F. 2006. P-glycoprotein in the placenta: expression, localization, regulation and function. Reprod Toxicol 22(3):400-10.

Cordon-Cardo C, O'Brien JP, Boccia J, Casals D, Bertino JR, Melamed MR. 1990. Expression of the multidrug resistance gene product (P-glycoprotein) in human normal and tumor tissues. J Histochem Cytochem 38(9):1277-87.

Davidson AL, Dassa E, Orelle C, Chen J. 2008. Structure, function, and evolution of bacterial ATP-binding cassette systems. Microbiol Mol Biol Rev 72(2):317-64, table of contents.

Davidson AL, Laghaeian SS, Mannering DE. 1996. The Maltose Transport System of Escherichia coli Displays Positive Cooperativity in ATP Hydrolysis 10.1074/jbc.271.9.4858. J. Biol. Chem. 271(9):4858-4863.

Dawson RJP, Locher KP. 2006. Structure of a bacterial multidrug ABC transporter. 443(7108):180-185.

Dawson RJP, Locher KP. 2007. Structure of the multidrug ABC transporter Sav1866 from Staphylococcus aureus in complex with AMP-PNP. FEBS Letters 581(5):935-938.

Dean M, Annilo T. 2005. Evolution of the ATP-binding cassette (ABC) transporter superfamily in vertebrates. Annu Rev Genomics Hum Genet 6:123-42.

Gohon Y, Popot J-L. 2003. Membrane protein-surfactant complexes. Current Opinion in Colloid & Interface Science 8(1):15-22.

Gottesman MM, Ambudkar SV. 2001. Overview: ABC transporters and human disease. J Bioenerg Biomembr 33(6):453-8.

Gottesman MM, Pastan I, Ambudkar SV. 1996. P-glycoprotein and multidrug resistance. Curr Opin Genet Dev 6(5):610-7.
Grisshammer R, White JF, Trinh LB, Shiloach J. 2005. Large-scale expression and purification of a G-protein-coupled receptor for structure determination -- an overview. J Struct Funct Genomics 6(2-3):159-63.
Heerklotz H. 2008. Interactions of surfactants with lipid membranes doi:10.1017/S0033583508004721. Quarterly Reviews of Biophysics 41(3-4):205-264.
Helenius A, Simons K. 1975. Solubilization of membranes by detergents. Biochim Biophys Acta 415(1):29-79.
Holash JA, Harik SI, Perry G, Stewart PA. 1993. Barrier properties of testis microvessels. Proc Natl Acad Sci U S A 90(23):11069-73.
Holland IB, Blight MA. 1999. ABC-ATPases, adaptable energy generators fuelling transmembrane movement of a variety of molecules in organisms from bacteria to humans. J Mol Biol 293(2):381-99.
Holland IB, Cole, S.P.C., Kuchler , K. and Higgins, C.F. 2003. ABC proteins: From Bacteria to Man. Academic, London.
Huet AA, Raygada JL, Mendiratta K, Seo SM, Kaatz GW. 2008. Multidrug efflux pump overexpression in Staphylococcus aureus after single and multiple in vitro exposures to biocides and dyes 10.1099/mic.0.2008/021188-0. Microbiology 154(10):3144-3153.
Juliano RL, Ling V. 1976. A surface glycoprotein modulating drug permeability in Chinese hamster ovary cell mutants. Biochim Biophys Acta 455(1):152-62.
Kartner N, Evernden-Porelle D, Bradley G, Ling V. 1985. Detection of P-glycoprotein in multidrug-resistant cell lines by monoclonal antibodies. Nature 316(6031):820-3.
Kartner N, Riordan JR, Ling V. 1983. Cell surface P-glycoprotein associated with multidrug resistance in mammalian cell lines. Science 221(4617):1285-8.
Lage H. 2003. ABC-transporters: implications on drug resistance from microorganisms to human cancers. Int J Antimicrob Agents 22(3):188-99.
Li XZ, Zhang L, Nikaido H. 2004. Efflux pump-mediated intrinsic drug resistance in Mycobacterium smegmatis. Antimicrob Agents Chemother 48(7):2415-23.
Ling V. 1997. Multidrug resistance: molecular mechanisms and clinical relevance. Cancer Chemother Pharmacol 40 Suppl:S3-8.
Litman T, Druley TE, Stein WD, Bates SE. 2001. From MDR to MXR: new understanding of multidrug resistance systems, their properties and clinical significance. Cell Mol Life Sci 58(7):931-59.
Lomovskaya O, Totrov M. 2005. Vacuuming the periplasm. J Bacteriol 187(6):1879-83.
McMurry L, Petrucci RE, Jr., Levy SB. 1980. Active efflux of tetracycline encoded by four genetically different tetracycline resistance determinants in Escherichia coli. Proc Natl Acad Sci U S A 77(7):3974-7.
O'Mara ML, Tieleman DP. 2007. P-glycoprotein models of the apo and ATP-bound states based on homology with Sav1866 and MalK. FEBS Letters 581(22):4217-4222.
Overington JP, Al-Lazikani B, Hopkins AL. 2006. How many drug targets are there? 5(12):993-996.

Paulsen IT, Brown MH, Skurray RA. 1996. Proton-dependent multidrug efflux systems. Microbiol Rev 60(4):575-608.
Poole K. 2005. Efflux-mediated antimicrobial resistance. J Antimicrob Chemother 56(1):20-51.
Rees DC, Johnson E, Lewinson O. 2009. ABC transporters: the power to change. Nat Rev Mol Cell Biol 10(3):218-27.
Rigaud JL, Mosser G, Lacapere JJ, Olofsson A, Levy D, Ranck JL. 1997. Bio-Beads: an efficient strategy for two-dimensional crystallization of membrane proteins. J Struct Biol 118(3):226-35.
Riordan JR, Ling V. 1979. Purification of P-glycoprotein from plasma membrane vesicles of Chinese hamster ovary cell mutants with reduced colchicine permeability. J Biol Chem 254(24):12701-5.
Schinkel AH. 1997. The physiological function of drug-transporting P-glycoproteins. Semin Cancer Biol 8(3):161-70.
Schinkel AH, Wagenaar E, Mol CA, van Deemter L. 1996. P-glycoprotein in the blood-brain barrier of mice influences the brain penetration and pharmacological activity of many drugs. J Clin Invest 97(11):2517-24.
Schneider E, Hunke S. 1998. ATP-binding-cassette (ABC) transport systems: functional and structural aspects of the ATP-hydrolyzing subunits/domains. FEMS Microbiol Rev 22(1):1-20.
Seelig A. 1998. A general pattern for substrate recognition by P-glycoprotein. Eur J Biochem 251(1-2):252-61.
Shapiro AB, Ling V. 1997. Positively cooperative sites for drug transport by P-glycoprotein with distinct drug specificities. Eur J Biochem 250(1):130-7.
Shen DW, Fojo A, Chin JE, Roninson IB, Richert N, Pastan I, Gottesman MM. 1986. Human multidrug-resistant cell lines: increased mdr1 expression can precede gene amplification. Science 232(4750):643-5.
Sheppard DN, Welsh MJ. 1999. Structure and function of the CFTR chloride channel. Physiol Rev 79(1 Suppl):S23-45.
Tan A, Ziegler A, Steinbauer B, Seelig J. 2002. Thermodynamics of sodium dodecyl sulfate partitioning into lipid membranes. Biophys J 83(3):1547-56.
Tanaka Y, Abe Y, Tsugu A, Takamiya Y, Akatsuka A, Tsuruo T, Yamazaki H, Ueyama Y, Sato O, Tamaoki N and others. 1994. Ultrastructural localization of P-glycoprotein on capillary endothelial cells in human gliomas. Virchows Arch 425(2):133-8.
Tatsuta T, Naito M, Oh-hara T, Sugawara I, Tsuruo T. 1992. Functional involvement of P-glycoprotein in blood-brain barrier. J Biol Chem 267(28):20383-91.
Thiebaut F, Tsuruo T, Hamada H, Gottesman MM, Pastan I, Willingham MC. 1987. Cellular localization of the multidrug-resistance gene product P-glycoprotein in normal human tissues. Proc Natl Acad Sci U S A 84(21):7735-8.
Thiebaut F, Tsuruo T, Hamada H, Gottesman MM, Pastan I, Willingham MC. 1989. Immunohistochemical localization in normal tissues of different epitopes in the multidrug transport protein P170: evidence for localization in brain capillaries and crossreactivity of one antibody with a muscle protein. J Histochem Cytochem 37(2):159-64.

Van Bambeke F, Balzi E, Tulkens PM. 2000. Antibiotic efflux pumps. Biochem Pharmacol 60(4):457-70.
Velamakanni S, Yao Y, Gutmann DAP, van Veen HW. 2008. Multidrug Transport by the ABC Transporter Sav1866 from Staphylococcus aureus† doi:10.1021/bi8006737. Biochemistry 47(35):9300-9308.
von Heijne G. 2006. Membrane-protein topology. 7(12):909-918.
Yeliseev AA, Wong KK, Soubias O, Gawrisch K. 2005. Expression of human peripheral cannabinoid receptor for structural studies. Protein Sci 14(10):2638-53.

2 Aim of research

The study of ABC-transporters requires the use of detergents for membrane solubilization and further purification of the protein. These proteins are reconstituted into model membranes in order to investigate their biophysical and biochemical properties. To quantify an important step during the reconstitution process of membrane proteins we addressed the question in chapter 3 of how efficiently detergents are removed from proteoliposomes by the common used Bio-Beads SM2 method.

All ABC-transporters have a basal ATP hydrolysis rate, which is different from organism to organism. The basal ATPase activity of SAV1866 has to our knowledge not been quantified under different conditions yet. In chapter 4 Sav1866 was solubilized in detergent micelles and we addressed the question of the stability and activity in those mixed micellar systems. Moreover we addressed the question of how the ATPase activity of Sav1866 changes under different experimental conditions in micelles and vesicles in terms of pH, ATP concentration dependence and NaCl dependence. Further the results were compared with the well known basal ATPase activity of P-glycoprotein.

The MDR-related ABC-transporters like P-gp transport their substrates from one membrane leaflet to the other. Thus the quantification of the substrate/protein interaction requires knowledge about the membrane and the transporter. Chapter 5 addresses the question of how drug stimulate ATPase activity of Sav1866 compared to P-gp. As a first step isothermal titration calorimetry, dynamic light scattering and zetapotential measurements were performed to get insight into the membrane properties where Sav1866 was reconstituted in. Further we investigated how the drug stimulated ATPase activity of Sav1866 is influenced by additional lipids and by different lipid/protein ratios. As last we propose a different function of Sav1866 than to be involved in multi-drug resistance. The ATPase activity of Sav1866 is not only stimulated upon addition of various structurally unrelated drugs but can also transport a cationic lipid by the name of lysyl-DPPG.

ABC-transporters are related with multi-drug resistance in bacteria as well as in humans. Over-expression of P-gp in human cancer cells leads to multi-drug resistance. In bacteria there are ABC-transporters present which transport toxic compounds out of the cell. Such

toxic compounds are for example quaternary ammonium compounds which are known to act as bactericides. However there is no quantitative data available of how much cationic detergent incorporates into a membrane or how a membrane is solubilized. We investigated the self assembly of a model compound dodecyltimethylammonium chloride (DTAC). As a next step we asked how does DTAC incorporate and solubilize a model lipid membrane. The incorporation and the solubiliaztion behaviour were investigated by means of isothermal titrations calorimetry and dynamic light scattering. The thermodynamic parameters were compared with the incorporation and solubilization properties of the negatively charged counterpart sodium dodecyl sulphate (SDS). Further we investigated the movement of the lipid headgroup upon incorporation of the two oppositly charged detergent molecules by means of ^{2}H-NMR. We provide the first quantitative comparison of anionic (SDS) and cationic (DTAC) detergents interacting with lipid membranes.

The last part of the work deals with the interaction of c-di-GMP with TipF. C-di-GMP is a second messenger in many bacteriae and is involved in the decision whether a bacteria lives in multicellular assemblies or as a single motile cell. Recently two important proteins involved in flagellum construction, TipN and TipF, could be identified. The protein TipF was shown to bind d-ci-GMP *in vivo*. The binding constant was however not known. Therefore we adressed the question in chapter 7 of how strong c-di-GMP binds TipF in order to get insight into the TipF pathway.

3 Detergents Removal by Bio-Beads SM2

3.1 Summary

The increasing amount of available crystal structures of membrane proteins led to a better understanding of these proteins. However the major drawback to study these proteins is the requirement of a stabilizing membrane or detergent environment, respectively, that keeps the membrane protein native. Biophysical studies of membrane proteins need pure and native proteins. Membrane proteins are purified by the use of single detergents or detergents mixtures. In order to bring the protein back to its typical environment, the membrane, it is reconstituted into model membrane vesicles. Upon reconstitution the detergent has to be removed. The most often used technique nowadays is the detergents removal by the use of Bio-Beads SM2. However the reconstitution process is still a semi-empirical task. Here we quantified the amount of detergent molecules left upon reconstitution by a label-free technique. The approach can be used to any detergent and gave insight into the removal efficiency of Bio-Beads SM2. We found for a specific lipid/detergent system upon removal of detergents by Bio-Beads SM2 that there are still 9 detergent molecules per 100 lipid molecules left in suspension. We show that the removal efficiency was independent of the amount of lipids and detergents used. We concluded that the removal efficiency is dependent on the balance of the detergents affinity to the membrane and to the Bio-Beads.

3.2 Memo

List of Abbreviations

GPCR: G-protein coupled receptor

R_b^{sat}: Critical detergent/lipid molar ratio where solubilization starts

$C_{12}E_8$: Octaethylene glycol monododecyl ether

POPC: 1-palmitoyl-2-oleoyl-*sn*-glycero-3-phosphocholine

ITC: Isothermal titration calorimetry

DLS: Dynamic light scattering

ABC-tansporter: **A**TP-**b**inding **c**assette transporter (integral membrane protein)

P-gp: P-glycoprotein (belongs to the family of ABC-transporter)

TX-100: Triton X-100

LM: Laurylmaltoside

Introduction

Integral membrane proteins are of great importance in pharmaceutical research as they are the main drug targets (Drews 2000). More than 60 % of all drug target molecules are located at the cell surface, and half of them are GPCRs (Overington and others 2006). However, compared to soluble proteins only very few structures have been solved up to date (on August 2009: 218 structures). This limitation arises from the lack of reproducible methods for solubilization, reconstitution and crystallisation of membrane proteins. Integral membrane proteins are permanently embedded in biological membranes. These proteins can be separated from the biological membranes only with detergents, nonpolar solvents, or denaturing agents.

Membrane proteins are difficult to handle since they have an amphipatic character, which requires the use of detergents for disintegration of the structure of native membranes in the initial purification step (Lambert and others 1998). Figure 1 shows a crystal structure of a typical ABC-transporter from *Staphylococcus aureus* at a 3Å resolution (Dawson and Locher 2006). The hydrophilic and the hydrophobic environments are depicted in blue and red respectively.

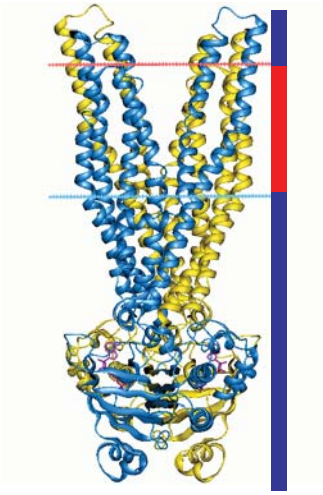

Figure 1 shows a typical bacterial membrane protein of the familiy of ABC-transporters, Sav1866. The hydrophilic part is depicted in blue whereas the hydrophobic part is shown in red.

In order to mimic the hydrophobic character of a membrane, detergents are used for solubilization and purification of membrane porteins. As a next step membrane proteins are reconstituted into model membranes to study the activity and function. During the reconstitution process detergents are slowly removed from the protein/lipid/detergent mixture. There are several methods available for detergents removal as e.g. dilution, dialysis or Bio-Beads SM2 treatment. Here the use of Bio-Beads SM2 is discussed in detail as it is nowadays a commonly used technique to remove detergent molecules.

Bio-Beads SM2 (registered name for polystyrene beads from Bio-Rad; Richmond, California) are macroporous divinyl benzene cross-linked polystyrene beads with a large surface with hydrophobic pores (pore sizes of ~ 9 nm) which allows the uptake of monomeric or micellar detergent molecules (Lambert and others 1998). We studied the use of Bio-Beads SM2 in detail and quantified the amount of detergent molecules remaining in the liposomes and the amount of detergent molecules which is removed during reconstitution. The lipid concentration after treatment was deterimend by a colorimetric assay proposed by (Itaya and Ui 1966) and dynamic light scattering measurements were carried out to get structural insight into the reconstitution process. We determined the final detergent concentration remaining in suspension by means of isothermal titration calorimetry (ITC). The method we have used to determine the detergents concentration does not require labeling and has the advantage that it can be

used for virtually any detergent. We started out with a model system containing POPC and $C_{12}E_8$ and we compared our results with previous values found by a different technique.

The final molar ratio $C_{12}E_8$/POPC after biobead treatment was found to be 0.09 +/- 0.02 (mol/mol). This ratio was neither significantly influenced by the initial detergent nor lipid concentration nor the volume of suspension. The amount of detergent which is removed from the liposomes upon treatment with Bio-Beads SM2 has been quantified in 1990 by means of radiolabled $C_{12}E_8$ (Levy and others 1990). It was found that 5 to 7 mol detergent remained per 100 mol of lipid. At first glance this value seems to be low as described by other authors (Rigaud and others 1997). However, Li-Blatter et al. have shown that for example the ABC-transporter P-gp, a close structural homologue of Sav1866 (Figure 1), transports various detergents among them also $C_{12}E_8$ (Li-Blatter and others 2009). Our findings suggest that detergents may influence the activity of the transporter especially if the reconstitution protocol contains detergents mixtures.

The period of time needed to add Bio-Beads SM2 and their amount are crucial factors in the detergent removal process. Upon fast detergent removal (e.g. all the beads are added at once) usually smaller and unilamellar vesicles are found in suspension (Levy and others 1990; Levy and others 1992). In contrast generally large and multilamellar vesicles are obtained when detergents are removed slowly. Multilamellar vesicles have the disadvantage that not all lipid molecules have access to the bulk solution. In this work the Bio-Beads SM2 were added according to well established protocols. The same amount of beads was added (40 mg/ml of wet Bio-Beads per ml of mixed detergent/lipid suspension) time dependently (see methods).

As an outlook other commercialy available detergents, such as TX-100 or LM have to be investigated. An interesting question that remains to be solved is how the detergent removal is related to the binding constant of the detergents towards the membrane.

Materials and Methods

Materials. Bio-Beads SM2 Adsorbent reagent was purchased from Bio-Rad Laboratories, Inc. (CA 94547, USA) and was washed extensively before use. POPC was obtained from Avanti polar lipids (Alabaster, AL). The detergent $C_{12}E_8$ was obtained from Fluka

(Buchs, Switzerland). The lipids and the detergents were used without further purification. The lipids were obtained in a chloroform suspension. The chloroform was evaporated under a gentle stream of nitrogen and the samples were put in high vacuum overnight. The dry lipid was weighted and re-suspended in buffer (25 mM HEPES containing 100 mM NaCl, pH 7.5 at 25 °C) by vortexing rigorously. Multilamellar vesicles (MLVs) were obtained by 5 freeze/thaw cycles. Large unilamellar vesicles (LUVs) were prepared by 12 extrusion runs through a Nucleopore polycarbonate filter at 23°C in a Lipex extruder (Northern Lipids, Vancouver, Canada). All steps were performed under argon in order to limit lipid exposure to air. The vesicle size was determined using dynamic light scattering. All results are given as z.average size. Z. average size is the intensity weigthed size distribution (given as diameter) of all species found in suspension or solution. Further the polydispersity index (PDI) is discussed as a width parameter, characterizing the polydispersity of the solution or suspension. Generally PDI values below 0.1 are typical for a monodisperse solution or suspension.

Bio-Beads SM2 washing step. Bio-Beads SM2 were washed according to instructions from the manufacturer (Biorad). Briefly, they were washed with methanol and followed by several washes with water. Clean Bio-Beads SM2 were stored in the same buffer used for the ITC study.

Detergent removal. Bio-Beads SM2 were added according to commonly used and well established protocols. Wet Bio-Beads SM2 (40 mg per ml of lipid/detergent suspension) were added after 15 min, 15 min, 30 min, overnight, and 60 minutes incubation period. The suspension was incubated on a tabletop shaker at a speed of 700 min^{-1} at 4°C.

Concentration Determination of Lipid. The lipid concentration was determined after removal of the Bio-Beads SM2 since (i) the sample is diluted upon addition of wet Bio-Beads SM2 and (ii) the Bio-Beads SM2 may remove lipids from the suspension. The concentration was determined using a phosphate assay according to (Itaya and Ui 1966). The vesicles were diluted in perchloric acid and heated until the suspension became clear. After addition of malachite green the free phosphate concentration was determined by measuring absorbance at 670 nm and was compared to standards.

Isothermal titration calorimetry. The partition experiment was done according to (Zhang and Rowe 1992). After Bio-Beads SM2 treatment the syringe was loaded with the mixed

lipid/detergent suspension and the mixture was injected into solutions containing different $C_{12}E_8$ concentrations.

Thermodynamics of Membrane Partitioning of $C_{12}E_8$. The apparent binding constant of $C_{12}E_8$ towards POPC, K_{app}, as well as the lipid concentration, C_L, is known. ITC titration experiments were performed to determine the free concentration of detergent, $C_{D,eq}$, in the syringe. Uptake of the nonionic detergents is exothermic whereas the release of the detergent molecules from the vesicles is exothermic at 25°C. The mixed vesicles were injected into solutions containing different $C_{12}E_8$ concentration. The free detergent, $C_{D,eq}$, in the syringe corresponds to the titration pattern where no heat is released or taken up (plus heat of dilution of the vesicles alone). Knowing the lipid concentration, C_L, the apparent partition coefficient, K_{app}, and the free concentration, $C_{D,eq}$, allows the determination of the detergent concentration which is left in suspension after Bio-Beads SM2 treatement according to

$$X_b = K_{app} / C_{D,eq} \quad (1)$$

where X_b is the molar ratio of bound detergent molecules per total lipid molecules, defined as

$$X_b = C_{D,b} / C_L \quad (2)$$

where $C_{D,b}$ is the bound detergent concentration and C_L the lipid concentration. Combining equation (1) and equation (2) yields

$$C_{D,b} / C_L = K_{app} / C_{D,eq} \quad (3)$$

The bound, $C_{D,b}$, and the free concentration, $C_{D,eq}$, in sum, is the total concentration, $C_{D,0}$ according to

$$C_{D,0} = C_{D,eq} + C_{D,b} \quad (4)$$

Results

Vesicle Size during Bio-Beads SM2 Treatment. Figure 1A shows a volume weighted size distribution plot of a vesicle suspension during the reconstitution process. The extrusion run (100 nm pores size) led to vesicle (5 mM) diameter of 100 – 110 nm (i). Detergent addition to a final concentration of 4 mM, which is above the critical saturation value, R_b^{sat} (R_b^{sat} = 0.62 (POPC/$C_{12}E_8$ at 25°C) (Edwards and Almgren 1991)), led to vesicle

disintegration. Two populations were found, one at around 30 nm and another at around 200 nm (ii). A close description of R_b^{sat} can be found in chapter 6.

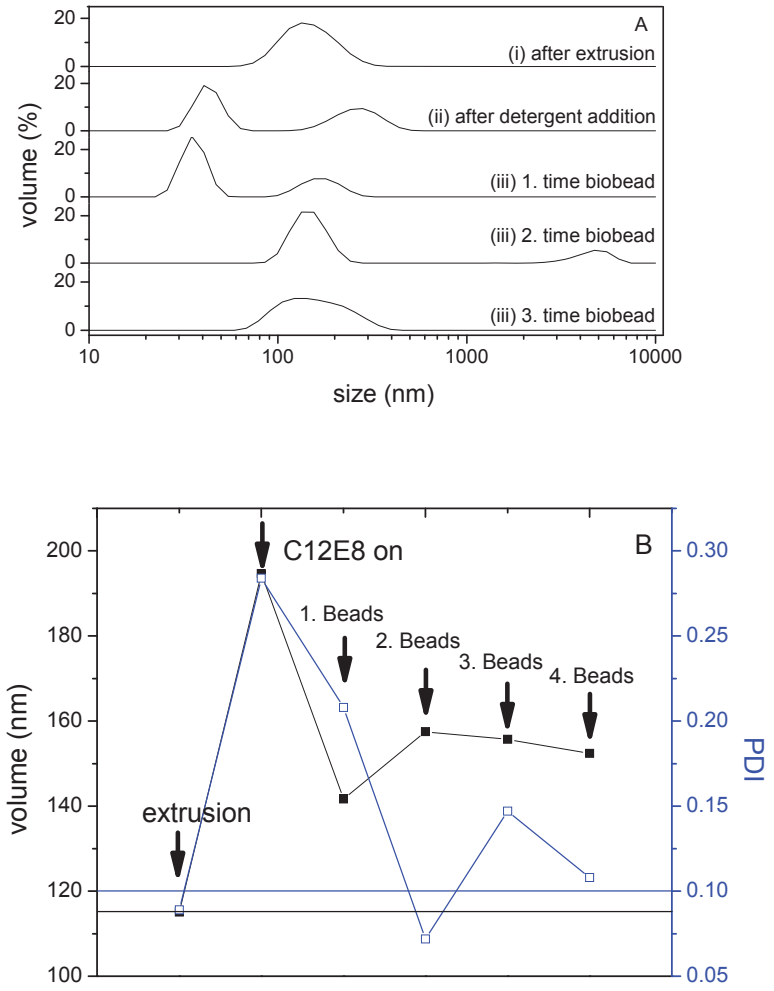

Figure 2A, B. *Vesicle size during Bio-Beads SM2 treatment.* (A) Volume weighted size distribution plot of the vesicles (i) after extrusion, (ii) after addition of C12E8 and (iii) after Bio-Beads SM2 treatment. (B) shows the average size in black of (A) and the polydispersity index in blue for each individual measurement.

Biobeads were consecutively added according to protocol (see methods). The suspension was incubated on a tabletop shaker at a speed of 700 min^{-1} at 4°C. The final lipid concentration after treatment was 3.46 mM according to phosphate assay. The final detergent concentration, $C_{D,0}$, after Bio-Beads SM2 treatment was 0.41 mM. Figure 2B shows the z.average size distribution of the species found in suspension and in the same

figure the polydispersity index (PDI). After Bio-Beads SM2 treatment the vesicles were generally bigger and had a broader size distribution than directly after extrusion.

Concentration Determination of Lipids after Bio-Beads SM2 Treatment. Figure 2 shows a plot of the initial *vs.* the final lipid concentration. The straight line has a slope of 0.83 (M/M).

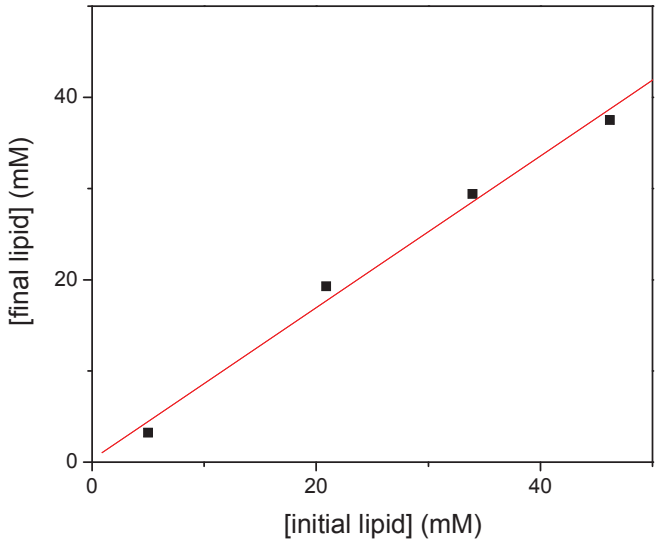

Figure 3. *Initial vs. final lipid concentration.* The final lipid concentration was determined according to the phosphate assay proposed by (Itaya and Ui 1966). The x-axis shows the initial lipid concentration and the y-axis the final lipid concentration. The slope of the straight line is 0.83 (M/M), (R^2 : 0.995)

Concentration Determination of Detergents by a Thermodynamic Approach. The concentration of detergents left in suspension after treatment with Bio-Beads SM2 is unknown. Isothermal titration calorimetry (ITC) reveals the amount of detergent which is removed. The experiments were performed as described in (Zhang and Rowe 1992). The binding constant of $C_{12}E_8$ to POPC vesicles (K_{app} = 6 mM^{-1}) is known from (Edwards and Almgren 1991) and the final lipid concentration is known from the phosphate assay. The free detergent concentration in suspension was determined by using equation (1). Figure 4 shows raw ITC-data for lipid vesicles (19.28 mM) initially preloaded with $C_{12}E_8$ (7 mM) titrated into different concentrations of $C_{12}E_8$ (0 – 40 μM). A detergent concentration of 15 – 20 μM in the cell equals the free detergent concentration in the

syringe. Figure 3B shows the integrated titration peaks. The black line corresponds to the heat of dilution of the vesicles (- 8 cal/mol). A lipid concentration, C_L, of 19.28 mM, a binding constant, K_{app}, of $C_{12}E_8$ to POPC of 6 mM^{-1} and a free detergent concentration, $C_{D,eq}$, of 15.5 µM leads to a final detergent concentration, C_0, of 2.05 mM $C_{12}E_8$ which remains in suspension.

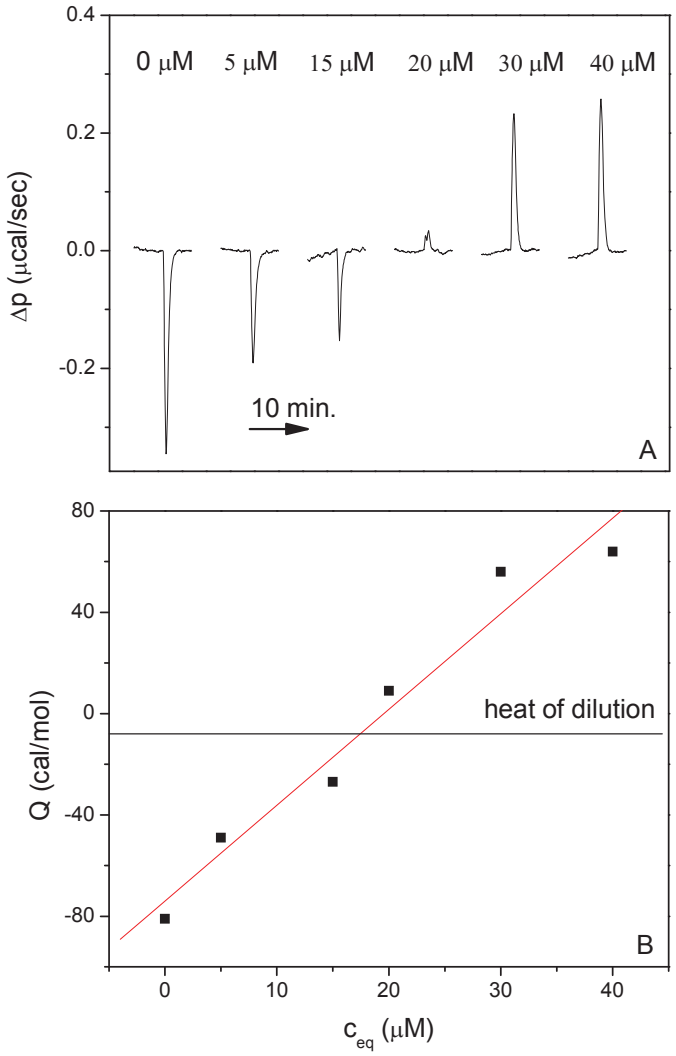

Figure 4. *Detergent concentration determination by a thermodynamic approach*. (A) shows the raw titration pattern for a vesicular suspension preloaded with $C_{12}E_8$ titrated into different concentrated $C_{12}E_8$ solutions (0 – 40 µM). The arrow corresponds to a time interval of 10 min. (B) shows the integrated data peaks plotted vs. the detergent concentration in the cell. The black horizontal line corresponds to the heat of dilution of the vesicles alone (-8 cal/mol).

The same approach was applied to higher lipid concentrations and higher detergent concentrations in order to check whether the binding affinity between the bilayer and Bio-Beads SM2 or Bio-Beads SM2 saturation with detergent, respectively, limits the detergent removal. We can exclude the latter point since lipid vesicles (37.52 mM) preloaded with $C_{12}E_8$ (15 mM) led to a final detergent concentration after Bio-Beads SM2 removal of 3.17 mM $C_{12}E_8$. From this we can conclude that the Bio-Beads SM2 are not overloaded since removal of detergent is in similar range (final detergent/lipid molar ratio (mol/mol) ~ 0.09) as found with lower $C_{12}E_8$ concentrations. All thermodynamic parameters are summarized in table 1.

Table 1. *Thermodynamic parameters upon detergents removal by Bio-Beads SM2.*

Volume	C_L initial	C_L final	C_D initial	C_D final	$C_{D,bound}$	$C_{D,eq}$	C_D/ C_L initial	C_D/ C_L final
ml	mM	mM	mM	mM	mM	μM	(mol/mol)	(mol/mol)
2	20.88	19.28	7	2.05	2.03	17.5	0.34	0.11
1	46.21	37.52	15	3.17	3.16	14	0.32	0.08
8.5	5	3.21	2.5	0.23	0.22	11.2	0.50	0.07
3	5	3.46	4	0.41	0.39	16.9	0.80	0.12

The study presented here reveals a final detergent/lipid molar ratio of 0.09 +/- 0.02 after Bio-Beads SM2 treatment. Figure 5 shows the initial molar ratios vs. the final molar ratios present in suspension.

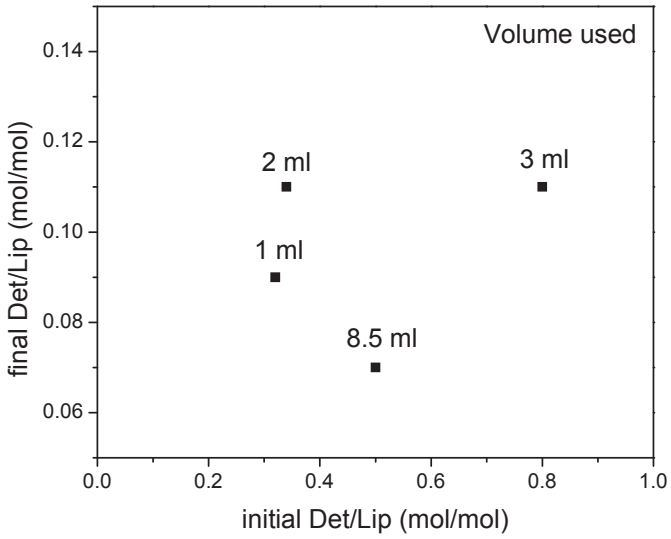

Figure 5. *Det/Lip molar ratio vs. final Det/Lip molar ratio.* Figure 5 shows the initial detergent/lipid molar ratio *vs.* the final detergent/lipid molar ratio. The final molar ratio was found to be 0.09 +/- 0.02 (M/M) which is independent on the volume or the initial concentrations used.

However, as described in the protocol, the proteoliposomes are centrifuged down and resuspended in the appropriate buffer after Bio-Beads SM2 treatment. This last step of the reconstitution protocol was skipped due to the lack of protein in the vesicles. 100 nm vesicles cannot be centrifuged down in contrast to e.g. vesicles containing proteins or multilamellare vesicles. It is expected that upon dilution of the mixed vesicles additional detergent molecules will be removed from the suspension.

Here we have shown that the technique is applicable. The use of different commonly used detergents as for example LM or Tx-100 could reveal general features of the Bio-Beads SM2 removal process. A possibility to quantify the Bio-Beads SM2 treatment would be to correlate the binding constant of the detergents towards the membrane with the removal efficiency (the final detergent/lipid molar ratio). This study dealt with the lipid-detergent interaction part of the reconstitution process and neglected any detergent-protein interactions.

References

http://blanco.biomol.uci.edu/Membrane_Proteins_xtal.html.

Dawson RJP, Locher KP. 2006. Structure of a bacterial multidrug ABC transporter. 443(7108):180-185.
Drews J. 2000. Drug discovery: a historical perspective. Science 287(5460):1960-4.
Edwards K, Almgren M. 1991. Solubilization of lecithin vesicles by C12E8. Trends in Colloid and Interface Science V. p 472-473.
Itaya K, Ui M. 1966. A new micromethod for the colorimetric determination of inorganic phosphate. Clin Chim Acta 14(3):361-6.
Lambert O, Levy D, Ranck J-L, Leblanc G, Rigaud J-L. 1998. A New Gel-like Phase in Dodecyl MaltosideLipid Mixtures: Implications in Solubilization and Reconstitution Studies. 74(2):918-930.
Levy D, Bluzat A, Seigneuret M, Rigaud JL. 1990. A systematic study of liposome and proteoliposome reconstitution involving Bio-Bead-mediated Triton X-100 removal. Biochim Biophys Acta 1025(2):179-90.
Levy D, Gulik A, Bluzat A, Rigaud JL. 1992. Reconstitution of the sarcoplasmic reticulum Ca(2+)-ATPase: mechanisms of membrane protein insertion into liposomes during reconstitution procedures involving the use of detergents. Biochim Biophys Acta 1107(2):283-98.
Li-Blatter X, Nervi P, Seelig A. 2009. Detergents as intrinsic P-glycoprotein substrates and inhibitors. Biochimica et Biophysica Acta (BBA) - Biomembranes Includes Special Section: Cardiolipin 1788(10):2335-2344.
Overington JP, Al-Lazikani B, Hopkins AL. 2006. How many drug targets are there? 5(12):993-996.
Rigaud JL, Mosser G, Lacapere JJ, Olofsson A, Levy D, Ranck JL. 1997. Bio-Beads: an efficient strategy for two-dimensional crystallization of membrane proteins. J Struct Biol 118(3):226-35.
Zhang F, Rowe ES. 1992. Titration calorimetric and differential scanning calorimetric studies of the interactions of n-butanol with several phases of dipalmitoylphosphatidylcholine. Biochemistry 31(7):2005-2011.

4 The Activity of Sav1866 in Lipid Vesicles and Detergent Micelles

4.1 Summary

We investigated the variation of the turn-over number of Sav1866 with the membrane environment, the extravesicular sodium chloride concentration and the p*H*. At the temperature, T = 25 °C the turnover number of Sav1866 varied by a factor of about 2.5 (tn = (1.1 – 2.7) s^{-1}) depending on the conditions applied. The lowest and highest turnover number was observed in lipid vesicles in the presence of high sodium chloride concentrations (C_{NaCl} = 150 mM) and in mixed micelles in the absence of sodium chloride, whereby the measurements were performed under optimal ATP concentrations. Although, the rate of ATP hydrolysis varied strongly, the dissociation constant of ATP varied only by a factor of 2 to 3. Binding of ATP at the interface between the two NBDs is thus neither dependent on the lipid environment nor is it very sensitive to the sodium chloride concentration of the environment. Arresting the activity cycle in the post-hydrolysis state with vanadate which means after phosphate, but not ADP release was in contrast strongly dependent on the conditions. The concentration of half-maximum inhibition of the Sav1866 ATPase activity with vanadate, IC_{50} (vandate) decreased with increasing turn-over number and remained constant at turnover numbers, nt ≥ 1 s^{-1}. The vanadate concentrations required to block the cycle in the post-hydrolysis state are thus lower if the turnover number is high i.e. if the lateral membrane packing density and the sodium chloride concentration are low. This suggests that the probability to bind to a molecule in the post-hydrolysis state increases with the rate of hydrolysis.

This suggests that formation of the release-competent conformation upon ATP binding at the interface of the two NBDs is less sensitive to variations of the environment than formation of the binding-competent conformation which corresponds to a resetting of the transporter. The present finding for Sav1866 seems to be in accordance with an occluded ATP in the course of the catalytic cycle for P-gp.

4.2 Manuscript

The Activity of the ATP-Binding Cassette Transporter Sav1866 from Staphylococcus aureus in Lipid Vesicles and Detergent Micelles

Andreas Beck[+], Päivi Äänismaa[+], Roger Dawson[§], Kaspar Locher[§] and Anna Seelig[+]*

[+]Biozentrum, University of Basel, Biophysical Chemistry,
Klingelbergstr. 50/70, CH-4056 Basel, Switzerland,
[§]ETH Zürich, Institute of Molecular Biology and Biophysics,
HPK D17 Schafmattstrasse 20, CH-8093 Zürich, Switzerland

*To whom correspondence should be addressed:
Tel. +41-61-267 22 06, Fax. +41-61-267 21 89, e-mail: anna.seelig@unibas.ch

Supported by the Swiss National Science Foundation Grant #

Sav1866 is an ATP binding cassette (ABC) transporter from *Staphylococcus aureus* which consist of an N-terminal transmembrane domain (TMD), comprising six α-helices, and a cytosolic nucleotide-binding domain (NBD). The functional protein is a homodimer (130 kDa) whereby the two TMDs form the translocation path and the NBDs bind and hydrolyze ATP at their interface. Sav1866 is a homolog of other bacterial half-transporters such as LmrA from *Lactococcus lactis* (Federici and others 2007; Pleban and others 2004; van Veen and others 1996) and MsbA from *E. coli* (Reyes and others 2006). It is also a homolog of the mammalian P-glycoprotein (P-gp, ABCB1, MDR1) that is expressed as a single polypeptide chain and transports or flips many hydrophobic compounds from the cytosolic to the extracellular membrane leaflet or to the cytosol, depending on the hydrophobicity of the compound. The crystal structures of Sav1866 has been resolved in the nucleotide-bound form, showing an outward facing conformation (Dawson and Locher 2006) whereas the crystal structure of P-gp has been resolved in the nucleotide-free form showing an inward facing conformation (Aller and others 2009).. The comparable topologies of different ABC transporters suggest that the transport mechanism is conserved among the ABC transporter superfamily. In analogy to P-gp it can be assumed that the catalytic/transport cycle is initiated by ATP binding to the NBDs and substrate binding to the TMDs, followed by substrate release and subsequent ATP hydrolysis which resets the transporter to the binding-competent conformation.

The amino acid sequence as well as the structure of the NBDs was similar to those NBDs of other full transporters and also to NBDs crystallized in free form. The structure was used for many structural models like P-gp (O'Mara and Tieleman 2007) or the transmission interface in the complex TAP (Oancea and others 2009). The nucleotide binding domain of Sav1866 showed the same crucial amino acid residues involved in the catalytic step of ATP hydrolysis found in other transporters.

We investigated the ATPase activity of Sav1866 in two highly different environments. Sav1866 was reconstituted in *E.coli* polar lipid extract:egg yolk PC (3:1 w:w) and into mixed micelles containing lipids and the detergent $C_{12}E_8$. We show that the ATPase activity is strongly enhanced in the mixed micellar system, which had strong influence on the pH and the vanadate dependence, respectiviely, of the ATPase activity. The ATPase activity of Sav1866 in lipid vesicles showed similar narrow sensitivity to pH as

previously reported for HlyB and the double mutant of TAP1 (Zaitseva and others 2005) (Ernst and others 2006). However upon reconstitution into mixed micelles the ATPase activity showed broad pH dependence as reported for P-glycoprotein (Aanismaa and Seelig 2007; al-Shawi and Senior 1993). Sav1866 has the same crucial motives in the NBDs thought to be involved in the pH dependence as HylB and the double mutant of TAP1.

Further we investigated the basal ATPase activity in two different buffer systems used previously either for the ATPase activity measurements of the ButCD and the Sav1866 transporters or for the ATPase activity measurements of P-glycoprotein, respectively. The two conditions differ mainly in terms of ionic conditions. The found turn-over number of ATP hydrolysis is in the same range as reported for P-gp. We found that the ATPase activity shows sodium chloride dependence. Upon increasing the sodium chloride concentration the ATPase activity is reduced. The highest activity was found in buffer systems were no sodium chloride was present.

Materials

Compounds. The polyoxyethylene alkyl ether $C_{12}EO_8$ or $C_{12}E_8$ was obtained from Fluka (Buchs, Switzerland). N-nonyl-β-D-maltoside (NM), n-decyl-β-D-maltoside (DM), n-dodecyl-β-D-maltoside (LM), n-tetradecyl-β-D-maltoside (TM), dodecyltrimethyl ammonium chloride (DTAC) and tetradecyltrimethyl ammonium chloride (TTAC) were purchased from Anatrace (Maumee, Ohio, USA). 3-[(3-Cholamidopropyl)dimethylammonio]-1-propanesulfonate (CHAPS) was purchased from Sigma. BCA, protein assay reagents A and B were from Pierce (Rockford, IL) and Bovine serum album, BSA, from Sigma. The lipids egg yolk phosphatidyl choline (POPC) and *E.coli* polar lipid extract were from Avanti polar lipids (Alabaster, Alabama, USA). All other chemicals were from Sigma or Merck.

Methods

Buffers. Buffer II (25 mM HEPES, 150 mM NaCl, 10 mM $MgSO_4$, final concentrations) was adjusted to pH 7.5 at 25°C and ATP was added in H_20 at pH 7.0 to the reaction mixture to a final concentration of 7 mM unless otherwise mentioned. An similar buffer was previously used for activity tests of E. coli vitamin B12 transporter BtuCD (Borths and others 2005a) as well as for activity tests of Sav1866 (Dawson and Locher 2006) Buffer I (25 mM HEPES, 50 mM NaCl, 2.5 mM MgSO4) was adjusted to pH 7.0 at 37°C. ATP was added to the reaction mixture to a final concentration of 3 mM unless otherwise mentioned. An equivalent buffer was previously used for activity tests of P-gp (Aanismaa and Seelig 2007; Litman and others 1997).

Purification and Reconstitution of Sav1866 into Lipid Vesicles. For detailed protocol see (Dawson and Locher 2006). Briefly, the gene encoding Sav1866 fused to an N-terminal His-tag was overexpressed in *E. coli*, solubilized and purified in octaethylene glycol monododecyl ether ($C_{12}E_8$). Sav1866 was reconstituted in lipid vesicles according to the protocol described for the E. coli vitamin B12 transporter BtuCD (Borths and others 2005a). The lipid vesicles were composed of egg yolk PC and *E. coli* polar lipid extract (1:3 w/w) (see ref. (Dawson and Locher 2006)) for detailed protocol. *E. coli* polar lipid extract contains phosphatidylethanolamine, phosphatidylglycerol and cardiolipin

(67:23.2:9.8 w/w). Vesicles were suspended either in 25 mM HEPES, pH 7.5 (1st batch) or in 25 mM Tris/HCl (2nd batch) containing 150 mM NaCl. The diameter of the lipid vesicles was 400 nm as determined by dynamic light scattering (DLS). In the course of the reconstitution process the protein and lipid concentration, respectively, decreased especially during detergent removal by Bio-Beads SM2. Therefore the lipid and the protein concentration, respectively, in the final vesicles suspension were determined as described below.

Sav1866 Reconstituted in Detergent Micelles. Mixed lipid/$C_{12}E_8$ micelles containing Sav1866 were formed by adding high concentrations of $C_{12}E_8$ to lipid vesicles containing Sav1866. The final concentration of $C_{12}E_8$, was $C_{C_{12}E_8}$ = 1.8 mM which is twenty fold the CMC (CMC = 0.09 mM (Heerklotz and Seelig 2000)).

Determination of the Lipid Concentration. The lipid concentration was quantified by a colorimetric phosphate assay (Itaya and Ui 1966). Briefly, lipid vesicles were diluted in prechloric acid and flamed until the suspension became clear. The free phosphate was detected at 670 nm after addition of malachite green and was quantified by comparing with standards.

Determination of the Protein Concentration with (BCA) Assay. A standard curve (0-10 µg in 10 µL) was prepared from BSA; BSA and BCA solutions were prepared by mixing reagent A and reagent B in 50:1 v/v. To each BSA standard and protein sample 1 mL of BCA working solution was added. The samples were incubated 20 min at 60 °C and then cooled to room temperature before measuring the absorbance at 562 nm.

Determination of the Protein Concentration According to Edelhoch (Edelhoch 1967). The lipid vesicles were solubilized in $C_{12}E_8$ solution (1.9 mM or 2.2 mM) and equilibrated for 30 min. The solution was then diluted and guanidinium chloride was added (6 M). The molar extinction coefficient was measured at 280 nm and the corresponding protein concentration was calculated according to (http://www.expasy.ch/tools/protparam-doc.html). Results are summarized in Table 1.

Table 1

For the following the protein concentration was determined in $C_{12}E_8$ according to the BCA determination as C_{Sav} = 1.8 mg/ml for the first proteoliposome preparation and as C_{Sav} = 2.7 mg/ml for second proteoliposome preparation.

ATPase Assay. The Sav1866 associated ATP hydrolysis was measured according to Litman et al. (Litman and others 1997) in 96-well microtiter plate (Nunc F96 MicroWell^{TM} plate, non-treated) with small modifications. Each experiment contained ~0.9 or ~0.2 µg protein / 60 µL in phosphate release assay buffer I or II (i.e. C_{Sav} = 0.114 µM or C_{Sav} = 0.028 µM). The reaction was started by transferring the plate from ice to a water bath kept at the temperature of choice for 30 min (at 37°C or at 25°C for 30 min or 1h, respectively) and was terminated by rapidly cooling the plate on ice. The inorganic phosphate, P_i, concentration was determined by adding ice-cold solution (200 µL) containing ammonium molybdate (0.2 % (w/v)), sulphuric acid (1.43 % (v/v)), freshly prepared ascorbic acid (1 % (w/v)) and SDS (0.9 % (w/v)). After incubation at room temperature for 30 min the phosphate released was quantified colorimetrically at 820 nm using a Spectramax M2 (Molecular Devices, Sunnyvale, USA). Reference phosphate standards were included to each 96-well plate. To correct for nonspecific ATP hydrolysis induced by the acidic color reagent the optical density (OD) of an ATP solution in buffer or water or a suspension of the transporter inhibited by vanadate (0.5 mM) was subtracted form the optical density of the sample. The optical density of the background control was usually about OD = 0.1 - 0.2 and that of the sample OD = 0.3 to 0.7.

Isothermal Titration Calorimetry (ITC). ITC experiments were performed with VP-ITC calorimeter from MicroCal (Northampton, MA).

Demicellisation Experiments in this study are described in detail elsewhere (Kresheck 1998; Kresheck and Hargraves 1974). Briefly, the syringe was filled with a micellar detergent concentration usually ten fold higher than the critical micelle concentration (CMC). The calorimeter cell was filled with matched buffer (25 mM HEPES, 150 mM NaCl, 10 mM $MgSO_4$ pH 7.5 at 25°C). All solutions were degassed before filling. The temperature was kept constant at 25°C. Typically 29 injections (a 10 µl each) were sufficient to go from complete demicellisation to no demicellisation.

Surface Activity Measurements. The air-water partition coefficient, K_{aw}, and the cross-

sectional area of the detergents molecules, A_d, were determined from the surface pressure, π, measurements, as a function of drug concentration (Gibbs adsorption isotherm) (for details see (Fischer and others 1998; Gerebtzoff and others 2004).

Circular Dichroism Measurements. CD-spectra of Sav1866 in the presence of $C_{12}EO_8$ (1.8 mM), LM (1.8 mM) and TTAC (2 mM) were measured in ATPase assay buffer (25 mM HEPES, 150 mM NaCl, 10 mM $MgSO_4$, pH7.5 at 25°C). The buffer was filtered trough a 0.2 μm regenerated cellulose filter prior to use. Sav1866 (C = 0.8 μM) and lipid (C = 163.9 μM). Detergent was mixed with lipids 30 min before measurements to ensure complete solubilization. The blank sample contained *E. coli* polar lipid extract: POPC in 1:3 (w/w) and detergent in the same concentration as in samples containing Sav1866. The path-length of the cuvette was 0.2 mm and the band width was adjusted to 2 nm. The spectra were recorded from 190 nm to 260 nm.

Data Evaluation. The vanadate and the ATP dependence of the ATPase activity was fitted to the Hill equation according to:

$$y = \frac{1}{1 + (x / IC_{50})^n} \tag{1}$$

where y is the ATPase activity, x the concentration of the added molecule, IC_{50} the concentration of half maximum inhibition/activation and n the Hill coefficient describing cooperativity of the binding process.

Evaluation of the ATPase activity curves. Kinetic model. The ATPase activity profiles of Sav1866 were evaluated using a modified Michaelis-Menten equation as proposed by (Litman and others 1997). The same compound which activates the transporter by interacting with the first binding site inhibits the ATPase activity, at higher concentration, by interacting with the second binding site.

$$V_S = \frac{K_1 K_2 V_0 + K_2 V_1 C_S + V_2 C_S^2}{K_1 K_2 + K_2 C_S + C_S^2} \tag{1}$$

where K_1 is the concentration of half-maximum activation, K_2 the concentration of half-maximum inhibition, V_0 basal velocity, V_1 activation velocity, V_2 inhibition velocity, C_S aqueous substrate concentration.

Results and Discussion

The Basal Turnover Number of Sav1866 in Lipid Vesicles and Mixed Micelles. In order to choose optimal protein concentration for the following experiments we first measured the basal ATPase activity of Sav1866 reconstituted into lipid vesicles as a function of the Sav1866 concentration, C_{Sav}. Measurements were performed in buffer I adjusted to pH 7.0 at 37°C. In the concentration range, C_{Sav} = 0.028 μM to C_{Sav} = 0.154 μM (i.e., 0.2 μg to 1.2 μg Sav1866 per 60 μl of reaction mixture) the ATPase activity increased linearly with the concentration, C_{Sav} (data not shown). For the following experiments Sav1866 was used at the concentrations, C_{Sav} = 0.028 μM or C_{Sav} = 0.114 μM.

Figure 1A, B shows the basal ATPase activity of Sav1866 (C_{Sav} = 0.114 μM) measured as a function of time in lipid vesicles and mixed lipid/$C_{12}E_8$ micelles in buffer I at pH 7.0 and T = 37°C. The Sav1866 ATPase in mixed micelles was measured in buffer I at pH 7.0 and T = 37°C and buffer II at pH 7.5 and T = 25°C (open circles). As seen in Figure 1A the basal ATPase activity as a function of time was linear up to 40 min for vesicles in buffer I (T = 37°C) and for mixed micelles in buffer II (T = 25°C).

The turnover number in mixed lipid/$C_{12}E_8$ micelles in buffer II at pH 7.5 and T = 25 °C was assessed as tn = 1 s^{-1}. At the temperature, T = 25°C the turnover number in mixed micelles remained constant over time (Figure 1B). The turnover number of Sav1866 in lipid vesicles at pH 7.0 and T = 37°C, calculated by taking into account the total protein concentration (i.e., assuming that all NBDs were exposed to the outside of the vesicles), was determined as tn = 1 s^{-1}. However, in contrast to micelles where all NBDs are accessible to ATP, not all molecules are oriented such that the NBDs are exposed to the extravesicular side of the membrane where ATP has access. For ButCD reconstituted into lipid bilayers 93% of all molecules were shown to expose the NBDs to the extravesicluar side of the membrane (Borths and others 2005b). This relatively high number was explained with the geometry of large NBDs. A similar arrangement of the NBDs was also assumed for Sav1866 (Dawson and Locher 2006). This is consistent with the relatively low activity increase upon addition of high concentrations of CHAPS to lipid vesicles containing Sav1866 which lead to the micellisation of the vesicles (see below) and to a concomitant exposure of all NBDs to ATP (Sharom and others 1993). The turnover number, tn, in lipid vesicles in buffer I at pH 7.0 and T = 37°C is therefore most likely 1

$s^{-1} < tn < 2\ s^{-1}$.

The ATPase activity of Sav1866 in mixed micelles in buffer I at pH 7 and T = 37°C was linear up to about 20 min only. In this range the number was determined as tn = 3.5 s^{-1} which is comparable to the turnover number of P-gp (tn = 3-5 s^{-1}) in MDR1-transfected mouse embryo fibroblasts (Aanismaa and Seelig 2007). After 30 min the ATPase activity of Sav1866 in mixed micelles decreased from 3.5 fold to 3 fold basal activity (~ 15 % decrease).

The decrease could be due either to the depletion of ATP or to competitive binding of ADP. Assuming that 3.5 ATP molecules (2.4 10^{-11} mol ATP/well) were hydrolysed per second at 37°C and that the NBDs of all Sav1866 molecules (6.86 10^{-12} mol Sav1866/well) were accessible only 24% of all available ATP molecules were consumed. We therefore concluded that the decrease in ATPase activity was rather due to an inhibition of ATP hydrolysis by ADP (i.e., product inhibition) than to a lack of ATP. This finding is consistent with the concentration of half-maximum activation by ATP and the concentration of half-maximum inhibition by ADP determined below (see Figure 3) (K_1 = 2.0 mM and K_2 = 2.2 mM (Table 1) as discus for Sav1866 in mixed micelles. These values can be considered as dissociation constants for ATP and ADP from the NBDs to a first approximation and are similar. Almost identical dissociation constants for ATP ($K_{d,\ ATP}$ = 2.12 mM) and ADP ($K_{d,\ ADP}$ = 2.107 mM) were also determined for MsbA reconstituted into *E. coli* lipids (Eckford and Sharom 2008). For P-gp (Liu and others 2000) (Kerr and others 2001) the dissociation constants for ATP ($K_{d,\ ATP}$ = 0. 280 mM) and ADP ($K_{d,\ ADP}$ = 0.330 mM) were about ten times lower than for Sav1866.

Figure 1

The Sav1866 ATPase Activity as a Function of the ATP Concentration. The ATPase activity of Sav1866 in lipid vesicles and mixed lipid/$C_{12}EO_8$ micelles was measured as a function of the ATP concentration (Fig. 2). Measurements were performed at pH 7.5 and T = 25 °C in the absence (C_{NaCl} = 0 mM) and presence of sodium chloride (C_{NaCl} = 150 mM). Under all four conditions the ATPase activity increased with increasing ATP concentration up to a maximum around 5 mM ATP and decreased again

at higher concentrations.

Considering the activating ATP concentration range only (C_{ATP} = 0 - 5 mM) data in Fig. 2 could be well fitted with the Hill equation (eq. 1). Data suggest a positive cooperativity for ATPase activity with a Hill coefficient in the range of 1.1 - 1.5. A similar positive cooperativity for the ATPase activity of isolated NBDs of HlyB wt was observed (Zaitseva, Jenewein et al. 2005). The maximum ATPase activity of Sav1866 in lipid vesicles was determined as V_{max}(ATP) = 547 ± 38 nmole mg^{-1} min^{-1} and V_{max}(ATP) = 511 ± 116 nmole mg^{-1} min^{-1} in the absence and presence (C_{NaCl} = 150 mM) of sodium chloride. The concentration of half-maximum activation induced by ATP in the absence and presence of sodium chloride was K_m(ATP) = 2.7 ± 0.3 mM and K_m(ATP) = 4.9 ± 1.9 mM, respectively, and thus varied only slightly with the sodium chloride concentration.

In mixed micelles the maximum ATPase activity of Sav1866, V_{max}(ATP), was also about 2 fold higher in the absence of sodium chloride (Tab. 2). The concentration of half-maximum activation by ATP was independent of the sodium chloride concentration K_m(ATP) = 0.9 ± 0.1 mM. The kinetic parameters are summarized in Tab 2.

Figure 2

Independent measurements of the ATPase activity as a function of decreasing extravesicular sodium chloride concentration were performed in Buffer I at 25 °C at a constant ATP concentration of (C_{ATP} = 2 mM) and are shown in Fig. 3. The intravesiclular ATP concentration was 150 mM. The highest ATPase activity was observed in the absence of salt. If the extravesicular sodium chloride concentration was lower the lipid vesicles were subjected to a slight osmotic swelling due to water influx which gives rise to a small decrease in the lateral membrane packing density (Nebel and others 1997). A decrease in the lateral membrane packing density is in principle consistent with an increase in the basal activity of ATP driven transporters (Aanismaa and others 2008). However, the maximum ATPase activity, V_{max}, also increased by a factor of two upon withdrawal of sodium chloride in mixed micelles where osmosis plays no role (see Figure 2). We therefore concluded that the activity reducing effect of sodium chloride is rather due to the direct effect of sodium chloride on the NBDs.

For comparison a similar measurement performed with in inside-out plasma membrane vesicles of mouse embryo fibroblast over-expressing P-gp (NIH-MDR1-G185) was included in Figure 3. As the plasma membrane includes Na/K pumps we used potassium chloride instead of sodium chloride. In the measured concentration range P-gp ATPase activity is barely changed with the extra-vesicular potassium chloride concentration. The arrows in Figure 3 indicate the monovalent salt concentrations used in the ATPase buffer II and I, respectively.

Figure 3

Inhibition of the Sav1866 ATPase Activity by Vanadte. Vanadate is a pentavalent phosphate analog which mimics the structure of the terminal or γ-phosphate of ATP and is often used to trap ABC-transporters in the post-hydrolysis state (Urbatsch and others 1995). Figure 4A shows the inhibition of the Sav1866 ATPase activity by vanadate in lipid vesicles and mixed lipid/$C_{12}E_8$ micelles in buffer II (C_{NaCl} = 150 mM) at pH 7.5 and 25 °C. Measurements were moreover performed at lower sodium chloride concentrations (C_{NaCl} = 50 mM) and in the absence of sodium chloride (C_{NaCl} = 0 mM)) but otherwise the same conditions.

In buffer II in the presence of sodium chloride (C_{NaCl} = 150 mM) the ATPase activity of Sav1866 in lipid vesicles was inhibited to 10% at a concentration of vanadate, $C_{VO_4^-}$ > 5mM. This is in agreement with previously reported data (Dawson and Locher 2006). The concentration of half-maximum inhibition of Sav1866 in lipid vesicles was determined using the Hill equation (eq. 1) as IC_{50} = 180 μM (at C_{NaCl} = 150 mM), IC_{50} = 90 μM (at C_{NaCl} = 50 mM) and IC_{50} = 50 μM (at C_{NaCl} = 0 mM). The concentration of half-maximum inhibition of Sav1866 in mixed micelles in the presence (C_{NaCl} =150 mM) and in the absence of sodium chloride was determined as IC_{50} = 9 μM. While vanadate inhibition of the ATPase in lipid vesicles was clearly dependent on the sodium chloride concentration, vanadate inhibition of the ATPase in mixed micelles was independent of sodium chloride. The concentrations of half-maximum inhibition by vanadate, IC_{50}, determined according to Hill are displayed as a function of the sodium chloride

concentration, C_{NaCl}, in Figure 3B. A linear increase in IC_{50} values with concentration was observed if Sav1866 was embedded in lipid vesicles. If Sav1866 was embedded in micelles the IC_{50} values remained constant at a low level. Figure 3C shows a plot of IC_{50} values as a function the turnover number which suggests that a limiting lower value of the concentrations of half-maximum inhibition, IC_{50}, for vanadate is reached at a turnover number, $nt \geq 1$. Inhibition by vanadate thus depends on the velocity of ATP hydrolysis.
For comparison the concentration of half-maximum inhibition of P-gp expressed in multidrug-resistant Chinese hamster ovary cells (CR1R12) was determined as IC_{50} = 9 μM (Urbatsch and others 1995). Vanadate inhibition was also measured for the related bacterial transporter MsbA and was lower if expressed in *E. coli* membranes than when reconstituted into liposomes (Eckford and Sharom). In isolated HlyB NBDs vanadate showed a dissociation constant of $K_i \sim 16$ μM (Benabdelhak and others 2005). Compared to other transporters the sensitivity of the ATPase activity of Sav1866 in lipid vesicles to vanadate was thus rather low.

Figure 4

Basal Sav1866 ATPase Activity as a Function of the pH. As seen in Figure 5 the pH dependence of the basal Sav1866 ATPase activity in lipid vesicles and mixed mixed lipid/$C_{12}E_8$ micelles was investigated in the range of pH 5.4 - pH 9 using three different buffer systems with the ionic conditions of buffer II at T = 25 °C. MES buffer (25 mM) was used for the range of pH 5.6 – pH 6.4, HEPES buffer (25 mM) for the range of pH 6.8 – pH 8.4 and Tris/HCl buffer (25 mM) in the range of pH 8.5 – pH 9. The ATPase activity of Sav1866 in lipid vesicles shows a maximum at pH 6.8 and decreases to negligibly low values below pH 5 and above pH 8.0. Data were fitted to a Gaussian peak distribution yielding an optimum for ATP hydrolysis at pH 6.7 and half maximum activity, V_{max} (50%) at pH 5.9 and pH 7.6. The full activity was thus reached in a very narrow pH range for Sav1866 reconstituted in lipid vesicles of the given composition. The pH dependence of the Sav1866 ATPase activity in mixed micelles was broader with a half maximum at pH 5.2 and pH 9.4, respectively.

Figure 5

A similarly steep pH-dependence of the ATPase activity as observed for Sav1866 in lipid vesicles was also reported for the transporter HlyB (Zaitseva and others 2005) and for the double mutant (D668E and Q701A) of isolated TAP1-NBDs (Ernst and others 2006). HylB and the double mutant of TAP1-NBDs (D668E/Q701H) showed a half-maximum activity at pH 6.1 and ~pH 5.0, and pH 8.2 and ~7.0, respectively, with an optimum at pH 7.0 and ~pH 6.0 respectively, which is similar to Sav1866. A similarly broad pH dependence as observe for Sav1866 in mixed micelles was also reported for P-gp in plasma membranes vesicles (half-maximum activity at pH 5.5 and pH 9.5) (Aanismaa and Seelig 2007; al-Shawi and Senior 1993).

The single mutant of the TAP1 NBDs (Q701H) also showed distinctly broader pH dependence (Ernst and others 2006; Zaitseva and others 2005). It is accepted that the histidine (H) residue from the H-loop interacts on one hand with the γ-phosphate form ATP and on the other hand with a glutamate (E) from Walker B. The interaction of histidine (H) and glutamate (E) residue is likely to become inefficient at low pH where all protonable groups are protonated as well as at high pH where all protonable groups are deprotonated. The different pH dependencies in the two mutants were suggested to arise from the fact that the former carries an aspartate (D) and the latter a glutamate (E) residue in the same position and that the different length of the amino acid side chains could alter the interaction with histidine (H). For closer inspection of the situation we aligned the amino acid residues known to be relevant for ATPase activity in the homodimers Sav1866 and HlyB, the heterodimer TAP1/2 and N- and C-terminal half of the monomer, P-gp to find potential differences. All transporters listed carry the typical catalytically important glutamate (E) in Walker B and histidine (H) in the H-loop except TAP1 and the single mutant of TAP1 (Q701H) (Figure 4). Because the catalytically relevant amino acids in Sav1866 and P-gp seem to be identical or at least very similar we suggest that the different pH dependences observed in Figure 2 are due to other factors. In the present case the membrane environment of the protein may also play a role.

Figure 6

The Detergent-Induced Transition between Lipid Vesicles and Mixed Micelles and the Concomitant Change of Sav1866 ATPase Activity. The influence of non-ionic (NM, DM, LM, TM and $C_{12}E_8$), cationic (TTAC and DTAC) and zwitter ionic (CHAPS) detergents on the ATPase activity of Sav1866 in lipid vesicles in buffer II at 25°C was studied in detail. We stimulated the ATPase activity as a function of the detergent concentration, starting at concentrations that were two to three orders of magnitude below the CMC up to concentrations well above the CMC. The activity profiles obtained with non-ionic and ionic detergents are displayed in Figure 7A and Figure 7B, respectively. The CMC (arrow) for each individual detergent is included in Figure 7. Thermodynamic parameters are summarized in Table 3.

Figure 7

Non-Ionic detergents stimulated Sav1866 ATPase activity up to 3 fold (Figure 7A). As seen in Figure 7A stimulation started at concentrations almost one order of magnitude below the CMC, which suggests a weak interaction of detergents with Sav1866. The interaction must however be weaker than for P-glycoprotein which showed the typical bell-shaped ATPase activity profiles with a concentration of half-maximum activation and a maximum activity determined as K_1 = 0.9 μM and V_{max} = 175 % for $C_{12}E_8$ in the range between the inverse of the air-water partition coefficient, $1/K_{aw}$ and the CMC of the detergent (Li-Blatter and others 2009).

Above the CMC Sav1866 ATPase activity still increased ~20% in the presence of tetradecyl-, dodecylmaltoside and $C_{12}E_8$, respectively, and stayed at a high fold value even exceeding 20 times CMC as seen for $C_{12}E_8$. At the CMC the lipid vesicles are solubilized and an increasing number of NBDs become accessible to ATP. Therefore the solubilization leads to an increase in the ATPase activity which was estimated to be less than a factor of two (Dawson). On the other hand the presence of high concentrations of nonyl- and decylmaltoside (above CMC) decreased the Sav1866 ATPase activity below basal activity. No typical bell-shaped ATPase activity curves as a function of concentration were observed as reported for other transporters (Aanismaa and Seelig

2007; Litman and others 1997). The carbon chain lengths (m = 9, 10) seem to be too short to stabilize the hydrophobic trans-membrane domains (TMDs) of Sav1866. The high increase of the Sav1866 ATPase activity of the detergents with higher hydrophobic anchors suggests an additional effect. The splay of the head groups of amphiphilies (detergents and lipids) in mixed micelles is larger than in lipid bilayers and the packing density of the membrane environment is lower which has been shown to lower the activation energy of membrane embedded ATP driven compounds ().

Charged Detergents. Cationic detergents (DTAC and TTAC, respectively) increased the Sav1866 ATPase activity at detergent concentrations clearly below the CMC (~two orders of magnitude) suggesting that these detergents directly interacted with Sav1866. At concentration exceeding the CMC the ATPase activity was not detectable anymore (TTAC ~ 1 mM and DTAC ~ 5 mM, respectively). We conclude that TTAC as well as DTAC are not able to stabilize the membrane protein in mixed micellar form. Structural properties of Sav1866 were investigated in mixed micelles containing $C_{12}E_8$, LM or TTAC, respectively (see Figure 8).

The ATPase activity profile for P-gp stimulated with the two cationic compounds DTAC and TTAC is shown in Figure 8. The ATPase activity curve looks very similar to Sav1866 see Table 4 for detailed evaluation). At high detergents concentration the ATPase activity goes towards zero, suggesting denaturation of the transporter by the detergents. Sav1866 and P-gp data were evaluated with the modified Michaelis-Menten equation and were summarized in Table 4.

The zwitterionic detergent CHAPS however seems not to interact with Sav1866. A slight increase in Sav1866 ATPase activity (~20%) above the CMC of CHAPS is again due to the solubilization of lipid vesicles and increased amount of active Sav1866 molecules. However CHAPS can not stabilize the protein well since the ATPase activity goes under basal ATPase at high CHAPS concentration (similar to NM).

The typical bell shaped activity profile curves are expected between the inverse of the air water partition coefficient, K_{aw}, and the CMC, as compounds interact from the membrane with the transporter. At lower concentration than the inverse of K_{aw} the substance is not surface active and therefore not present in the membrane.

Effect of Detergents on the Structure of Sav1866 Monitored by Circular Dichroism Measurements (CD-measurements). In order to test whether detergents change the secondary structure of Sav1866 the CD-spectrum of Sav1866 was recorded in the presence of LM (1.8 mM), $C_{12}E_8$ (1.8 mM) and TTAC (2 mM) (Figure 9).

Figure 9

The CD-spectra of Sav1866 in lipid vesicles had low quality due to the light scattering caused by the broad size distribution of 400 nm lipid vesicles. Note that reference spectra can not easily be subtracted as 400 nm vesicles have a broad size distribution and therefore complex scattering properties. In the presence of LM (1.8 mM, shown as open down-triangles) and in the presence of $C_{12}E_8$ (1.8 mM, shown as open up-trinagles) the secondary structure of Sav1866 is almost identical (~66-68% α-helix, ~3-6 % β-sheet, 16-24 % random coil and β-turn 4.5-11.5%). The predicted secondary structure derived from the crystal structure according to protein data bank (PDB) was 63–67 % α-helix and 9 % β-sheet, in good agreement with present observations.

In TTAC (2 mM, shown closed circles) solution the secondary structure of Sav1866 is a clearly shifted to more random coil (~48 % α-helix, ~21 % β-sheet, 31 % random coil, β-turn 0%). However the effect of TTAC on the secondary structure is rather small, but the ATPase activity at the given concentration is completely abolished. The change in the α-helical structure suggested a distortion of the TMDs by TTAC.

Table 1

Concentration of Sav1866 and lipid.

Preparation		SDS-page	BCA (vesicles)	BCA (5% SDS)	BCA (C12E8)	Edelhoch (C12E8)	Lipid	Lipid/protein ratio
1	mg/ml	6-8	2.08 ± 0.15	1.81 ± 0.5	1.84 ± 0.2+ 1.7 ± 0.22*	1.97+	4	314:1
	uM		16	14	14.2+ 13.1*	15.2	4400	
2	mg/ml	5	-	-	2.69 ± 0.16*	3.9* 6.44*	3.7	194:1
	uM		-	-	20.8*	30.3* 49.7*	4000	

+ measured in 2.2 mM $C_{12}E_8$

* measured in 1.9 mM $C_{12}E_8$

Table 2

	Sav1866 in	pH	NaCl (mM)	T °C	tn (Hill) (s^{-1})	tn (MM) (s^{-1})	V_{max} (Hill) (nmol/mg*min^{-1})	K (Hill) (mM)	n (Hill)	V_{max} (MM) (nmol/mg*min^{-1})	K_1 (mM)	K_2 (mM)	IC_{50} Vanadate (mM)
II	vesicles	7	50	37	1[A]								
I	vesicles	7.5	0	25	1.2	1.9	547±38	2.7±0.3	1.3±0.1	900	5.0	7.6	0.05
I	vesicles	7.5	50	25									0.09
I	Vesicles	7.5	150	25	1.1	1.5	511±116	4.9±1.9	1.1±0.1	690	6.7	8.6	0.18
II	mix. micelles	7	50	37	3.5[A]								
I	mix. micelles	7.5	0	25	2.7	5.5	1229±30	0.87±0.04	1.5±0.1	2530	2.4	5.0	0.009
I	mix. micelles	7.5	50	25									
I	mix. micelles	7.5	150	25	1.3	3.1	592±9	0.98±0.03	1.5±0.1	1410	3.5	5.0	0.009

[A] Taken from time dependence measurements

Table 3

Thermodynamic parameters of the detergents used in the study.

Compound	MW (g/mol)	CMC (SAM)[f] mM	CMC (ITC)[g] mM	K_{aw}[†] (M^{-1})	A_D[†] (m^2)	K_{app} mM^{-1}	c_d^{wsat} mM	R_b^{sat}
TM	-	0.01[h]	-	-	-	-	-	-
LM	510.6	0.17	0.19	9.76E5	5.5E-19	3.42[a,b]	0.32	0.2
DM	482.6	2.48	-	1.55E5	6.86E-19	0.25	2.7	0.45[b,e]
NM	468.5	4	6.54	4.39E4	6.53E-19	-	-	-
$C_{12}E_8$	539	-	0.08	2.2E6	5.8E-19	4[a]	0.5	0.33[c,d]
DTAC	263.9	7.15	5.25	1.54E4	-	-	-	-
TTAC	-	0.7	-	2.11E5	-	-	-	-
CHAPS	615	4.9	-	7.83E4	9.3E-19	0.6[a]	-	-

a) LM: 5 (mM^{-1}), $C_{12}E_8$ 6 (mM^{-1}), Heerklotz, H., and J. Seelig. 2000. Correlation of membrane/water partition coefficients of detergents with the critical micelle concentration. Biophys J 78:2435-2440.

b) LM: 8-19 (mM^{-1}) de la Maza, A., and J. L. Parra. 1997. Solubilizing effects caused by the nonionic surfactant dodecylmaltoside in phosphatidylcholine liposomes. Biophys J 72:1668-

c) H Heerklotz et al. (1996)

d) H Heerklotz et al. (1997)

e) Heerklotz, H. 2001. Membrane stress and permeabilization induced by asymmetric incorporation of compounds. Biophys J 81:184-195.

f) this work; 25 mM Tris/HCl, 114 mM NaCl, pH 7.4 at RT

g) this work; 25 mM HEPES, 150 mM NaCl, 10 mM $MgSO_4$, pH7.5 at 25°

h) Anatrace catalogue

Table 4

Parameters derived from figure 7 and 8, respectively. The DTAC and TTAC induced ATPase activity profiles of Sav1866 and P-gp were fitted to the modified Michaelis-Menten equation described in methods.

		TTAC		DTAC	
		Sav1866	P-gp	Sav1866	P-gp
K_1	(M)	49×10^{-6}	30×10^{-6}	479×10^{-6}	316×10^{-6}
K_2	(M)	75×10^{-6}	63×10^{-6}	674×10^{-6}	971×10^{-6}
V_1	(fold)	3.02	2.96	3.3	4.59

Legends to Figures

Figure 1. *The Turn-Over Number of Sav1866 under Different Conditions.*
A: Time dependence of Sav1866 ATPase activity was measured in lipid vesicles (open triangles) and mixed lipid/ $C_{12}E_8$ micelles ($C_{12}E_8$ 1.8 mM) containing (filled circles) in buffer I (25 mM HEPES, 50 mM NaCl, 2.5 mM $MgSO_4$, 3 mM ATP) adjusted to pH 7.0 at 37°C and in mixed micelles in buffer II (25 mM HEPES, 150 mM NaCl, 7 mM ATP, 10 mM $MgSO_4$) adjusted to pH 7.5 at 25°C (open circles). **B:** The turnover numbers were calculated from data in Figure 1A. Note that in lipid vesicles only half of the NBDs are accessible to ATP and turnover number measured in lipid vesicles were multiplied by a factor of two (see text).

Figure 2. *ATP Dependence of Sav1866 with and without NaCl.*
The basal ATPase activity in lipid vesicles (triangles) and mixed lipid/$C_{12}E_8$ micelles ($C_{12}E_8$ 1.8 mM) (circles) is shown as a function of the ATP concentration. Measurements were performed in the presence (open symbols) and absence of sodium chloride (150 mM) (closed symbols). The measurements were performed in buffer II (25 mM HEPES, with or without 150 mM NaCl, 7 mM ATP, 10 mM $MgSO_4$, pH 7.5) at 25°C. The line represents curve fit according to equation (1).

Figure 3. *Effect of NaCl on Sav1866 ATPase Activity in Lipid Vesicles.*
The effect of the extra-vesicular salt concentration was measured in buffer II (25 mM HEPES, 150 mM NaCl, 7 mM ATP, 10 mM $MgSO_4$, pH 7.5) at 25°C. The data is normalized to the basal Sav1866 ATPase activity in the presence of 150 mM NaCl. The intra-vesicular sodium chloride concentration was 150 mM.

Figure 4 A-D. *Vanadate Inhibition of Sav1866 ATPase Activity.*
The vanadate sensitivity of Sav1866 in lipid vesicles (triangles) was measured in buffer II (25 mM HEPES, 10 mM $MgSO_4$, 7 mM ATP) at 25°C with different amount of sodium chloride present in suspension (150 mM NaCl (open down-triangles), 50 mM NaCl (filled up-triangles) and 0 mM NaCl (open up-triangles), respectively). The vanadate sensitivity

of Sav1866 was further measured in mixed lipid/$C_{12}E_8$ micelles (circles) in buffer II (25 mM HEPES, 10 mM $MgSO_4$, 7 mM ATP) at 25°C. The concentration of half maximum inhibition of the ATPase activity of Sav1866 in lipid vesicles containing 0 mM NaCl, IC_{50} = 50 μM, 50 mM NaCl, IC_{50} = 90 μM, 0 mM NaCl IC_{50} = 180 μM, and in mixed lipid/$C_{12}E_8$ micelles, IC_{50} = 9 μM, respectively. NaCl present shown as average of two measurements at each NaCl concentration) and in mixed lipid/$C_{12}E_8$ micelles (buffer II at 25 °C, average of three different measurements) as a function of the vanadate concentration.

Figure 5. *Effect of pH on the Basal Sav1866 ATPase Activity*.

The basal ATPase activity of Sav1866 in lipid vesicles (triangles) and mixed lipid/$C_{12}E_8$ micelles (circles) was measured in the pH the range pH 5.6 – pH 9, using MES buffer (25 mM) in the range pH 5.6 – 6.4, HEPES buffer (25 mM) in the range pH 6.8 – 8.4 and Tris/HCl (25 mM) in the pH range of 8.5 - 9 using a colorimetric assay. The measurements were performed in buffer II (25 mM HEPES, 150 mM NaCl, 7 mM ATP, 10 mM $MgSO_4$) at 25°C.

Figure 2 shows the average of five different measurements in lipid vesicles and the average of two different measurements in mixed lipid/$C_{12}E_8$ micelles shown as relative values. Different protein batches were used showing different ATPase activities. Therefore the ATPase activity of each individual measurement was normalized to the pH where the highest ATPase activity was observed.

Figure 6. *Sequence Alignment of Sav1866 with other ABC-transporters.* Figure 3 shows the sequence alignment of SAV1866 with other ABC-transporters. The important catalytically active amino acids in Walker B and H-loop motif are shown as bold letters.

Figure 7A, B. *Effect of Non-Charged Detergents on Sav1866 ATPase Activity.*

The effect of various detergents on the ATPase activity of Sav1866 (0.114 μM) in lipid vesicles was measured in buffer II (25 mM HEPES, 150 mM NaCl, 7 mM ATP, 10 mM $MgSO_4$, pH 7.5) at 25°C. The detergents used in A were TM (open circles), LM (open star), DM (open down-triangle), NM (open up-triangle) and $C_{12}E_8$ (filled circles). The

CMC is indicated with arrows for each individual detergent. B shows the ATPase activity measurements of TTAC (open up-triangles) and DTAC (filled circles) fitted to the modified Michaelis-Menten equation (2). The zwitterionic detergents CHAPS is shown as closed up-triangles.

Figure 8. *Effect of Charged Detergents on the ATPase Activity P-Glycoprotein in Plasma Membrane Vesicles.* The ATPase activity of P-gp induced by TTAC (open up-triangles) and DTAC (filled circles) was measured in Tris/HCl (25 mM) including 50 mM KCl, 3 mM ATP, 2.5 mM MgSO4, 3 mM DTT, 0.5 mM EGTA, 2 mM ouabain, and 3 mM sodium azide. The ATPase activity measurements of TTAC and DTAC were fitted to the modified Michaelis-Menten equation (2).

Figure 9. *CD-Spectra of Sav1866 in Mixed Micelles*.
CD-spectra of Sav1866 in the presence of $C_{12}E_8$ (1.8 mM, filled circles), LM (1.8 mM, open stars), and TTAC (2 mM, open up-triangles) were measured in buffer II (25 mM HEPES, 150 mM NaCl, 7 mM ATP, 10 mM $MgSO_4$, pH 7.5) at 25°C with 0.8 μM Sav1866 and 163.9 μM lipid present. Baseline measurements without Sav1866 present were recorded and were subtracted.

References

Aanismaa P, Gatlik-Landwojtowicz E, Seelig A. 2008. P-glycoprotein senses its substrates and the lateral membrane packing density: consequences for the catalytic cycle. Biochemistry 47(38):10197-207.

Aanismaa P, Seelig A. 2007. P-Glycoprotein kinetics measured in plasma membrane vesicles and living cells. Biochemistry 46(11):3394-404.

Aller SG, Yu J, Ward A, Weng Y, Chittaboina S, Zhuo R, Harrell PM, Trinh YT, Zhang Q, Urbatsch IL and others. 2009. Structure of P-glycoprotein reveals a molecular basis for poly-specific drug binding. Science 323(5922):1718-22.

al-Shawi MK, Senior AE. 1993. Characterization of the adenosine triphosphatase activity of Chinese hamster P-glycoprotein. J Biol Chem 268(6):4197-206.

Benabdelhak H, Schmitt L, Horn C, Jumel K, Blight MA, Holland IB. 2005. Positive co-operative activity and dimerization of the isolated ABC ATPase domain of HlyB from Escherichia coli. Biochem J 386(Pt 3):489-95.

Borths EL, Poolman B, Hvorup RN, Locher KP, Rees DC. 2005a. In vitro functional characterization of BtuCD-F, the Escherichia coli ABC transporter for vitamin B12 uptake. Biochemistry 44(49):16301-9.

Borths EL, Poolman B, Hvorup RN, Locher KP, Rees DC. 2005b. In Vitro Functional Characterization of BtuCD-F, the Escherichia coli ABC Transporter for Vitamin B12 Uptakeâ€ Biochemistry 44(49):16301-16309.

Davidson AL, Laghaeian SS, Mannering DE. 1996. The Maltose Transport System of Escherichia coli Displays Positive Cooperativity in ATP Hydrolysis
10.1074/jbc.271.9.4858. J. Biol. Chem. 271(9):4858-4863.

Dawson RJP, Locher KP. 2006. Structure of a bacterial multidrug ABC transporter. 443(7108):180-185.

Eckford PD, Sharom FJ. The reconstituted Escherichia coli MsbA protein displays lipid flippase activity. Biochem J.

Eckford PD, Sharom FJ. 2008. Functional characterization of Escherichia coli MsbA: interaction with nucleotides and substrates. J Biol Chem 283(19):12840-50.

Edelhoch H. 1967. Spectroscopic determination of tryptophan and tyrosine in proteins. Biochemistry 6(7):1948-54.

Ernst R, Koch J, Horn C, Tampe R, Schmitt L. 2006. Engineering ATPase activity in the isolated ABC cassette of human TAP1. J Biol Chem 281(37):27471-80.

Federici L, Woebking B, Velamakanni S, Shilling RA, Luisi B, van Veen HW. 2007. New structure model for the ATP-binding cassette multidrug transporter LmrA. Biochemical Pharmacology 74(5):672-678.

Fischer H, Gottschlich R, Seelig A. 1998. Blood-brain barrier permeation: molecular parameters governing passive diffusion. J Membr Biol 165(3):201-11.

Gerebtzoff G, Li-Blatter X, Fischer H, Frentzel A, Seelig A. 2004. Halogenation of drugs enhances membrane binding and permeation. Chembiochem 5(5):676-84.

Heerklotz H, Seelig J. 2000. Correlation of Membrane/Water Partition Coefficients of Detergents with the Critical Micelle Concentration. 78(5):2435-2440.

Itaya K, Ui M. 1966. A new micromethod for the colorimetric determination of inorganic phosphate. Clin Chim Acta 14(3):361-6.

Kerr KM, Sauna ZE, Ambudkar SV. 2001. Correlation between steady-state ATP hydrolysis and vanadate-induced ADP trapping in Human P-glycoprotein.

Evidence for ADP release as the rate-limiting step in the catalytic cycle and its modulation by substrates. J Biol Chem 276(12):8657-64.
Kresheck GC. 1998. A Calorimetric Determination of the Standard Enthalpy and Heat Capacity Changes that Accompany Micelle Formation for Four Long Chain Alkyldimethylphosphine Oxides in H2O and D2O Solution from 15 to 79 Â°C. Journal of the American Chemical Society 120(42):10964-10969.
Kresheck GC, Hargraves WA. 1974. Thermometric titration studies of the effect of head group, chain length, solvent, and temperature on the thermodynamics of Micelle formation. Journal of Colloid and Interface Science 48(3):481-493.
Li-Blatter X, Nervi P, Seelig A. 2009. Detergents as intrinsic P-glycoprotein substrates and inhibitors. Biochimica et Biophysica Acta (BBA) - Biomembranes
Includes Special Section: Cardiolipin 1788(10):2335-2344.
Litman T, Zeuthen T, Skovsgaard T, Stein WD. 1997. Structure-activity relationships of P-glycoprotein interacting drugs: kinetic characterization of their effects on ATPase activity. Biochim Biophys Acta 1361(2):159-68.
Liu R, Siemiarczuk A, Sharom FJ. 2000. Intrinsic fluorescence of the P-glycoprotein multidrug transporter: sensitivity of tryptophan residues to binding of drugs and nucleotides. Biochemistry 39(48):14927-38.
Nebel S, Ganz P, Seelig J. 1997. Heat changes in lipid membranes under sudden osmotic stress. Biochemistry 36(10):2853-9.
Oancea G, O'Mara ML, Bennett WF, Tieleman DP, Abele R, Tampe R. 2009. Structural arrangement of the transmission interface in the antigen ABC transport complex TAP. Proc Natl Acad Sci U S A 106(14):5551-6.
O'Mara ML, Tieleman DP. 2007. P-glycoprotein models of the apo and ATP-bound states based on homology with Sav1866 and MalK. FEBS Letters 581(22):4217-4222.
Pleban K, Macchiarulo A, Costantino G, Pellicciari R, Chiba P, Ecker GF. 2004. Homology model of the multidrug transporter LmrA from Lactococcus lactis. Bioorganic & Medicinal Chemistry Letters 14(23):5823-5826.
Reyes CL, Ward A, Yu J, Chang G. 2006. The structures of MsbA: Insight into ABC transporter-mediated multidrug efflux. FEBS Letters
ABC Transporters 580(4):1042-1048.
Sharom FJ, Yu X, Doige CA. 1993. Functional reconstitution of drug transport and ATPase activity in proteoliposomes containing partially purified P-glycoprotein. J Biol Chem 268(32):24197-202.
Urbatsch IL, Sankaran B, Weber J, Senior AE. 1995. P-glycoprotein is stably inhibited by vanadate-induced trapping of nucleotide at a single catalytic site. J Biol Chem 270(33):19383-90.
van Veen HW, Venema K, Bolhuis H, Oussenko I, Kok J, Poolman B, Driessen AJ, Konings WN. 1996. Multidrug resistance mediated by a bacterial homolog of the human multidrug transporter MDR1. Proc Natl Acad Sci U S A 93(20):10668-72.
Zaitseva J, Jenewein S, Wiedenmann A, Benabdelhak H, Holland IB, Schmitt L. 2005. Functional Characterization and ATP-Induced Dimerization of the Isolated ABC-Domain of the Haemolysin B Transporterâ€ Biochemistry 44(28):9680-9690.

Figures

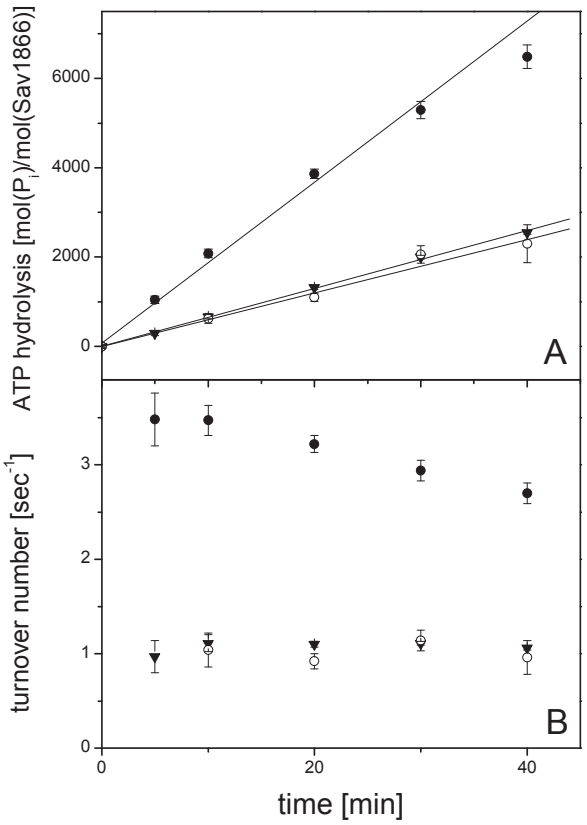

Figure 1

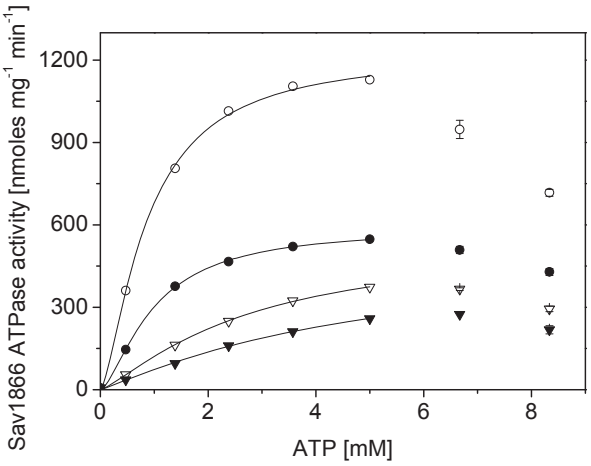
Sav1866 ATPase activity [nmoles mg-1 min-1]
1200
900
600
300
0
0
2
4
6
8
ATP [mM]

Figure 2

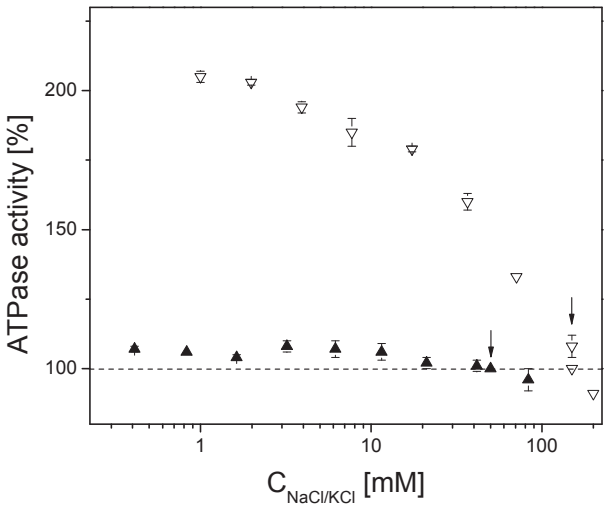

Figure 3

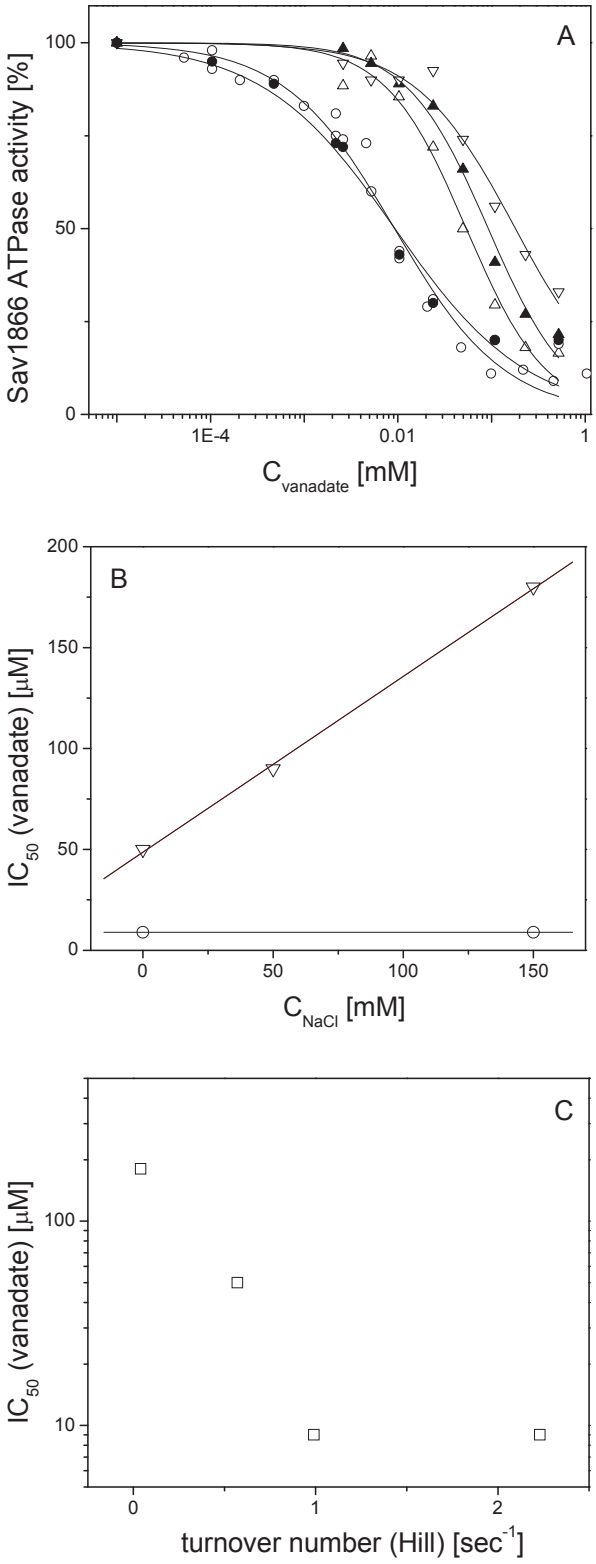
A
Sav1866 ATPase activity [%]
100
50
0
1E-4
0.01
1
C vanadate [mM]
B
IC50 (vanadate) [µM]
200
150
100
50
0
0
50
100
150
C NaCl [mM]
C
IC50 (vanadate) [µM]
100
10
0
1
2
turnover number (Hill) [sec-1]

Figure 4A, B, C

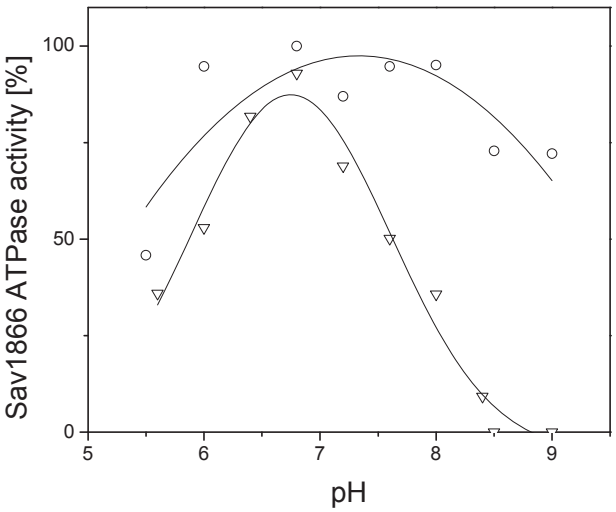

Figure 5

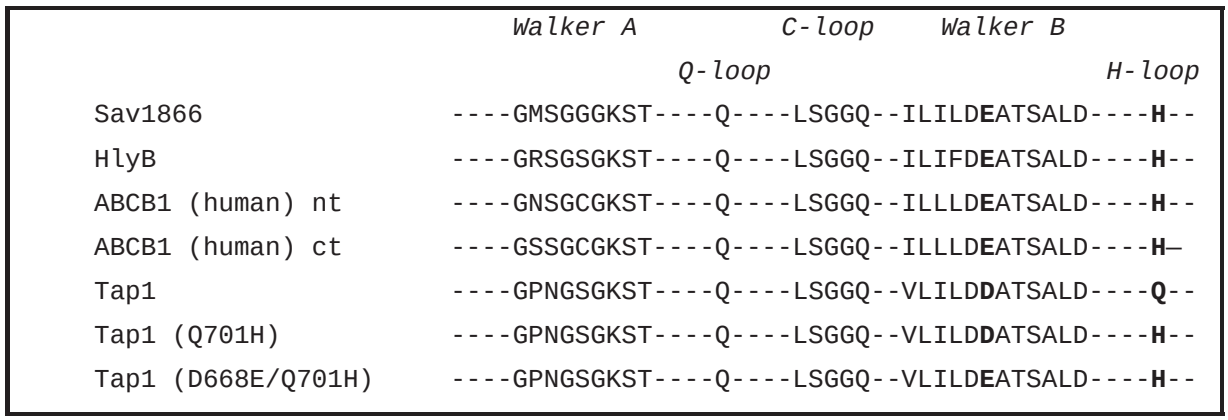
Walker A
C-loop
Walker B
Q-loop
H-loop
Sav1866 ----GMSGGGKST----Q----LSGGQ--ILILDEATSALD----H--
HlyB ----GRSGSGKST----Q----LSGGQ--ILIFDEATSALD----H--
ABCB1 (human) nt ----GNSGCGKST----Q----LSGGQ--ILLLDEATSALD----H--
ABCB1 (human) ct ----GSSGCGKST----Q----LSGGQ--ILLLDEATSALD----H—
Tap1 ----GPNGSGKST----Q----LSGGQ--VLILDDATSALD----Q--
Tap1 (Q701H) ----GPNGSGKST----Q----LSGGQ--VLILDDATSALD----H--
Tap1 (D668E/Q701H) ----GPNGSGKST----Q----LSGGQ--VLILDEATSALD----H--

Figure 6

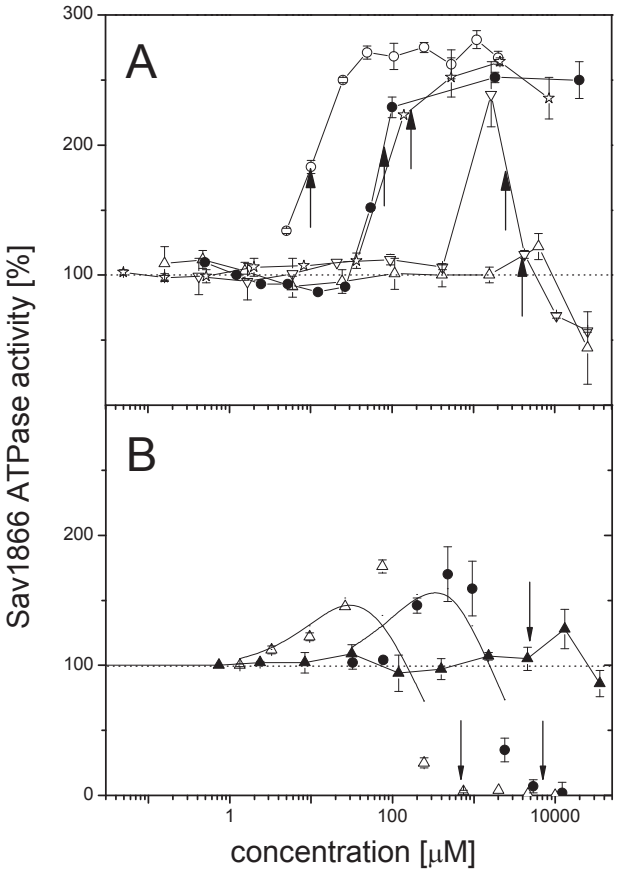
A
B
300
200
100
200
100
0
1
100
10000
Sav1866 ATPase activity [%]
concentration [μM]

Figure 7

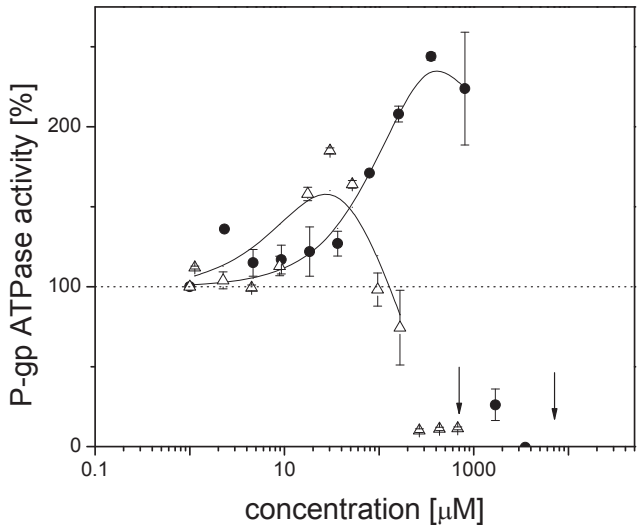

Figure 8

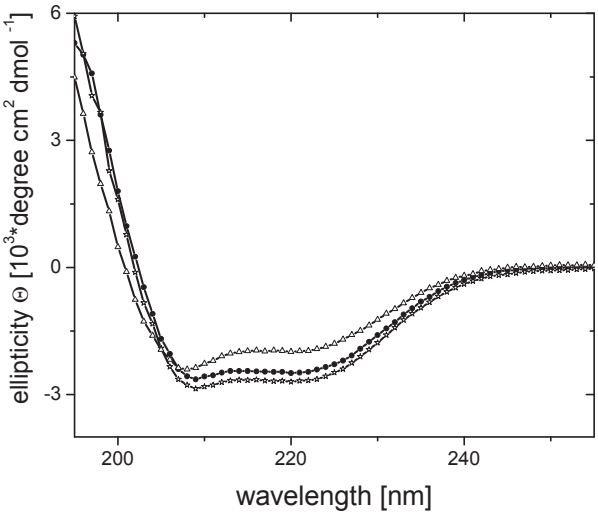
6
3
0
-3
200
220
240
wavelength [nm]
ellipticity Θ [10^3*degree cm^2 dmol^-1]

Figure 9

5 Sav1866: Multidrug Transporter or Lipid Flipase?

5.1 Summary

Sav1866 is a homo-dimeric ABC-transporter from *Staphylococcus aureus* and the structure could be solved to high resolution. Sav1866 was shown to be involved in multidrug transport similar to the eukaryotic homologue P-glycoprotein (P-gp). Here we extended the search for possible substrates for Sav1866 and found that the ATPase activity of Sav1866 was generally activated upon addition of cationic compounds and was inhibited by the addition of neutral or anionic compounds. We tested the ATPase activity of Sav1866 under the same conditions as we tested P-gp previously and found that different substrates induced different ATPase activity profiles. Progesterone showed inhibition of the ATPase activity of Sav1866 but stimulated the ATPase activity of P-gp, Hoechst33342 activated the ATPase activity of Sav1866 but inhibited the ATPase activity of P-gp to mention two representative compounds. Sav1866 can bind structurally unrelated compounds according to the same principles as P-gp. However, it binds them with a different affinity than P-gp. We calculated the free energy per H-bond acceptor pattern and found that the free energy from lipid to the transporter is slightly lower than observed for P-gp. Further we found that the Sav1866 ATPase activity is stimulated upon addition of an intrinsic double cationic charged lipid, lysyl-DPPG. Lysyl-DPPG is asymmetrically distributed across the lipid bilayer of *Satphylococcus aureus*. Sav1866 may be involved in the transport of the lipid across the membrane.

5.2 Manuscript

Sav1866: Multidrug Transporter or Lipid Flipase?

Päivi Äänismaa+, Andreas Beck+, Roger Dawson, Kaspar Locher and Anna Seelig*

+Both authors have equally contributed

Biozentrum, University of Basel, Div. of Biophysical Chemistry, Klingelbergstr. 50/70, CH-4056 Basel, Switzerland

*To whom correspondence should be addressed:

Tel. +41-61-267 22 06, Fax. +41-61-267 21 89, e-mail: anna.seelig@unibas.ch

Supported by the Swiss National Science Foundation Grant #

Introduction

The ATP binding cassette transporter Sav1866 from *Staphylococcus aureus* is a half-transporter with an N-terminal membrane domain followed by a nucleotide binding domain similar to LmrA from *Lactococcus lactis* (Federici and others 2007; Pleban and others 2004; van Veen and others 1996). Sav1866 has been crystallized to high resolution in the dimeric, nucleotide bound form (Dawson and Locher 2006). Due to the homology with ABCB1 (P-gp) Sav1866 was thought to be involved in multi-drug resistance. However, so far little is known on the endogenous function of this transporter. Expressed in the gram-positive bacterium *Lactococcus lactis* Sav1866 displayed a Hoechst33342-, verapamil-, tetraphenylphosphonium-, and vinblastine-stimulated ATPase activity (Velamakanni and others 2008). An extended search for Sav1866 substrates revealed that the ATPase activity of Sav1866 is stimulated by compounds with one cationic charge such as promazine and even more efficiently by compounds with two cationic charges such as Hoechst33342. The analysis revealed that Sav1866 is susceptible to hydrogen bond acceptor groups in substrates as shown previously for P-gp (Gatlik-Landwojtowicz and others 2006; Seelig 1998). Knowledge of the characteristics of Sav1866 substrates allowed us to search for possible endogenous substrates.

Here we have investigated the endogenous lysyl phosphatidyl glycerol (L-PG) that arises from estrification of PG with L-lysine (Short and White 1971). The positively charged L-PG accounts for up to 38% of the *Staphylococcus aureus* membrane lipids, whereas the other phospholipids (PG and DPG) are negatively charged. L-PG synthesis has significant impact on membrane surface charge and interactions with cationic antimicrobial peptides. The *mprF* mutant that no loner produces the unusual L-PG lipid was much more susceptible to a broad variety of cationic antimicrobial peptides whereas the neutral gramicidin D was equally active toward wild-type and *mprF* mutant (Kristian and others 2003). It remains to be determined whether *mprF* encodes the as yet unidentified L-PG synthase or whether it is involved in some other essential aspect of L-PG biosynthesis.

How the newly synthesized lipids are moved across the bacterial membrane to the extracellular side remained unclear. Due to the highly charged lysyl head group passive

flip-flop is energetically very unfavourable and active transport is therefore required. Whether other lipid translocators like energy-dependent flippases or energy-independent scramblases are responsible for transport is not clear.

We reconstituted Sav1866 into lipid vesicles containing *E.coli* polar lipid extract/egg yolk PC (3:1 w %). First, we investigated the substrate-induced ATPase activity of Sav1866 by means of a colorimetric phosphate release assay and compared the ATPase activity of Sav1866 with that of P-gp. Second, we demonstrated that lysyl-DPPG activated the ATPase activity of Sav1866 when provided in vesicular or mixed micellar form together with CHAPS. We have shown that CHAPS does not lead to changes in the ATPase activity of SAV1866 below the critical micellar concentration (CMC).

We found that usually positively charged compounds activated the ATPase activity in a concentration dependent manner, and further showed that neutral and negatively charged compounds decreased the ATPase activity of Sav1866. The results are in qualitative agreement with previous published results, showed however verapamil- and Hoechst33342-stimulated ATPase activation in a different concentration range (Velamakanni and others 2008). The concentration of half maximal ATPase activity, K_1, of P-glycoprotein for various substances was found to be highly different from system to system. K_1 values of verapamil are reported from 1 μM (Aanismaa and Seelig 2007) to 62 μM (Omote and Al-Shawi 2002). Here we found K_1 values for verapamil in the order of 130 μM whereas previous finding was ~ 10 μM (Velamakanni and others 2008). For Hoechst33342 the difference was bigger, however Hoechst33342 has more charges than verapamil and therefore the incorporation behaviour is more affected by conditions and membranes used.

Materials

Proteoliposomes. Purified Sav1866 was reconstituted into lipid vesicles (400 nm) composed of egg yolk PC and *E.coli* polar lipid extract (1:3 w/w). (See ref. (Dawson and Locher 2006)) for detailed protocol. *E.coli* polar lipid extract contains phosphatidylethanoamine, phosphatidylglycerol and cardiolipin (67 : 23.2 : 9.8 w-%). Proteoliposomes were suspended either in 25 mM HEPES, pH 7.5 (1st batch) or in 25

mM Tris/HCl (2nd batch) containing 150 mM NaCl.

Compound. Progesterone, promazine/HCl, (R/S)-verapamil/HCl, Methicillin sodium salt monohydrate were obtained from Sigma-Aldrich (Steinheim, Germany), and Hoechst 33342 were from Fluka (Buchs, Switzerland). 3-[(3-Cholamidopropyl)dimethylammonio]-1-propanesulfonate (CHAPS) was purchased from Sigma. Lysyl-DPPG (1,2-dipalmitoyl-sn-glycero-3-[phospho-rac-(3-lysyl(1-glycerol))] (chloride salt)), E.Coli polar lipid extract, POPC were obtained from Avanti polar lipids (Alabaster, Alabama, USA). BCA, protein assay reagents were from Pierce (Rockford, IL) and Bovine serum album, BSA, from Sigma. All other chemicals were from Sigma or Merck.

Chemical Structures of Studied Compounds (in alphabetical order). Possible hydrogen bond acceptor patterns are show as dotted circles. Quaternary ammonium groups are highlighted with dotted squares.

Chlorpromazine, EU_H 2

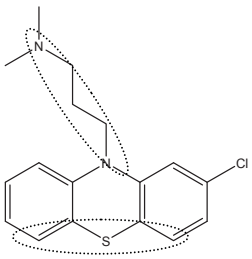

Hoechst 33342, EU_H 3

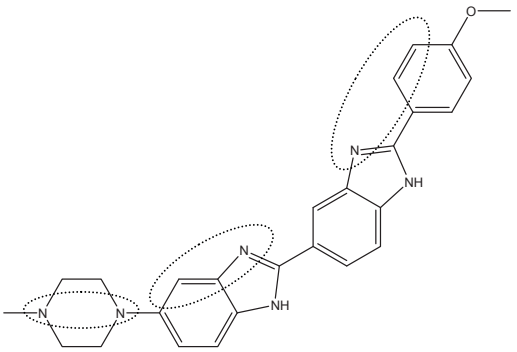

Penicillin G, EU_H 5

Progesterone, EU_H 1.5

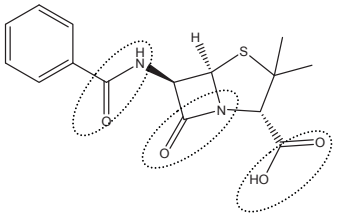

Promazine, EU_H 2

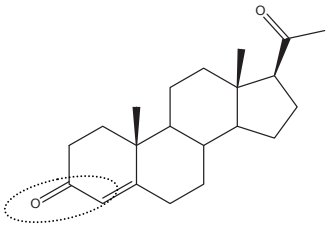

R/S-verapamil, EU_H 5

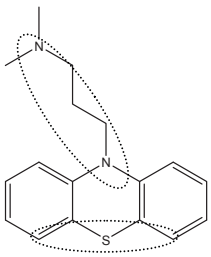

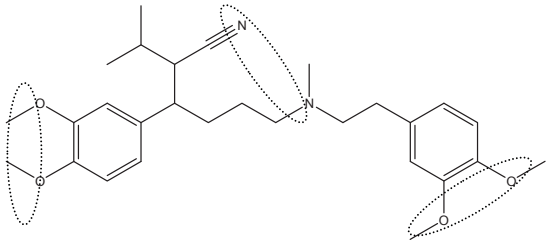

Lysyl-DPPG, EU_H 10

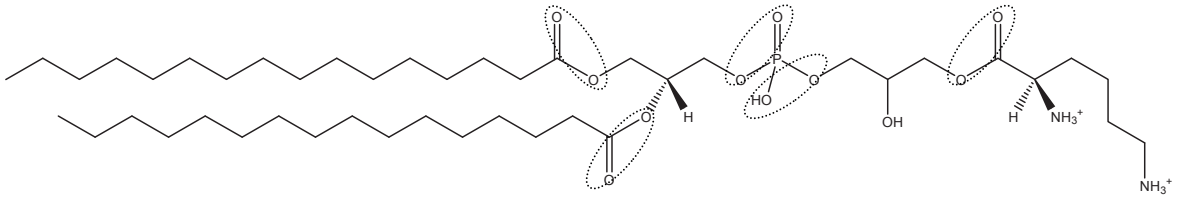

CHAPS, EU_H 3.5 + EU 1

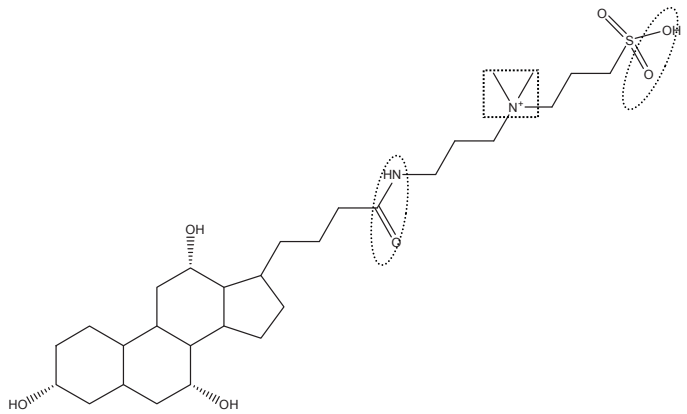

Methods

ATPase Assay. The Sav1866 associated ATP hydrolysis was measured according to Litman et al. (Litman and others 1997) in 96-well microtiter plate (Nunc F96 MicroWell^{TM} plate, non-treated) with small modifications. Each experiment contained either ~0.9 μg or ~0.2 μg of protein per total assay volume of 60 μL in phosphate release assay buffer (total protein concentration ~14.9 μg/mL per sample in 25 mM HEPES, 150 mM NaCl, 10 mM $MgSO_4$, 7 mM ATP or in 25 mM HEPES, 50 mM NaCl, 2.5 mM $MgSO_4$, 3 mM ATP) (determined according to the protein concentration 1.8 mg/mL (first preparation) and 2.7 mg/mL (second preparation) unless otherwise stated. The reaction was started by transferring the plate from ice to a water bath kept at the temperature of choice for 30 min (at 37°C or at 25°C respectively) and was terminated by rapidly cooling the plate on ice. The inorganic phosphate, P_i, concentration was determined by addition of ice-cold solution (200 μL) containing ammonium molybdate (0.2 % (w/v)), sulphuric acid (1.43 % (v/v)), freshly prepared ascorbic acid (1 % (w/v)) and SDS (0.9 % (w/v)). After incubation at room temperature for 30 min the phosphate released was quantified colorimetrically at 820 nm using a Spectramax M2 (Molecular Devices, Sunnyvale, USA). Reference phosphate standards were included to each 96-well plate.

Purification and Reconstitution of Sav1866. For detailed protocol see (Dawson and Locher 2006). Briefly, the gene encoding Sav1866 fused to an N-terminal His-tag was overexpressed in *E.coli*, solubilized and purified in octaethylene glycol monododecyl ether ($C_{12}E_8$). Sav1866 was reconstituted in lipid vesicles as the E. coli vitamin B12 transporter BtuCD (Borths and others 2005). The reconstitution of the protein into lipid vesicles containing 3:1 (w/w) *E.Coli* polar lipid extract and POPC leads to a loss of protein as well as of lipids. Lipid concentration as well as protein concentration was determined as described below.

Determination of the Lipid Concentration. The concentration of the lipid was quantified by a colorimetric phosphate assay (Itaya and Ui 1966). Briefly, proteoliposomes were diluted in prechloric acid and flamed until the suspension became clear. The free phosphate was detected at 670 nm after addition of malachite green and was quantified

by comparing with standards.

Determination of the Protein Concentration with BCA Assay. Standard curve (0-10 μg in 10 μL) was prepared from Bovine serum albumin; BSA and BCA working solution were prepared by mixing reagent A and reagent B in 50:1 v/v. To each BSA standards and protein samples 1 mL of BCA working solution were added. The samples were incubated 20 min at 60 °C and then cooled to room temperature before measuring the absorbance at 562nm.

Determination of the Protein Concentration According to Edelhoch (Edelhoch 1967). The proteoliposomes were solubilized in $C_{12}E_8$ solution (1.9 mM or 2.2 mM) and equilibrated for 30 min. Afterwards the solution was diluted and suspended to a final concentration of 6 mM Guanidinium chloride. The molar extinction coefficient was measured at 280 nm. From the extinction coefficient the concentration was calculated according to http://www.expasy.ch/tools/protparam-doc.html. Results are summarized in Table 1.

Table 1

For the following calculations we used a protein concentration, c = 1.8 mg/ml, for the first proteoliposome preparation and c = 2.7 mg/ml for second proteoliposome preparation.

Preparation of Lipid Vesicles. Large unilamellar vesicles (LUVs) containing *E.coli* polar lipid extract:POPC (3:1 w/w) were prepared as follows. The lipids were obtained in chloroform and were dried first with a stream of N_2 and then overnight under high vacuum. For the binary lipid mixtures the second lipid was added in dichlormethane solution to the dried film of the first lipid and treated as before. Subsequently, buffer solution (either 25 mM HEPES, 150 mM NaCl or 25 mM HEPES, 50 mM NaCl) was added to the lipid film and the mixture was rigorously vortexed. After 5 freeze/thaw cycles the lipid suspension was extruded 12 times through 400 nm pores and if stated further 12 times through 100 nm pores. The size was controlled by dynamic light scattering (DLS).

Small unilamellar vesicles (SUVs) were prepared as follows. The preparation of the lipid suspension was same as described for LUVs. After buffer addition the lipid suspension was sonicated for 20-30 min with a tip sonifier. Next, the suspension was centrifuged for 5 min on a Tabletop centrifuge. The metal debris from the sonifier tip were removed and the size was checked by DLS.

Isothermal Titration Calorimetry (ITC). ITC experiments were performed with VP-ITC calorimeter from MicroCal (Northampton, MA).

Partitioning Experiments. A high concentrated lipid suspension (c_{lipid} > 20 mM) was injected into a sub-micellar verapamil solution. Typically there were 30 injections a 10 µl each to reach heat of dilution. The time between the injections was set to 5 – 10 min. to ensure re-equilibration of the system. All solutions and suspensions were thoroughly degassed before filling into the calorimeter cell.

Surface Activity Measurements. The air-water partition coefficient, K_{aw}, and the cross-sectional area of the drugs, A_d, were determined from the surface pressure, π, measurements, as a function of drug concentration (Gibbs adsorption isotherm) (for details see (Fischer and others 1998; Gerebtzoff and others 2004).

Dynamic Light Scattering. The size of the lipid vesicles was checked by dynamic light scattering (DLS) by Zetasizer NanoZS instrument (ZEN3600) (Malvern Inst., Worcestershire, UK). The device was equipped with a 4 mW HeNe laser with a wavelength of 633 nm. Due to the principle of non-invasive back scattering the scattering angle was 173°. The attenuator and the measuring points were set automatically by the instrument. Three individual measurements were performed for each system to test the reproducibility. The experimental data were analyzed using DTS software for DLS as provided by Malvern.

Zetapotential Measurements. The zeta potentials of the lipid vesicles were measured in double-distilled water. The zeta potential was analysed by measuring the electrophoretic mobility using a Zetasizer NanoZS instrument (ZEN3600) (Malvern Inst., Worcestershire, UK). The experimental data were analyzed using DTS software for DLS

as provided by Malvern. Measurements are usually given as z.average size which is an intensity mean.

Kinetic model for Evaluation of the ATPase Activity Curves. The ATPase activity profiles of Sav1866 were evaluated using a modified Michaelis-Menten equation as proposed by Litman et al. The same compound which can activate the transporter by interacting with the first binding site can, inhibit the ATPase activity, at higher concentration, by interacting with the second binding site.

$$V_S = \frac{K_1 K_2 V_0 + K_2 V_1 C_S + V_2 C_S^2}{K_1 K_2 + K_2 C_S + C_S^2} \quad (1)$$

where K_1 is the concentration of half-maximum activation, K_2 the concentration of half-maximum inhibition, V_0 basal velocity, V_1 activation velocity, V_2 inhibition velocity, C_S aqueous substrate concentration.

Evaluation of ITC Data. The apparent binding constant of verapamil to *E.coli* polar lipid extract : POPC (3:1), K_{app}, was determined according to:

$$X_b = K_{app} / C_{D,eq} \quad (2)$$

where X_b is the membrane bound mole fraction of detergent molecules. The bound, $C_{D,b}$, and the free concentration, $C_{D,eq}$, in sum, is the total concentration, $C_{D,0}$ according to

$$C_{D,0} = C_{D,eq} + C_{D,b}$$

Note that the apparent partition coefficient, K_{app}, of a charged molecule is only valuable in the concentration range studied, as K_{app} is dependent on the effective membrane charge density and the effective charge of the molecule.

Gouy-Chapman Theory. To account for electrostatic contribution $C_{D,eq}$ is replaced by C_M, the concentration immediately above the plane of binding. For charged system $C_{D,eq} \neq C_M$, whereas for a neutral system $C_{D,eq} = C_M$. Negatively charged membranes will attract cationic compounds and repulse anionic compounds, respectively. C_M varies therefore strongly from the bulk solution. The concentration difference is governed by the Boltzman relation:

$$C_{D,M} = C_{D,eq}\, e^{-z_D \psi F_0 / RT}$$

where $z_D F_0$ is the molar electric charge, and RT is the thermal energy. The partition equilibrium (2) can then be modified as

$X_b = K_p C_{D,M}$.

K_p is referred to the intrinsic binding constant. Furthermore the binding of Na^+ to the negatively charged headgroup (POPG) was taken into account ($K_{(Na^+)} = 0.6\ M^{-1}$).

Determination of the Packing Density of Vesicles. The packing density was estimated according to:

$$K_{lw} = K_{aw} e^{-\frac{A_D \pi_M}{kT}} e^{-\frac{zF_0 \psi}{RT}} \quad (3)$$

where K_{lw} is the lipid water apparent partition coefficient, K_{aw}, the air water partition coefficient (taken from surface activity measurements (SAM)), A_D is the crossectional area of the molecule (from SAM), π_M, is the lateral packing density, z the formal charge of the molecule, F_0 the Faraday constant, ψ, the surface potential, k the Boltzmann constant, R, the gas constant and T the temperature.

Results

Characterization of the Lipid Mixture under ATPase Activity Assay Conditions. The lipid mixture, Sav1866 was reconstituted in, was studied in detail, as the compounds first have to incorporate into the membrane before they bind from the membrane to the transporter similar to P-gp (for review see (Higgins and Gottesman 1992). The lipid mixture containing *E. coli* polar lipid extract: POPC (3:1 w%) was extruded 12 times through 400 nm and as a next step through 100 nm pores. The size distribution of the vesicles was checked by dynamic light scattering under the ATPase assay conditions. The ATPase conditions were either 25 mM Hepes (150 mM NaCl, 10 mM $MgSO_4$, 7 mM ATP) pH 7.5 at T = 25°C or 25 mM Hepes (50 mM NaCl, 2.5 mM $MgSO_4$, 3 mM ATP) pH 7.0 at T = 37°C, respectively. The lipid mixture contains 24 mol-% charged lipid head groups (for cardiolipin two charges were taken into account) and exhibits a zetapotential, ζ, of -17.1 ± 0.7 mV as determined by zetapotential measurements at 25°C and showed an

intensity weighted average size distribution of 173 ± 12 nm after extrusion through 100 nm pores. At 37°C the lipid vesicles showed an average size distribution of 220 ± 10 nm and a zetapotential, ζ, of -30.6 mV. The results are summarized in Table 2.

The lipid vesicles were not smaller after increasing the extrusion runs. Moreover after sonication of the lipid suspension they were larger than the usually observed 30 nm vesicles like observed for POPC. The vesicles were larger and had generally a size of ~ 60 nm after 30 min of sonication. The chain segments of the prokaryotic lipids contain cyclopropane rings which are not present in eukaryotic lipids. These cyclopropane rings suggest more rigid chain segment in prokaryotic organism than in eukaryotic.

Table 2

We performed isothermal titration calorimetry experiments to get more insight into the incorporation behavior of a drug into the specific lipid mixture. We performed titrations with verapamil and *E. coli* polar lipid extract: POPC (3: 1 w%) at same conditions as in (Meier and others 2006) with POPC:POPG (3:1 mol%) and compared the results. The comparison is appropriate as the surface charge of the two systems was similar and we had accounted for electrostatic contributions. *E. coli* polar lipid extract: POPC (3: 1 w%, SUVs ~ 60 nm, 29.33 mM) were injected into verapamil solutions (100.8 μM) at 37°C. The measurement is shown in Figure 1. All thermodynamic parameters derived from the ITC experiments are summarized in Table 3. The intrinsic partition coefficient, K_p, was determined as 170 M^{-1} and the enthalpy of binding, ΔH, was -1.9 kcal/mol. POPC:POPG (3:1) titrations showed intrinsic partition coefficients, K_p, of 400 M^{-1} and an enthalpy of reaction, ΔH, of -2.1 kcal/mol at 37°C (50 mM Hepes, 50 mM NaCl, 30 nm SUVs (Meier and others 2006)). The intrinsic binding constant of verapamil towards PC:PG membranes is 2-3 times larger than for *E. coli* polar lipid extract: POPC. To a first approximation the lateral packing density of *E. coli* polar lipid extract: POPC exhibits therefore a ~ 2 mN/m higher packing density than a POPC:POPG (3: 1 mol%) membrane (equation 3), as the effective surface charge is similar in both systems investigated. Here the lipid mixture used contained ~ 40 mol-% PC. The lateral packing density of POPC was previously determined as π_M = 32 ± 1 mN/m (Seelig 1987). The lateral packing

density of E.coli:PC (3:1 w/w) was therefore estimated as π_M = ~ 34 mN/m at 37°C which is in reasonable agreement with an estimate of the lateral packing density of *E. Coli* polar lipid extract from the pressure-area isotherm at room temperature (π_M = 35 mN/m) (Kamaraju and Sukharev 2008).

The lipid-water partition coefficients of all drug molecules investigated were derived from the air-water partition coefficients, K_{aw}, taking into account a lateral packing density of 34 mN/m (for details see (Gerebtzoff and others 2004)).

The surface potential of the vesicles changes upon incorporation of a charged molecule. Moreover the surface potential of the lipid vesicles is altered in the presence of the ABC-transporter. Therefore the surface potential as determined by zetapotential measurements of the pure vesicles does not reflect the exact situation in the ATPase assay for charged drugs. We calculated the lipid/water partition coefficient, K_{lw}, as described in methods by taking the two extreme values of the surface potential into account, either -30 mV or 0 mV. The difference in the affinity from water to the membrane, ΔG_{lw}^0, does maximally change by ~ 3 kJ/mol. For all further calculations we therefore choose a surface potential of 0 mV as proposed previously (Gatlik-Landwojtowicz and others 2006).

Figure 1

Sav1866 ATPase Activity Stimulated with Different Compounds at 25°C. The effect of different compounds on the Sav1866 ATPase activity was studied in 25 mM Hepes (150 mM NaCl, 10 mM $MgSO_4$, 7 mM ATP) pH 7.5 at T = 25°C. Figure 2 shows the ATPase activity profiles induced by the various structurally unrelated compounds normalized to the basal ATPase activity of Sav1866 (100 %). All drugs were applied in the range of the inverse of the air/water partition coefficient, $1/K_{aw}$, and the critical micelle concentration (CMC) as determined by surface activity measurements (SAM), summarized in Table 4. The activation profiles were fitted to the modified Michaelis-Menten equation (eq. 1) described in methods. Hoechst33342, promazine, chlorpromazine, and verapamil (cationic compounds) stimulated Sav1866 ATPase activity clearly at low aqueous substrate concentrations and inhibited the ATPase activity at high concentrations. Progesterone (neutral) and penicillin G (anionic) inhibited the Sav1866 ATPase activity

already at low concentrations. All parameters derived from Figure 2 are summarized in Table 4. Higher aqueous concentration of compounds than used led to drug aggregation or drops in pH and was therefore not used.

Figure 2

Sav1866 ATPase Activity Stimulated with Different Compounds at 37°C

The ATPase assays for P-gp were previously performed at T = 37°C at pH 7.0, with 50 mM KCl, 2.5 mM MgSO4 and 3 mM ATP plus additional compounds to inhibit other transporters in native membranes (DTT, Ouabain and EGTA for details see (Aanismaa and Seelig 2007)). In order to compare Sav1866 with P-gp, the ATPase measurement conditions of Sav1866 were adjusted to the measuring conditions of P-gp except for the additional compounds.

Figure 3A shows all neutral and anionic compounds investigated whereas Figure 3B shows the cationic compounds. Progesterone was measured as a neutral compound in both conditions. The ATPase activity of Sav1866 inhibited by progesterone shows no large shift of the concentration of half minimum activity, K_2 = 1.4E-5 *vs.* 5E-5 and similar change in the minimum ATPase activity, V_{max} = 0.63 *vs.* 0.5.

Hoechst 33342 did not change the ATPase activity profile in the different conditions. The verapamil stimulated ATPase activity of Sav1866 as seen in Figure 2 was not observed anymore. Verapamil under the conditions studied inhibited the ATPase activity of Sav1866. We tried to restore the ATPase activation profile by the addition of lipids to the ATPase reaction mixture. The lipid to protein molar ratio (~ 200:1) is low in the proteoliposome preparation. Verapamil incorporates at lower concentrations when buffer contains low ionic strength as verapamil is attracted by the oppositely charged membrane. Verapamil, being present to high extend in the membrane, immediately binds to the transporter leading to an inhibition of the ATPase activity. By the addition of external lipids we diluted verapamil out and therefore less verapamil was present in the membrane where Sav1866 was reconstituted in (see Figure 4).

Figure 3

Effect of Additional Lipids on the Verapamil Stimulated ATPase Activity. As verapamil upon addition, immediately occupied the second binding site at 37°C we tried to add additional lipids to restore the verapamil stimulated ATPase activity increase. Table 2 suggests that verapamil binds at lower concentrations to the membrane at the 37°C conditions than at 25°C. The external lipid concentration was increased assuming the added lipid vesicles do not mix, or only to a small extend, with the proteoliposomes. The verapamil induced ATPase activity was measured and is shown in Figure 4.

The fold increase in the ATPase activity was restored by the addition of either small unilamellar vesicles (SUVs, Figure 4A) or large unilammellar vesicles (LUVs, Figure 4C) containing *E. coli* polar lipid extract: POPC (3: 1 w%), respectively. Addition of small unilammellar vesicles containing POPC: POPG (3: 1 mol%) (Figure 4B) did not show any significant difference compared to the addition of SUVs containing *E.coli* polar lipid extract: POPC. At a molar ratio of lipid/protein of ~ 7000 the fold increase in the ATPase activity was highest. Further addition of lipids did not show any significant ATPase activity increase. The lowest concentration of half maximum activity, K_1, was observed for the addition of *E. coli* polar lipid extract: POPC (3: 1 w%) SUVs to a final protein/lipid molar ratio of 1: 20300. There we found K_1 ~ 10 μM, what is similar to previous findings (Velamakanni and others 2008).

Figure 4

Effect of Additional Lipids on the Drug Stimulated ATPase Activities. Verapamil displayed under distinct conditions only inhibitory effect on the ATPase activity of Sav1866. However by the addition of additional lipids the stimulating effect of verapamil on the ATPase activity could be restored. We were wondering whether other drugs displaying inhibitory effects on the ATPase activity of Sav1866 could lead to activation of the ATPase activity by the addition of more lipids. Two drugs displaying strong inhibitory effects on ATPase activity of Sav1866 were used, progesterone and DPH-TMA. Promazine was tested as well as we observed a rather big shift in the ATPase activity profile. The measurements with additional lipids are shown in Figure 5.

Figure 5 reveals that the ATPase activity curve did not drastically change by the addition of lipid vesicles. A general trend is observed towards higher maximum activities. However the change from inhibition to activation could not be observed as previously for verapamil.

Figure 5

Effect of Lysyl-DPPG on Sav1866 and Pgp ATPase Activity. Close inspection of the ATPase activity profiles induced by compounds led to the conclusion that positive charged drugs lead often to activation (except DPH-TMA) whereas neutral or negative charged drugs inhibited the ATPase activity of Sav1866. As the role in lipid transport of the close homology model P-gp is unclear we were wondering whether Sav1866 can transport a lipid, like other ABC-transporters e.g. MsbA (Doerrler and Raetz 2002). The interaction of the cationic lipid, lysyl-DPPG (1,2-dipalmitoyl-*sn*-glycero-3-[phospho-*rac*-(3-lysyl(1-glycerol))]) with the ATPase activity of Sav1866 and Pgp was studied in detail. Lysyl-DPPG is present to high amount in the membrane of gram positive bacteria (Kristian and others 2004). For *Staphylococcus aureus* a lysyl-DPPG content of 38 % in the stationary phase has been reported compared to 57 % PG, the main component of the membrane ((Mukhopadhyay and others 2007). Since lysyl-DPPG has a very low critical aggregation concentration (for comparison 14:0 PG has a critical aggregation concentration of, CAC = 11 μM, (Avanti polar lipids)) it is impossible to provide it in monomeric form at higher concentrations to the proteoliposomes without any additions. Lysyl-DPPG was extruded trough 100 nm pores to ensure unilamellar vesicles and provided to the proteoliposemes either in vesicular form or in mixed micellar form together with CHAPS. Since lysyl-DPPG is double cationic charged and the lipid mixture, Sav1866 is reconstituted in, is anionic charged we assumed that the lipid vesicles at least partially mix. However providing the lysyl-DPPG in a mixed CHAPS/lysyl-DPPG solution which is diluted below the CMC upon addition, most of the lipids are thought to mix with the proteoliposomes.

Figure 6A shows the ATPase activity of Sav1866 (open up-triangles) and P-gp (filled up-triangles), respectively, with increasing concentration of CHAPS. Sav1866 does not

interact with CHAPS whereas the ATPase activity of P-gp was slightly inhibited by CHAPS. Figure 6B shows the ATPase activity of the two proteins upon addition of lysyl-DPPG in vesicular form (Sav1866: open squares, P-gp: filled squares). The ATPase activity of both proteins was stimulated by the lipid. For Sav1866 a typical activation/inhibition profile was observed whereas P-gp showed only activation in the concentration range studied. The apparent concentration of half maximum activation, K_1, was lower for Sav1866 (K_1 = 21.7 μM) than for Pgp (K_1 = 87 μM, lower limit) whereas the maximum activity increase (fold) was similar (V_1 = 2.1 *vs.* V_1 = 2.2). Figure 6C shows the ATPase activity measurement of lysyl-DPPG provided in mixed micellar form together with CHAPS (Sav1866: open down-triangles, P-gp: filled down-triangles). Lysyl-DPPG was solubilized in CHAPS (6 mM) and the size of the aggregates was checked after half an hour by dynamic light scattering to ensure solubilization. After addition to the reaction mixture, the CHAPS solution was diluted clearly below the CMC to a concentration of 0.5 mM leading to the incorporation of CHAPS and lysyl-DPPG into the Sav1866 containing proteoliposomes. The ATPase activity of Sav1866 was stimulated up to 3.8 fold whereas the concentration of half maximum activation, K_1, stayed unchanged. On the other hand lysyl-DPPG inhibited the ATPase activity of P-gp in the presence of 0.5 mM CHAPS (Figure 6C). CHAPS alone inhibited the ATPase activity of P-gp as seen in Figure 6A. Lysyl-DPPG was not able to restore the CHAPS induced inhibition of the P-gp ATPase activity.

Figure 6

Discussion

Sav1866 ATPase Activity Stimulated with Different Compounds at 25°C.

The ATPase activity of Sav1866 was monitored upon addition of various structurally unrelated compounds. We observed typical bell-shaped ATPase activity curves as previously found for P-gp (Aanismaa and Seelig 2007). Upon activation of the ATPase activity the drug binds to the first binding site of the transporter. At high concentration however the drug binds to the second binding site, leading to an inhibition of the ATPase

activity (Litman and others 1997). All curves were fitted to the modified Michaelis-Menten equation accounting for two binding sites. We found that positively charged compounds in general activated the ATPase activity of Sav1866. This is in agreement with previous findings (Velamakanni and others 2008). These authors have shown that Sav1866 can transport Hoechst33342 and that the ATPase activity is stimulated by the addition of Hoechst33342, verapamil, ethidium and tetraphenylphosphonium.
We found that neutral or negatively charged compounds led to inhibition of the ATPase activity of Sav1866. Our results implied that negatively or neutral charged compounds investigated bind to the transporter with high affinity, therefore immediately occupying the second binding site leading to inhibition of the ATPase activity of Sav1866.

Sav1866 ATPase Activity Stimulated with Different Compounds at 37°C. The ATPase activity was checked under different conditions (same as P-gp) in order to compare with P-gp. We expected a change of the ATPase the activity profile under the different conditions (see Figure 2 and 3) due to a change of the ionic strength in suspension. The ionic strength modulates (i) the basal ATPase activity of Sav1866 (see chapter 4) and (ii) the surface potential of the lipid vesicles. This in turn modulates the apparent binding constant of charged compounds from water to the bilayer phase, K_{lw}, as the charge density at the membrane surface is different.
At low ionic strength cationic compounds tend to incorporate at lower concentration as they are attracted by the anionic membrane. Anionic compounds on the other hand incorporate at higher concentrations as they are repelled. Neutral compounds incorporate at similar concentrations. Moreover additional effect from temperature and pH are expected.
We found that progesterone (neutral) induced a very similar ATPase activity profile under both conditions. The concentration of half minimal ATPase activity, K_2, for progesterone was either 5E-5 or 1.4E-5 M^{-1} with a maximal inhibition of 0.6 to 0.5. On the other hand the ATPase activity of P-gp under the same conditions gets activated by progesterone with a K_1 of 1.4E-5 M^{-1} and a K_2 of 1.4E-4 M^{-1} with a maximum activation V_{max} of 3.3 and a maximum inhibition of 0.7 (Aanismaa and Seelig 2007). Progesterone

inhibits the ATPase activities of Sav1866 in the same concentration range were P-gp gets activated suggesting higher affinity of progesterone for Sav1866 than for P-gp.
Hoechst33342 did not significantly change in the two conditions used. Hoechst33342 displayed a concentration of half maximum activation, $K_1 \sim 30$ μM, in Sav1866 whereas P-gp showed inhibition at a concentration of half maximum inhibition of, $K_2 = 5$ μM. On the other hand difference between the two conditions for the Sav1866 measurements was observed for verapamil. At the 25°C conditions the ATPase activity was increased upon addition of verapamil with a K_1 of 130 μM, at 37°C there was no activation at all detecTable.

Effect of Additional Lipids on the Drug Stimulated ATPase Activity. By addition of lipids to the reaction mixture, the verapamil induced ATPase activity of Sav1866 was restored under the conditions used. The lipid vesicles were supposed not to mix or to a low extend, as all vesicles have an anionic surface potential thus repelling each other.
What do additional lipids to the system assuming they do not mix? They bind additional verapamil and take it therefore out of suspension. Moreover additional lipids take $MgSO_4$ and NaCl out of suspension. But as the only concentration difference in an ATPase activity measurement is the drug concentration less NaCl or $MgSO_4$ can not account for an increase in the ATPase activity.
The addition of external lipid vesicles did not change the ATPase activity from inhibition to activation of strong inhibitory drugs, like e.g. DPH-TMA and progesterone, suggesting high affinities of these drugs from the membrane to the transporter.

Effect of Lysyl-DPPG on Sav1866 and Pgp ATPase Activity. The ATPase activity of Sav1866 was activated upon addition of lysyl-DPPG in vesicular form or in mixed micellar form. Previously it was shown that MsbA, a lipid A transporter from *E. coli* can not only transport the lipid, but also structurally unrelated drugs. The transport of structurally very diverse substrates as e.g. drugs and lipids implies a substrate/protein interaction according to a modular binding process as previously found for P-gp (Gatlik-Landwojtowicz and others 2006; Seelig 1998). A close description of the modular binding principle can be found in the next paragraph.

Thermodynamics of Drug/Transporter Interaction.

Lipid/Water Partitioning. The study of substrate/transporter interaction in multi-drug related ABC-transporters is difficult as the drug binds the transporter from the membrane. The concentration of the drug in the membrane is dependent on the structural properties of the substrate, the membrane and the experimental conditions. The concentration of the substrate in the membrane is described by the lipid/water partition coefficient, K_{lw}. In order to determine the affinity (partition coefficients can be converted into affinities, see equ. (5)) of the substrate to the protein knowledge of the lipid/water affinity of the substrate is required.

Transporter/Water Partitioning. The measurement of the substrate induced ATPase activity of an ABC-transporter concentration dependently allows the determination of the concentration of half maximal ATPase activity, K_1. K_1 is a kinetic parameter. However the ATPase activity measurement is performed under steady-state conditions. Steady-state conditions refer to conditions were the substrate, ATP, is present in excess concentration. The ATP hydrolysis is slower than the substrate binding step. Therefore, for a first approximation, K_1 can be converted into a thermodynamic binding constant, $1/K_1$. $1/K_1$ is referred to as K_{tw}, the transporter/water partition coefficient.

Transporter/Lipid Partitioning. Determination of K_{lw} allows calculation of the affinity of a substrate from the water to the lipid membrane. K_{tw} allows the calculation of the affinity of a substrate from the water to the transporter. Taking together we can calculate the effective affinity of the substrate from the membrane to the transporter, K_{tl}, using:

$$K_{tw} = K_{lw} * K_{tl} \quad (4)$$

Converting Binding Constants into Affinities. We discussed the determination of the different binding constants in detail. The free energy (affinity) of the different binding steps can be calculated by:

$$\Delta G^0 = - RT \ln (K*c_w) \quad (5)$$

where $c_w = 55.5$ is the molar concentration of water, R the gas constant and T the temperature. According to equation (5) the binding properties can be converted into affinities.

$$\Delta G_{tw}{}^0 = \Delta G_{lw}{}^0 + \Delta G_{tl}{}^0 \quad (6)$$

We have determined the effective membrane/transporter affinity, ΔG_{tl}^{0}, using the approach described above. All affinities found are summarized in Table 4 and 5.

The Modular Binding Concept. We have determined the effective affinity of the substrate from the membrane to the transporter. All the thermodynamic parameters for both conditions investigated are summarized in Table 4 and 5. Further we chose the same approach as previously done for P-gp and counted all possible hydrogen acceptor patterns in the substrates investigated. A close description of the possible hydrogen acceptor patterns can be found in (Seelig 1998). This allowed us to determine the affinity per hydrogen bond acceptor pattern. We found that the substrates investigated showed slightly less affinity to Sav1866 than to P-gp. As an average affinity we found at 25°C -4.3 kJ/mol*H-bond acceptor pattern^{-1} and -5.3 kJ/mol*H-bond acceptor pattern^{-1} at 37°C. The crystal structure of Sav1866 revealed a higher charge density in the binding pocket than in P-gp. The slightly lower affinities per hydrogen-bond acceptor patterns in Sav1866 is in line with the structural properties in the binding pocket as the hydrogen bonding energy is higher in more hydrophobic environments.

Table 1

Concentration of Sav1866 and Lipid in Proteoliposomes.

Preparation		SDS-page	BCA (vesicles)	BCA (5% SDS)	BCA (C12E8)	Edelhoch (C12E8)	Lipid	Lipid/protein ratio
1	mg/ml	6-8	2.08 ± 0.15	1.81 ± 0.5	1.84 ± 0.2+ 1.7 ± 0.22*	1.97+	4	314:1
	uM		16	14	14.2+ 13.1*	15.2	4400	
2	mg/ml	5	-	-	2.69 ± 0.16*	3.9* 6.44*	3.7	194:1
	uM		-	-	20.8*	30.3* 49.7*	4000	

+ measured in 2.2 mM C12E8

* measured in 1.9 mM C12E8

Table 2

Conditions	**Vesicle size [nm]**	**Zetapotential [mV]**
25 mM Hepes, 150 mM NaCl, 10 mM $MgSO_4$, 7 mM ATP, pH 7.5 at 25°C	173±12	-17.1±0.7
25 mM Hepes, 50 mM NaCl, 2.5 mM $MgSO_4$, 3 mM ATP, pH 7.0 at 37°C	220±10	-30.6

Table 3

Temp. °C	Lipid mM	Verapamil μM	HEPES mM	NaCl mM	pH	K_p M^{-1}	ΔH kcal/mol
37	43	117.08	25	50	7	110	-1.7
37	21.5	75	25	50	7	190	-1.53
37	29.33	100	25	50	7	160	-1.59
37	29.37 SUVs	103.5	25	50	7	120	-1.43
37	29.33	100.8	25	50	7	170	-1.9

Table 4

Calculated in 25 mM Hepes, 50 mM NaCl, 2.5 mM $MgSO_4$, 3 mM ATP, pH 7.0 at 37°C

Calculation: Π = 34 mN/m, psi = 0 mV

Compound	MW	pk_A	Possible reco. patterns	K_{aw}	A_D	CMC	K_{lw}	ΔG^0_{lw}	K_1	K_2	V_1	V_2	ΔG^0_{tw1}	ΔG^0_{tw2}	ΔG^0_{tl1}	ΔG^0_{tl2}	n ΔG^0_{tl1} /weighted patterns	P-gp
	g/mol			M^{-1}	m^2	M	M^{-1}	kJ/mol	M	M	fold	fold	kJ/mol		kJ/mol			
Cyclosporin A	1202.6	-	10.5	2E7[c]	1.4E-18[a]	1E-6	2.97E2	-25.0	1E-8[i]	1E-6	0.99	0.91	-57.9	-46	-32.81	-20.94	-3.1	-2.6
DPH	232.32	-	2	1.45E5[b]	3E-19[h]	-	1.34E4	-34.9	1.85E-7[i]	1.85E-6	0.99	0.62	-50.3	-44.4	-15.47	-9.54	-7.74	-
DPH-TMA	290.42	-	2	1.78E5[b]	3E-19[h]	-	1.64E4	-29.4	1.36E-6[i]	1.36E-5	1	0.1	-45.2	-39.3	-15.74	-9.8	-7.87	-
Hoechst33342	452.55	11.08[d]	2	7.19E5[c]	6.97E-19[c]	-	2.85E3	-30.9	3.1E-5	8.55E-5	3.56	1.6	-37.1	-34.5	-6.28	-3.64	-3.14	-
Methicillin	380.42	2.8[e]	3.5	1.23E2[b]	8.08E-19[b]	-	2.02E-1	-6.2	1.44E-4[i]	1.44E-2	1.1	0.1	-33.2	-21.3	-26.94	-15.06	-7.7	-
Progesterone	314.5	-	1.5	1.57E5[c]	4E-19[a]	8E-5	6.56 E3	-33.0	1.57E-4 [i]	1.57E-5	1	0	-38.9	-32.93	-5.9	0.07	-3.91	-5.1
Promazine	284.42	9.4[f]	2	4.8E3[c]	4.2E-19[a]	7E-3	1.71E2	-23.6	3.3E-5	4.35E-4	1.46	-	-37.0	-30.3	-13.37	-6.7	-6.68	-3.5
R/S-Verapamil	454.6	8.92[g]	5	1.66E5[c]	9E-19[a]	5E-3	1.31E2	-22.9	1.3E-4	1.22E-3	1.19	-	-33.5	-27.7	-10.58	-4.74	-2.12	-3.9
Lysyl-DPPG	924.06	10.4	10	-	-	-	-	-	2.2E-5	3.08E-5	2.11	-	-38.0	-37.1	-	-	-	-

a) pH 8.0
b) pH 7.0
c) pH 7.4
d) scifinder calculated
e) Rapson HDC, Bird AE. J Pharm Pharmacol. 1963; 15:226T
f) Sorby DL, et al. J Pharm Sci. 1966; 58:788
g) Hasegawa J et al Pharm Sci 1984
h) estimation
i) estimated from K_2: K_1 is a factor of 10 smaller for methicillin than K_2 and K_1 of cyclosporine A is a factor of 100 smaller than K_2 according to (Gatlik-Landwojtowicz and others 2006)

Table 5

Calculated in 25 mM Hepes, 150 mM NaCl, 10 mM $MgSO_4$, 7 mM ATP, pH 7.5 at 25°C

Calculation: Π = 34 mN/m, psi = 0 mV

Compound	MW	pk_A	Possible reco. patterns	K_{aw}	A_D	CMC	K_{lw}	ΔG^0_{lw}	K_1	K_2	V_1	V_2	ΔG^0_{tw1}	ΔG^0_{tw2}	ΔG^0_{tl1}	ΔG^0_{tl2}	n ΔG^0_{tl1} /weighted patterns	P-gp
	g/mol			M^{-1}	m^2	M	M^{-1}	kJ/mol	M	M	fold	fold	kJ/mol		kJ/mol		kJ/mol	
Chlorpromazine	318.87	9.2	2	2.15E4[c]	4.2E-19[a]	9.6E-4	9.09E2	-26.09	1.04E-4	1.76E-2	1.7	-	-32.7	-20.0	-6.6	6.12	-3.3	-4.9
Hoechst33342	452.55	11.08[d]	3	7.19E5[c]	6.97E-19[c]	-	3.79E3	-29.12	5.39E-5	1.86E-4	1.7	0.47	-34.3	-31.2	-5.2	-2.1	-2.6	-
PenicillinG	334.36	2.8[e]	3.5	1E2[c]	8.08E-19[b]	-	2.81E-1	-5.35	1.18E-4[h]	1.18E-2	-	0.31	-37.4	-21.0	-27.0	-15.6	-7.7	-
Progesterone	314.5	-	1.5	1.57E5[c]	4E-19[a]	8E-5	7.72E3	-31.42	1.37E-6[h]	1.37E-5	-	0.63	-43.4	-37.7	-12	-6.3	-8	-5.1
Promazine	284.42	9.4[f]	2	4.8E3[c]	4.2E-19[a]	7E-3	2.03E2	-22.37	1.24E-3	3.43E-3	3.3	-	-26.5	-24.0	-4.7	-1.7	-2.1	-3.5
R/S-Verapamil	454.6	8.92[g]	5	1.66E5[c]	9E-19[a]	5E-3	1.89E2	-21.32	8.04E-5	2.7E5	1.3	1.32	-33.3	nd	-12	nd	-2.4	-3.9

a) pH 8.0
b) pH 7.0
c) pH 7.4
d) scifinder calculated
e) Rapson HDC, Bird AE. J Pharm Pharmacol. 1963; 15:226T
f) Sorby DL, et al. J Pharm Sci. 1966; 58:788
g) Hasegawa J et al Pharm Sci 1984
h) estimation from K_2: K_1 is factor of 10 smaller for progesterone than K_2 and K_1 a factor of 100 smaller for Penicillin G according to (Gatlik-Landwojtowicz and others 2006)

Legends to Figures

Figure 1. *Binding of Verapamil to E.coli Polar Lipid Extract : POPC (3:1 w%) Vesicles.* (A) Vesicle-into-verapamil titration. A lipid vesicles suspension (SUVs) (29.33 mM) was titrated into verapamil (100 μM). The measuring conditions were 25 mM Hepes, 50 mM NaCl at 37°C (pH of 7.0). (B) shows the reaction heats as a function of the injection number, $N_{inj.}$ Each peak corresponds to the addition of 10 μL vesicle suspension to the verapamil solution in the calorimeter cell (1.4 mL). The experimental points are shown as black squares whereas the theoretical analysis is depicted as solid line. (C) depicts the extend of binding, X_b, as a function of the free verapamil concentration in the cell. X_b is defined as the molar ratio of bound verapamil per total lipid. The intrinsic partition coefficient, K_p, was 120 M^{-1} and the heat of reaction, ΔH, was -1.9 kcal/mol.

Figure 2. *Substrate Simulated ATPase Activity of Sav1866.* The interaction of structurally different substrates with the ATPase activity of Sav1866 was measured (25 mM Hepes, 150 mM NaCl, 7 mM ATP, 10 mM $MgSO_4$) at pH of 7.5 at T = 25°C. penicillin G (⌠), promazine (⟨), progesterone (◊), chlorpromazine (∫), verapamil (⌡), hoechst33342 (⌡). The solid lines show the fit to the modified Michaelis-Menten equation.

Figure 3A, B. *Substrate Simulated ATPase Activity of Sav1866.* The interaction of the substrates with the ATPase activity of Sav1866 was measured in 25 mM Hepes, 50 mM NaCl, 3 mM ATP, 2.5 mM MgSO4, pH 7.0 at 37°C. (A) Anionic and neutral substrates. Cyclosporine A (⌠), DPH (′), methicillin (⊙), progesterone (◊). (B) Positively charged substrates. Promazine (⟨), DPH-TMA (≤), hoechst33342 (⌡), verapamil (⌡), lysyl-DPPG (⌠). The solid line represents the fit according to the modified Michaelis-Menten equation.

Figure 4A-C. *Sav1866 ATPase Activity upon Addition of Verapamil and Additional Lipid Vesicles.*

(A) shows the ATPase activity of Sav1866 upon addition of verapamil and additional small unilammellare vesicles (SUVs) containing *E.coli* polar lipid extract : POPC (3:1

w%). The molar ratio of protein per lipid is shown in the left corner. (B) shows the measurement upon addition of POPC:POPG (3:1 mol%) SUVs. (C) shows the addition of a *E. coli* polar lipid extract:POPC (3:1 w%) mixture extruded trough 100 nm pores (LUVs).

Figure 5A-C. *Addition of extra Vesicles on the Substrate Induced Sav1866 ATPase Activity Profile.*

Figure 5 shows the ATPase activity profiles of Sav1866 (open up-trinagles) upon addition of external lipid vesicles (POPC/POPG 3:1 mol%) to a final molar ratio (protein/lipid) of 7163. The measurement with a final lipid/protein molar ratio of 192 is shown as filled squares. (A) shows the ATPase activity of Sav1866 stimulated with the promazine (filled squares) whereas the open up-triangles show the measurement with the addition of PC:PG vesicles. (B) shows the ATPase activity of Sav1866 inhibited with progesterone (filled squares) whereas the open up-triangles show the measurement with the addition of PC:PG vesicles and (C) the ATPase inhibition profile of Sav1866 induced by DPH-TMA (filled squares) and upon addition of lipids (open up-triangles). The solid line represents the fit according to the modified Michaelis-Menten equation. The vertical lines show the inverse of the air water partition coefficient (dotted line) and the CMC (dashed line).

Figure 6A-C. *ATPase activity change of Sav1866 and P-gp by Lysyl-DPPG.*

A: ATPase activity of Sav1866 (open up-triangles) and Pgp (filled up-triangles) with increasing concentration of CHAPS. Assay conditions were for Sav1866 (25 mM Hepes, 150 mM NaCl, 7 mM ATP, 10 mM $MgSO_4$) pH 7.5 at T = 25°C and for P-gp (25 mM Tris, 50 mM KCl, 3 mM ATP, 2.5 mM $MgSO_4$, 3 mM DTT, 2 mM Ouabain, 0.5 mM EGTA) pH 7.0 at T = 37°C. **B:** ATPase activity of Sav1866 (open squares) and P-gp (filled squares) by the addition of lysyl-DPPG in vesicular form. **C:** ATPase activity measurement of Sav1866 (open down-triangles) and Pgp (filled down-triangles) by addition of lysyl-DPPG in micellar form in CHAPS (6 mM). Upon addition to the reaction mixture CHAPS gets diluted 12 times to a final concentration of 0.5 mM, which

is clearly below the CMC. The final concentration of CHAPS in (C) is indicated as arrow in (A).

References

Avanti polar lipid.
Aanismaa P, Seelig A. 2007. P-Glycoprotein kinetics measured in plasma membrane vesicles and living cells. Biochemistry 46(11):3394-404.
Borths EL, Poolman B, Hvorup RN, Locher KP, Rees DC. 2005. In vitro functional characterization of BtuCD-F, the Escherichia coli ABC transporter for vitamin B12 uptake. Biochemistry 44(49):16301-9.
Dawson RJP, Locher KP. 2006. Structure of a bacterial multidrug ABC transporter. 443(7108):180-185.
Doerrler WT, Raetz CR. 2002. ATPase activity of the MsbA lipid flippase of Escherichia coli. J Biol Chem 277(39):36697-705.
Edelhoch H. 1967. Spectroscopic determination of tryptophan and tyrosine in proteins. Biochemistry 6(7):1948-54.
Federici L, Woebking B, Velamakanni S, Shilling RA, Luisi B, van Veen HW. 2007. New structure model for the ATP-binding cassette multidrug transporter LmrA. Biochemical Pharmacology 74(5):672-678.
Fischer H, Gottschlich R, Seelig A. 1998. Blood-brain barrier permeation: molecular parameters governing passive diffusion. J Membr Biol 165(3):201-11.
Gatlik-Landwojtowicz E, Aanismaa P, Seelig A. 2006. Quantification and characterization of P-glycoprotein-substrate interactions. Biochemistry 45(9):3020-32.
Gerebtzoff G, Li-Blatter X, Fischer H, Frentzel A, Seelig A. 2004. Halogenation of drugs enhances membrane binding and permeation. Chembiochem 5(5):676-84.
Higgins CF, Gottesman MM. 1992. Is the multidrug transporter a flippase? Trends Biochem Sci 17(1):18-21.
Itaya K, Ui M. 1966. A new micromethod for the colorimetric determination of inorganic phosphate. Clin Chim Acta 14(3):361-6.
Kamaraju K, Sukharev S. 2008. The Membrane Lateral Pressure-Perturbing Capacity of Parabens and Their Effects on the Mechanosensitive Channel Directly Correlate with Hydrophobicityâ€ Biochemistry 47(40):10540-10550.
Kristian SA, Durr M, Van Strijp JA, Neumeister B, Peschel A. 2003. MprF-mediated lysinylation of phospholipids in Staphylococcus aureus leads to protection against oxygen-independent neutrophil killing. Infect Immun 71(1):546-9.
Kristian SA, Golda T, Ferracin F, Cramton SE, Neumeister B, Peschel A, Gotz F, Landmann R. 2004. The ability of biofilm formation does not influence virulence of Staphylococcus aureus and host response in a mouse tissue cage infection model. Microb Pathog 36(5):237-45.
Litman T, Zeuthen T, Skovsgaard T, Stein WD. 1997. Structure-activity relationships of P-glycoprotein interacting drugs: kinetic characterization of their effects on ATPase activity. Biochim Biophys Acta 1361(2):159-68.
Meier M, Blatter XL, Seelig A, Seelig J. 2006. Interaction of verapamil with lipid membranes and P-glycoprotein: connecting thermodynamics and membrane structure with functional activity. Biophys J 91(8):2943-55.
Mukhopadhyay K, Whitmire W, Xiong YQ, Molden J, Jones T, Peschel A, Staubitz P, Adler-Moore J, McNamara PJ, Proctor RA and others. 2007. In vitro susceptibility of Staphylococcus aureus to thrombin-induced platelet microbicidal

protein-1 (tPMP-1) is influenced by cell membrane phospholipid composition and asymmetry. Microbiology 153(Pt 4):1187-97.
Omote H, Al-Shawi MK. 2002. A novel electron paramagnetic resonance approach to determine the mechanism of drug transport by P-glycoprotein. J Biol Chem 277(47):45688-94.
Pleban K, Macchiarulo A, Costantino G, Pellicciari R, Chiba P, Ecker GF. 2004. Homology model of the multidrug transporter LmrA from Lactococcus lactis. Bioorganic & Medicinal Chemistry Letters 14(23):5823-5826.
Seelig A. 1987. Local anesthetics and pressure: a comparison of dibucaine binding to lipid monolayers and bilayers. Biochim Biophys Acta 899(2):196-204.
Seelig A. 1998. A general pattern for substrate recognition by P-glycoprotein. Eur J Biochem 251(1-2):252-61.
Seelig J. 2004. Thermodynamics of lipid-peptide interactions. Biochim Biophys Acta 1666(1-2):40-50.
Short SA, White DC. 1971. Metabolism of phosphatidylglycerol, lysylphosphatidylglycerol, and cardiolipin of Staphylococcus aureus. J Bacteriol 108(1):219-26.
van Veen HW, Venema K, Bolhuis H, Oussenko I, Kok J, Poolman B, Driessen AJ, Konings WN. 1996. Multidrug resistance mediated by a bacterial homolog of the human multidrug transporter MDR1. Proc Natl Acad Sci U S A 93(20):10668-72.
Velamakanni S, Yao Y, Gutmann DAP, van Veen HW. 2008. Multidrug Transport by the ABC Transporter Sav1866 from Staphylococcus aureus† doi:10.1021/bi8006737. Biochemistry 47(35):9300-9308.

Figures

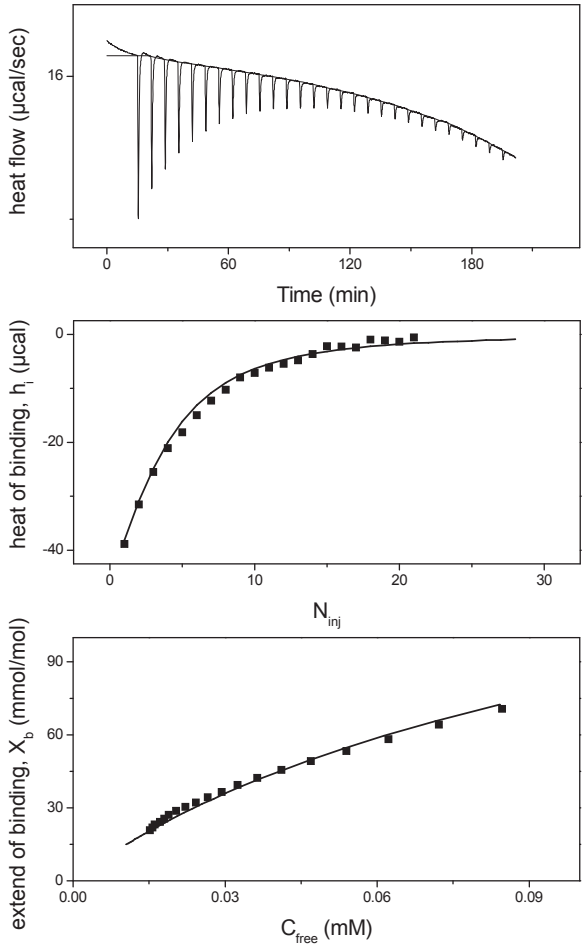

Figure 1

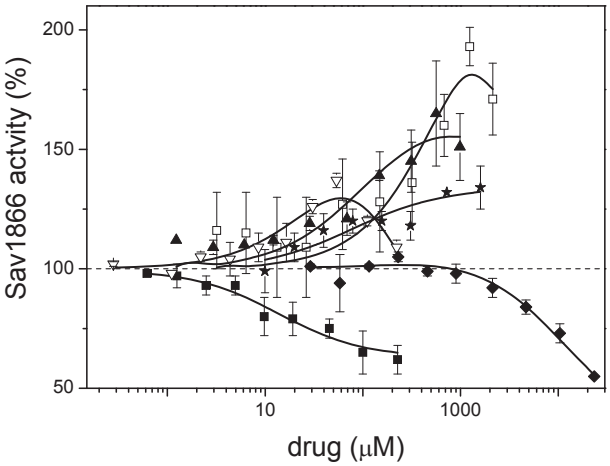

Figure 2

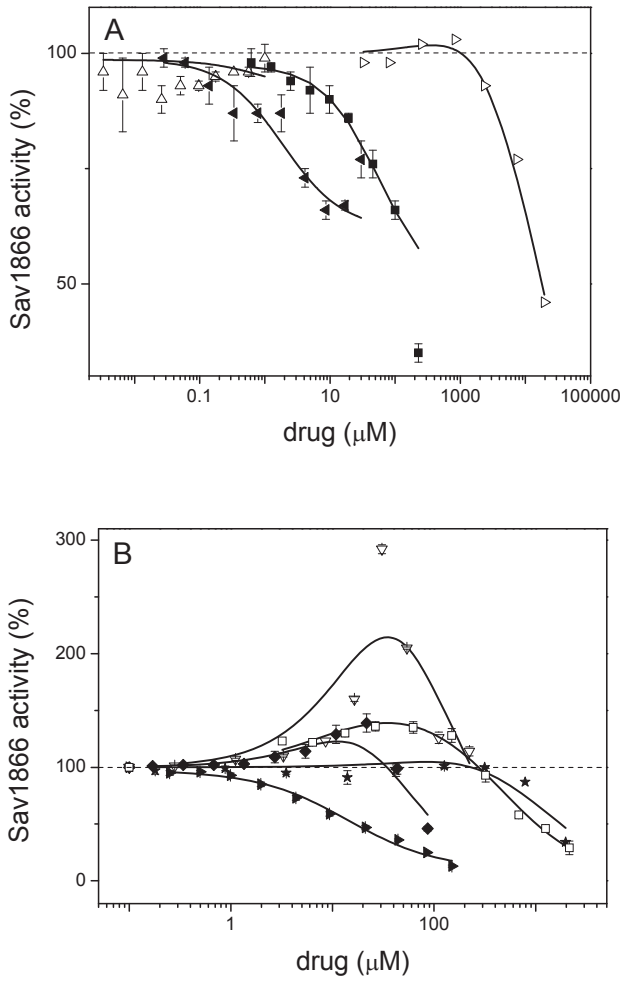
A
100
50
Sav1866 activity (%)
0.1
10
1000
100000
drug (μM)
B
300
200
100
0
Sav1866 activity (%)
1
100
drug (μM)

Figure 3

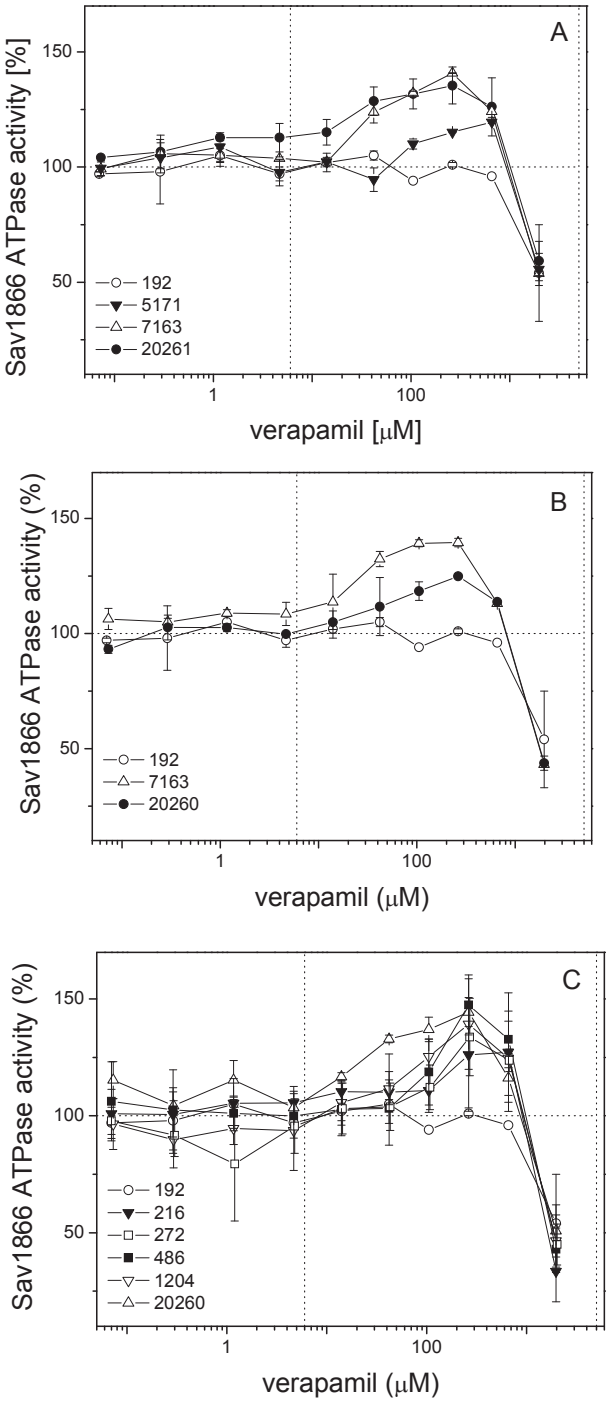
A
Sav1866 ATPase activity [%]
150
100
50
192
5171
7163
20261
1
100
verapamil [μM]
B
Sav1866 ATPase activity (%)
150
100
50
192
7163
20260
1
100
verapamil (μM)
C
Sav1866 ATPase activity (%)
150
100
50
192
216
272
486
1204
20260
1
100
verapamil (μM)

Figure 4

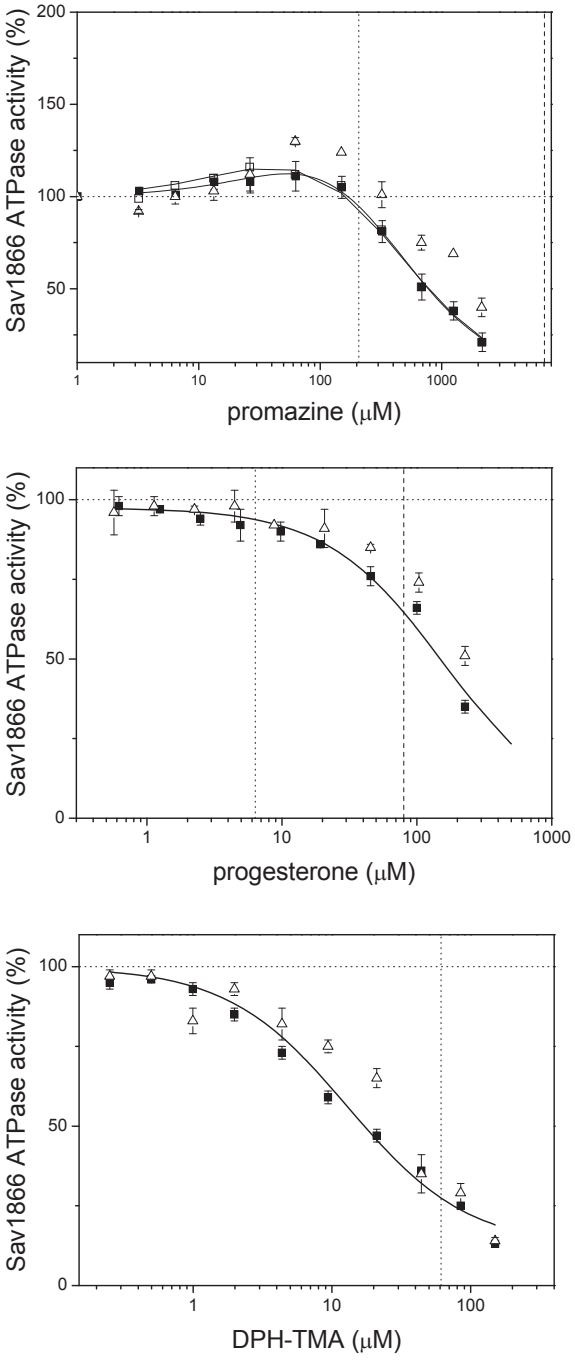
Sav1866 ATPase activity (%)
200
150
100
50
1
10
100
1000
promazine (μM)
Sav1866 ATPase activity (%)
100
50
0
1
10
100
1000
progesterone (μM)
Sav1866 ATPase activity (%)
100
50
0
1
10
100
DPH-TMA (μM)

Figure 5

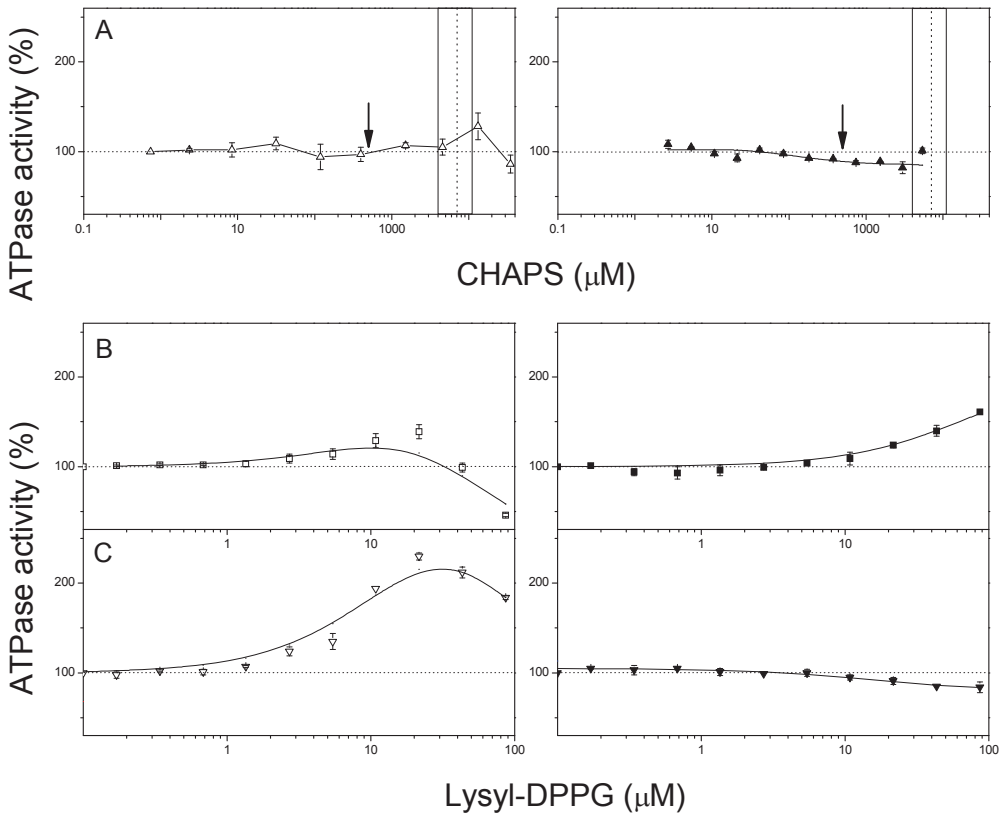
A
B
C
ATPase activity (%)
ATPase activity (%)
200
100
0.1
10
1000
1
100
CHAPS (μM)
Lysyl-DPPG (μM)

Figure 6

6 On the Interaction of Lipid Membranes with Ionic Detergents

6.1 Summary

A wide variety of detergents is employed in membrane biology for solubilization and purification. Most common are neutral detergents with their high critical micellar concentration and their low protein denaturating capabilities. Ionic detergents, on the other hand, are increasingly used as disinfectants, fungicides, or textile fiber softeners. Most detergents will easily insert into biological membranes altering membrane properties. Understanding the extent of membrane-detergent interactions requires the measurement and analysis of binding isotherms. For ionic detergents interacting with neutral or charged membranes the hydrophobic energy is modulated distinctly by electrostatic attraction/repulsion forces and ionic screening, influencing the shape of the binding isotherm. Using isothermal titration calorimetry (ITC) we have measured the thermodynamic parameters for the interaction of $CH_3(CH_2)_n$ - $^{+}N(CH_3)_3$ and $-SO_4^-$ (n = 10 – 16) with lipid bilayers composed of neutral and anionic lipids. Quite different binding isotherms were obtained depending on the charge of detergent and membrane. However, after correcting for electrostatic effects the actual binding followed a simple surface partition equilibrium and the intrinsic binding constant, K_D^0, was related to predominantly hydrophobic interactions. At 25 °C the binding enthalpies, ΔH_D^0, directly available from the ITC experiment, were small ($\Delta H^0_{^{+}N(CH_3)_3}$ = -0.4 to -2.5 kcal/mol; $\Delta H^0_{SO_4^-}$ = -1.3 to -3.8 kcal/mol) and showed no correlation with the length of the alkyl chains. In contrast, the free energies of the hydrophobic interaction as derived from the binding constant, K_D^0, was large (ΔG_D^0= -7.0 to -10 kcal) and showed a linear dependence on the chain length. The incremental contributions per CH_2 group were $\Delta G^0_{CH_2}$ = -520 cal/mol for n-alkyl$-SO_4^-$ and $\Delta G^0_{CH_2}$ = -560 cal/mol for n-alkyl-$^{+}N(CH_3)_3$ detergents interacting with charged POPC/POPG membranes, indicating very similar hydrophobic/van der Waals interactions of the two types of detergent. In contrast,

the *total* free energy of binding for $^{+}N(CH_3)_3$ detergents was consistently less negative by 1-2 kcal/mol compared to that of $-SO_4^-$ detergents of the same chain length leading to 15 fold smaller binding constants for n-alkyl-$^{+}N(CH_3)_3$ detergents. Membrane insertion was compared with micelle formation under the same conditions. We propose a cooperative aggregation model to describe micellization. Compared to the pseudo-phase separation model or the mass action model the aggregation model allows a continuous growth of the aggregates and provides an excellent fit of the ITC demicellization experiments.

6.2 Manuscript

On the Interaction of Ionic Detergents with Lipid Membranes. Thermodynamic Comparison of n-Alkyl-$^{+}N(CH_3)_3$ and n-Alkyl-SO_4^- †

Andreas Beck and Joachim Seelig*

Biozentrum, University of Basel, Div. of Biophysical Chemistry, Klingelbergstrasse 50/70, CH-4056 Basel, Switzerland

* To whom correspondence should be addressed:

Tel. +41-61-267 2190, Fax. +41-61-267 2189, e-mail: joachim.seelig@unibas.ch

† Supported by the Swiss National Science Foundation Grant # 3100-10779

Introduction

Membrane biology uses a wide variety of detergents to solubilize membranes and to purify lipids and membrane proteins. Most common are neutral detergents such as octyl glucoside or dodecyl maltoside as they provide a non-denaturing environment. In contrast, charged detergents such as sodium dodecyl sulfate (SDS) not only dissolve membranes but simultaneously denature membrane-bound proteins, allowing molecular weight determinations by SDS gel chromatography. We have analyzed in detail the thermodynamics of SDS partitioning into neutral and negatively charged lipid membranes [1]. Here we present the corresponding analysis for the positively charged counterpart dodecyl trimethylammonium chloride (DTAC). Using isothermal titration calorimetry (ITC) and dynamic light scattering (DLS) we measured the binding/insertion of DTAC into lipid vesicles of different composition. The binding process is analyzed by a surface partition equilibrium, taking into account chemical adsorption/binding and electric attraction/repulsion. The measurements are performed in the temperature range of 15-65 °C and are compared with the binding thermodynamics of SDS.

The insertion of detergents such as SDS or DTAC into lipid membranes is driven by the hydrophobic effect and the van der Waals interaction between the alkyl chains. The strength of these interactions can be modulated by the length of the alkyl chain and the chemical nature of the polar group. We have therefore varied the length of the hydrocarbon chains from 10 up to 16 carbon atoms and have measured the binding thermodynamics at 25 °C for the $^{+}N(CH_3)_3$ and $-SO_4^-$-carrying detergents. The data are compared with n-alkyl-glucoside and n-alkyl-maltoside for which chain length data in the range of 8-12 are available.

For charged detergents thermodynamic measurements are strongly influenced by the salt/buffer composition. In order to be comparable with biological studies on membrane transporters most of the present studies were performed at 0.1 M NaCl, 25 mM Hepes, pH 7.5. We have therefore also measured the CMC of the various detergents in this buffer and have analyzed the micellization data in terms of a cooperative aggregation model which is different from the mass action and the pseudo-phase separation models.

Materials and Methods

Materials. 1-palmitoyl-2-oleoyl-*sn*-glycero-3-phosphocholine (POPC) and 1-palmitoyl-2-oleoyl-*sn*-glycero-3-phosphoglycerol (POPG), dissolved in chloroform, were from Avanti Polar Lipids (Birmingham, AL). n-alkyl-trimethylammonium chlorides were from Anatrace (Maumee, OH, USA) and n-alkyl-sulfates were from Sigma Aldrich (Steinheim, Germany).

Liposome Preparation. Composite lipid films were prepared by appropriate mixing of the lipids in organic solvent. The dried lipid was suspended in buffer, vortexed, and freeze-thawed for five cycles. Unilamellar vesicles (LUVs) of diameter d = 100 nm were obtained by extrusion of multilamellar lipid suspensions through polycarbonate filters (Nuclepore, Pleasanton, CA) [2,3].

Lipid concentrations were determined gravimetrically by carefully weighing the samples and by adding defined amounts of buffer.

If not otherwise stated, the buffer composition was 25 mM Hepes (pH 7.5), 0.1 M NaCl. The phospholipid dispersions as well as the detergent solutions were prepared in the same buffer to minimize heats of dilution.

High-Sensitivity Titration Calorimetry. Isothermal titration calorimetry was performed using a VP high-sensitivity titration calorimeter from Microcal (Northampton, MA). To avoid air bubbles, solutions were degassed under vacuum before use. The calorimeter was calibrated electrically. The data were acquired by computer software developed by MicroCal. In control experiments the corresponding detergent solution (or vesicle suspension) was injected into buffer without lipid (or detergent). Injection of lipid suspensions into buffer alone yielded small reaction heats.

Light Scattering Measurements. Light scattering measurements were performed on a Zetasizer ZS90 instrument (ZEN3690; Malvern Inst., Worcestershire, UK). It was equipped with a 4 mW HeNe laser with a wavelength of 633 nm. Due to the principle of non-invasive back scattering the scattering angle was 173°. The buffer was filtered through 0.2 µm regenerated cellulose filter (Infochroma AG, Zug, CH) before using. The

results were evaluated using DTS-software provided by Malvern and are given as z-average size. The z-average size gives two values, a mean value for the size, and a width parameter known as the Polydispersity Index (PDI). This mean size is an intensity mean.

Thermodynamics of Micelle Formation. Micelle formation is usually quantitated by either the pseudo-phase separation model or by a mass action equilibrium. The mass action model describes the formation of a micelle with n monomers by the equilibrium

$$nA \rightleftarrows A_n$$

Both models describe an all-or-none process and neglect species with intermediate aggregation numbers. As an alternative we propose a cooperative aggregation model for micelle formation. This model has been employed successfully in other aggregation processes of biomolecules [4-6]. It starts with a nucleation step

$$A + A \overset{\sigma K}{\rightleftarrows} A_2 \qquad c_{A_2} = \sigma K c_A^2$$

followed by *n* growth steps.

$$A_2 + A \overset{K}{\rightleftarrows} A_3 \qquad c_{A_3} = K c_{A_2} \cdot c_A = \sigma K^2 c_A^3$$

$$\vdots$$

$$A_{n-1} + A \overset{K}{\rightleftarrows} A_n \qquad c_{A_n} = K c_{A_{n-1}} c_A = \sigma K^{n-1} c_A^n$$

K is the equilibrium constant of the growth step, $\sigma < 1$ is the nucleation parameter which makes the initial dimer formation more difficult than the further growth of the aggregates. c_A is the equilibrium concentration of monomers. Mass conservation requires

$$c_A^0 = c_A + 2\sigma K c_A^2 + 3\sigma K^2 c_A^3 ..... + n\sigma K^{n-1} c_A^n$$

where c_A^0 is the total concentration of A in monomer form. Using the definition

$$s = K c_A$$

this series can be written as

$$c_A^0 = c_A\left[1+\sigma\sum_{j=2}^{n} j\, s^{j-1}\right]$$

which can also be expressed in analytical form.

$$c_A^0 = c_A\left[1-\frac{\sigma\left(s^2-2s+s^n\left(1+n-sn\right)\right)}{\left(s-1\right)^2}\right]$$

The degree of dissociation can then be defined as

$$\alpha = \frac{c_A}{c_A^0}$$

and denotes the mole fraction of monomers in equilibrium with aggregates. For given total concentration c_A^0 and a given set of parameters K, σ, and n, the degree of dissociation, α, and the heat of dissociation per injection, δh_i, can be calculated and can be compared with the experimental result. As an obvious difference compared to the mass action model the aggregation model predicts small heat changes even once the concentration in the calorimeter cell is larger than the CMC. This will be discussed in more detail below.

Thermodynamics of Membrane Partitioning. The insertion of detergents into the lipid membrane is described by a surface partition equilibrium

$$X_b = K_D^0 \cdot c_M$$

$X_b = n_D^b / n_L^0$ is the "extent of binding" and is given by the molar ratio of bound detergent, n_D^b, over total lipid, n_L^0. If the detergent cannot flip to the inner membrane because of its charged head group, only the lipid molecules in the outer monolayer of unilamellar lipid vesicles are counted. X_b can also be expressed in terms of concentrations

$$X_b = \frac{c_D^b}{c_L^0}$$

c_M is the "surface concentration" i.e. the concentration of free detergent in the lipid-water interface, immediately above the plane of binding. For non-ionic detergents $c_M = c_{eq}$ where c_{eq} is the equilibrium concentration in bulk solution. For cationic detergents interacting with anionic lipid vesicles, electrostatic attraction yields $c_M > c_{eq}$. In contrast, insertion of cationic detergents into a neutral lipid bilayer leads to a positively charged membrane surface, making insertion increasingly difficult and $c_M < c_{eq}$.

The surface concentration, c_M, is related to the equilibrium concentration, c_{eq}, according to Boltzmann's law

$$c_M = c_{eq} \cdot e^{-zF_0\psi_0/RT}$$

(z = signed valence of detergent, F_0 = Faraday constant, ψ_0 = surface potential)

The surface potential, ψ_0, depends on the charge density of the membrane, the extent of detergent binding, X_b, on other bound ions, and the ionic strength of the buffer solution. Moreover, Na^+ will bind to the phosphoglycerol head group with a binding constant of $K_{Na^+} = 0.6\ M^{-1}$. The binding isotherm $X_b = f(c_{eq})$ can be measured with ITC in a model-independent manner [7]. It can then be analyzed by combining the surface partition equilibrium with the Gouy-Chapman theory. The details of this approach have been described in previous publications [1,8,9]. It is experimentally convenient to introduce an apparent binding constant $K_{app} = X_b/c_{eq}$ as both X_b and c_{eq} can be deduced directly from the ITC binding constant. However, K_{app} is not truly constant but will vary with the amount of bound detergent as $K_{app} = K_D^0 e^{-zF_0\psi_0/RT}$.

Experimental Results

Critical Micellar Concentration Measured by Isothermal Titration Calorimetry. Isothermal titration calorimetry is a convenient method to determine the critical micellar

concentration (CMC) of a detergent. A concentrated detergent solution with c >> CMC is injected in small steps into buffer and the heat of demicellization, δh_i, is recorded. Under ideal conditions δh_i should be constant during the first few injections until the concentration of detergent in the calorimeter cell approaches the CMC. Near the CMC the heat flow decreases rapidly as the injected micelles no longer disintegrate. Figure 1 shows a typical titration diagram and its evaluation by the model discussed above. Figure 1A displays the heat flow

Figure 1

measured for 10 µL injections of a buffered micellar solution of 100 mM dodecyl trimethylammonium chloride (DTAC) into buffer (0.1 M NaCl, 25 mM Hepes, pH 7.5) at 65 °C. Figure 1B shows the integrated heat flows, δh_i, as a function of the injection number, i. It may be noted that the very first δh_is are not exactly constant. Moreover, considerable heat evolves even beyond the CMC of 10.3 mM. In evaluations based on the mass action model the "tail" of the titration curve is often subtracted. In contrast, the aggregation model provides a quantitative explanation for this "tailing-off" behavior. The solid line in figure 1B was calculated with the aggregation model and the parameters listed in table 1. The model predicts a small, but distinct heat uptake (~300 µcal per injection) even if the detergent concentration in the calorimeter cell is larger than the CMC. In molecular terms this suggests small changes relating to the size, shape and the degree of counterion condensation of the micelle.

Table 1

Figure 1C describes the degree of dissociation, α, equivalent to the mole fraction of detergent monomers. During the first few injections the injected micelles completely disintegrate into monomers (degree of dissociation $\alpha = 1$). Under ideal conditions already the very first injection, $\delta h1$, could be used to calculate the heat of demicellization. As the injection continues the detergent concentration in the calorimeter cell rises and the degree

of dissociation, α, starts to decrease as the micelles only partially disintegrate. α can be calculated as a function of the injection number k:

$$\alpha_k = \frac{\sum_{i=1}^{k} \delta h_i}{k\delta h_1}$$

The measured heat, $\sum_{i=1}^{k} \delta h_i$, is divided by the maximum heat possible, $k\delta h_1$, expected for full dissociation. The experimental results are given by the solid symbols in figure 1C.

The solid lines in figures 1B and 1C are theoretical results of the aggregation model calculated with the parameters K = 1/CMC, σ, and n listed in table 1. The parameter σ determines primarily the length of the plateau region for which the degree of dissociation is α = 1. A small nucleation parameter makes nucleation difficult and extends the length of the plateau region.

The cooperative aggregation is sensitive to the size of the aggregates. In the present case a consistent fit of all measurements (temperature range 15-65 °C) required a minimum aggregate size of n = 35 monomers. Smaller n-values produced distinct discrepancies with the experiments; on the other hand, for n ≥ 40 the predicted aggregation isotherm changed only little. Thus the aggregation model predicts a minimum number of monomers forming a micelle. Data in the literature for the micellar size of DTAC vary in the range of $20 \le n \le 60$ [10].

Figure 2A shows the variation of the enthalpy of micelle *formation*, $\Delta H^0_{mic} = -\Delta H^0_{demic}$, with temperature. Endothermic heats of micelle formation are seen at low temperatures, exothermic values above 35 °C. Linear regression analysis yields ΔH^0_D (kcal/mol) = -0.095 T (°C) + 3.16. The molar heat capacity change is $\Delta C^0_{p,D}$ = -95 cal/molK. Figure 2B then displays the CMC as a function of temperature. The solid line is the theoretical fit based on the van't Hoff equation and calculated with the variable ΔH^0_{mic} of figure 2A. Figure 2B also includes previous CMC measurements evaluated by the mass action model [10].

Figure 2

Inspection of figure 1B shows that the initial heats of injection are not constant as theoretically expected but start out below the plateau region. Similar deviations from a constant initial plateau region have been reported before [10-12], and must be explained by additional dilution effects *after* micelle disintegration. We have measured the dilution of DTAC solutions with concentrations *below* the CMC. Injecting a 7.2 mM DTAC solution into buffer yields the results shown in figure 3. Considering only the very first 10 μL injection of each titration the temperature dependence of the heat of dilution can be approximated by ΔH_{dil} (cal/mol) = -52.2 T (°C) + 846.

Figure 3

Binding of DTAC to Lipid Vesicles. DTAC binds to lipid vesicles with high affinity. Both hydrophobic and electrostatic forces contribute to the binding process. Isothermal titration calorimetry in combination with suitable models allows a quantitative separation of the two energy contributions [8]. The present analysis follows the approach used for negatively charged sodium dodecyl sulfate [1]. Unilamellar lipid vesicles of 100 nm diameter were prepared by several extrusions through 100 nm Millipore filters. The lipid composition was either 100 % POPC or a POPC/POPG (75:25 mol/mol) mixture. Binding of DTAC to pure POPC vesicles creates a positive surface potential which makes DTAC binding increasingly difficult. In contrast, cationic POPC/POPG vesicles show the opposite effect. In the initial phase, electrostatic attraction distinctly enhances binding until the membrane surface charge is compensated. Once the membrane charge has been neutralized further DTAC binding experiences the same electrostatic repulsion as noted for POPC vesicles.

Binding isotherms were determined by lipid-into-detergent titration experiments [9]. The calorimeter cell contained DTAC solutions with concentrations between 20 - 80 μM in buffer (0.1 M NaCl, 25 mM Hepes, pH 7.5). Lipid vesicles (c_L ~ 23 - 26 mM) were injected in 10 μL steps and the corresponding heat release recorded as shown in figure 4.

Figure 4A displays the heat flow as a function of time, figure 4B shows the heats of reaction, δh_i, as a function of the injection number, n_i, figure 4C finally is the binding isotherm, that is the extent of binding,

Figure 4

X_b, vs. the equilibrium concentration, $c_{D,eq}$. The solid lines in figure 4B, C were calculated with the binding constant, K_D^0, and the heat of reaction, ΔH_D^0, listed in table 2, based on the model described previously [1]. It was assumed that DTAC binds to the outer lipid layer only as the charged molecule cannot easily flip to the inner half-layer (cf. below). Figure 5A shows

Figure 5

the temperature dependence of the detergent binding enthalpy, ΔH_D^0, for both neutral and anionic vesicles. The regression analysis of the data in figure 5A (solid lines) provides the

Table 2

molar heat capacity change with $\Delta C_{P,D}^0$ = -68 cal/molK (-80 cal/molK) for POPC (POPC/POPG) 100 nm vesicles. As the binding enthalpy, ΔH_D^0, is negative at all temperatures, the binding constant, K_D^0, will decrease at higher temperatures as evidenced experimentally by figure 5B. The solid lines are the predicted temperature dependencies for the two membranes using van't Hoff's law and the temperature-dependent ΔH_D^0-values listed in table 2.

Membrane Solubilization. At sufficiently high concentrations of DTAC the bilayer becomes destabilized leading to mixed micelles composed of lipid and detergent. We denote with $R_b^{sat} = c_D^{sat} / c_L^0$ the beginning of this process, that is, the phase boundary

between the pure bilayer phase and the coexistence phase of bilayers with mixed micelles. Likewise, $R_b^{sol} = c_D^{sol} / c_L^0$ denotes the detergent/lipid molar ratio at the end of the solubilization process and describes the phase boundary between the coexistence phase and the pure micellar phase.

When measuring the phase boundaries it must be noted that DTAC cannot easily translocate across the bilayer membrane because of its electric charge. This leads to a kinetic hindrance of the solubilization process as illustrated by figure 6. POPC/POPG (75:25 mol/mol) vesicles of 100 nm diameter and at a lipid concentration of 100 μM were suspended

Figure 6

in 80.4 mM DTAC (~10 × CMC) and the change in absorbance was measured in a UV spectrometer at 350 nm as a function of time and temperature. The figure demonstrates that membrane solubilization is a slow process with a half-time of about 50 min at room temperature, but decreases rapidly to a few minutes as the temperature is increased to 45 °C.

Long equilibration times of ~12 hrs were hence employed in order to deduce the phase diagram between bilayers and micelles. Lipid vesicles and DTAC were mixed together at defined ratios and the size of the mixed lipid/DTAC vesicles (with DTAC in both half-layers) was measured with dynamic light scattering (DLS) 12 hrs later. Figure 7 summarizes the results at 25 °C. Each data point in figure 7 corresponds to a separate lipid vesicle/detergent

Figure 7

preparation. The initial vesicle size (at low DTAC concentration) is 90-120 nm and is characterized by a monomodal size distribution (polydispersity index < 0.2). The vesicle size decreases rapidly after the point of membrane saturation, R_b^{sat}, is reached (PDI up to

0.7). As the total detergent concentration, c_D^0, is the sum of detergent free in solution, c_b^{sat}, and bound detergent $c_D^b = R_b^{sat} \cdot c_L^0$ it follows [13]:

$$c_D^0 = c_D^{sat} + R_b^{sat} c_L^0$$

A plot of the total detergent concentration, c_D^0, at saturation vs. the total lipid concentration should yield a straight line with a slope of R_b^{sat} and an intersect c_D^{sat}. Analysis of the data in figure 7 yields

$$c_D^0 = 6.34 + 1.42\ c_L^0 \qquad (R = 0.94)$$

The minimum concentration of DTAC to initiate bilayer disruption at 25 °C is 6.34 ± 0.50 mM which is clearly below the CMC of ~10 mM at this temperature. The minimum detergent-to-lipid ratio at which micelle formation sets in is R_D^{sat} = 1.42 ± 0.25 mol DTAC/mol lipid. For membrane solubilization purposes DTAC must be considered a "weak" detergent [9].

The phase boundary for *complete* solubilization, characterized by R_D^{sol}, can also be deduced from figure 7. C_D^0 of solubilization is the DTAC concentration where for a given lipid concentration the absorption reaches its minimum (polydispersity index < 0.25). A plot according to the above equation yields

$$c_D^0 = 6.6 + 2.20\ c_L^0 \qquad (R = 0.99)$$

The detergent-to-lipid ratio at complete solubilization is thus estimated as $R_D^{sol} \approx 2.20 \pm 0.20$ mol DTAC/mol lipid. The limiting concentrations is $c_D^{sol} = 6.6 \pm 0.5$.

Comparison of the SO_4^- *and* $^+N(CH_3)_3$ *Head Groups. Chain Length Dependence.* Using ITC we have measured the membrane binding properties of detergents of varying chain length (n = 10-16) and have compared the SO_4^- with the $^+N(CH_3)_3$ head group. The thermodynamic

Table 3

binding data are summarized in table 3. Also included are the corresponding data on micelle formation and data from the literature for two non-ionic detergents. The binding constants K_D^0 are corrected for electrostatic effects and define the hydrophobic part of the binding energy.

Discussion

Micelle Formation. Micelle formation is a 3-dimensional process and the linear aggregation model must be considered as an approximation. Nevertheless, the model allowed an excellent simulation of the ITC curves obtained in demicellization experiments. The cooperativity parameter σ was found to be independent of temperature with $\sigma = 10^{-4}$. The cooperative length, i.e. the length where aggregates become statistically independent, is $N_{coop} \sim \sigma^{-\frac{1}{2}} \sim 100$. In the present experiments, the minimum size of the aggregates to explain the demicellization ITC experiments was N ~ 35-40, consistent with this estimate. In contrast to the mass action and the pseudophase separation models the present model includes all molecular species with aggregate numbers between n = 1 and N. The smaller the cooperativity parameter, the steeper is the transition between monomers and large aggregates. The model also explains the "tail" of the ITC demicellization experiment once the detergent concentration in the calorimeter cell has increased above the CMC and micelles no longer disintegrate.

The CMCs of n-alkyl trimethylammonium chlorides have been investigated before [10-12,14,15]. Micelle formation is strongly influenced by the presence of salt. In order to mimic conditions of biological experiments the present studies were performed in the presence of 0.1 M NaCl, 25 mM Hepes, pH 7.5, explaining, in part, the small numerical differences to earlier measurements (cf. figure 2) . A systematic difference was noted between the present model and the standard analysis where ΔH^0_{demic} is evaluated by the distance between the two nearly horizontal regions in the ITC diagram (cf. figure 1 in [11]).

The ΔH^0_{demic} determined by this method is constantly ~10% smaller than that used to simulate the ITC curve by the cooperative aggregation model.

The free energy of micelle formation, ΔG^0_{mic}, can be calculated according to ΔG^0_{mic} = RT ln X_{mic} where X_{mic} = CMC/55.5 is the mole fraction of detergent in the aqueous phase (cf. table 3). A plot of ΔG^0_{mic} for detergents with different head groups (including non-ionic detergents) and different chain lengths is shown in figure 8A. ΔG^0_{mic} varies linearly with the chain length with a slope of $\Delta G^{mic}_{CH_2}$ = -620 to -700 cal/mol which defines the contribution on

Figure 8

an individual CH_2 group towards micelle formation. For the transition of a CH_2 group from water to a pure hydrocarbon phase the free energy is $\Delta G_{CH_2} \approx$ -820 to -880 cal/mol [16] which is distinctly more negative than micelle formation. The constant part in the regression analysis yields the contribution of the headgroup to the micellization process. $\Delta G_{headgroup}$ is positive for all headgroups, thus counteracting micelle formation.

Membrane Partitioning. The equilibrium between detergent free in solution (c_{eq}) and detergent bound to the lipid bilayer (X_b) is described here by a surface partition equilibrium $X_b = K^0_D c_M$ where the surface concentration, c_M, is determined by electrostatic attraction/repulsion. The binding constant, K^0_D, refers to the chemical affinity only. The free energy of hydrophobic binding can be calculated as

$$\Delta G^0_D = -RT \ln c_w K^0_D$$

where c_w = 55.5 is the molar concentration of water and corrects for the cratic contribution. If the apparent binding constant $K_{app} = X_b/c_{eq}$ is also evaluated, the electrostatic contribution to the free energy is

$$\Delta G^0_{el} = -RT \ln\left(K_{app} / K^0_D\right)$$

ΔG^0_{el} varies with the membrane surface charge, the concentration of the detergent and the ionic composition of the medium. In contrast, ΔG^0_D and K^0_D should be essentially independent of these parameters.

Inspection of table 3 reveals that the reaction enthalpies, ΔH^0_D, are rather small and are in the range of -0.4 to -4.2 kcal/mol for n-alkyl-$^+N(CH_3)_3$ and -1.3 to -4.23 kcal/mol for n-alkyl-SO_4^-, depending on chain length and temperature. No systematic variation of ΔH^0_D with chain length was observed. However, when the free energy is plotted against the chain length a linear decrease of ΔG^0_D with the number of carbon atoms is observed as illustrated in figure 8B. Compared to micelle formation a larger spread of the slopes of the different detergents can be observed. The free energy contributions per CH_2 group upon bilayer insertion, ΔG^{part}_D, for detergents with the maltose, SO_4^-, or $^+N(CH_3)_3$ head groups are $\Delta G^{part}_{CH_2}$ = -780 cal/mol, -770 cal/mol, and -650 cal/mol, respectively, (POPC membranes). Likewise, figure 8B predicts $\Delta G^{part}_{CH_2}$ = -560 cal/mol and -520 cal/mol for the $^+N(CH_3)_3$ and SO_4^- head groups upon insertion into anionic POPC/POPG membranes. In all systems an increase in the length of the alkyl chain by 2 CH_2 units increases the free energy of insertion by -1.0 kcal/mol to -1.6 kcal/mol, corresponding to an increase in the binding constant by a factor 5-15.

Table 2 demonstrates that enthalpy and entropy contribute equally to the free energy of DTAC binding at 55 °C. The exclusion of a hydrocarbon chain from water is thus not only an entropic effect but is favored by the van der Waals interaction between neighboring chains. The basic dispersion interaction between two CH_2 units in a paraffin crystal has been calculated as W = -1.24 × 10^3 (N/D^5) kcal/mol where N is the number of carbon atoms in the chain and D (Å) is the separation of the chains [17]. With D = 5.5 and N = 16 one calculates W = -3.94 kcal which agrees with the experimental result. A separation of D = 5.5 was chosen as it yields a cross sectional area of ~ 30 $Å^2$ per hydrocarbon chain corresponding to POPC in the liquid crystalline state. As the dispersion energy is inversely proportional to the 5th power of the chain-chain separation

even small changes in the packing density are sufficient to explain the free energy difference between different detergents and membrane systems. The calculations of Salem [17] were based on a crystalline lattice and the extension to semi-ordered liquid crystalline membranes is only an order of magnitude estimate.

If one compares the membrane binding energies of detergents with identical chain lengths but different head groups (fig 8B) it is obvious that the maltose and TAC compound have almost identical binding energies. These are about 1-2 kcal/mol less negative than those of the sulfate and glucose- containing detergents. A possible explanation are the larger surface area requirements of the maltose and $^{+}N(CH_3)_3$ head groups compared to the glucose or SO_4^- moieties. The insertion of a head group of area A_D into the bilayer surface requires work against the lateral packing pressure π according ot $\Delta G = \pi A_D$. π has been determined as $\pi \sim 32$ mN/m [18] and insertion of a head group with area $A_D = 55$ Å (glucose) would require an energy of 2.5 kcal/mol. Extrapolation of the straight lines in 8B to n = 0 yields only $\Delta G_{gluc} = 0.92$ kcal/mol for the contribution of the glucose head group and $\Delta G_{malt} = 2.1$ kcal/mol for the larger maltose group. The same extrapolation for the ionic detergents yields $\Delta G_{N(CH_3)_3} = -0.29$ kcal/mol $\Delta G_{SO_4^-} = -2.4$ kcal/mol. Such large extrapolations must be considered with caution, they nevertheless reflect at least qualitatively the size differences in the molecular areas. The differences in the binding constants at a given chain length are essentially the result of the size differences of the detergent head groups.

Figure 4C reveals a non-linear dependence of membrane-bound DTAC on the equilibrium concentration of detergent free in solution. The open symbols in figure 4C represent the binding isotherm as derived from the calorimetric measurements without assuming a specific binding model (except considering binding to the outer halflayer only). The solid line is calculated with the surface partition model as described above. The apparent binding constant, K_{app}, can be deduced from figure 4C by $K_{app} = X_b/c_{eq}$. K_{app} varies with c_{eq} and is large for the initial phase of binding where the anionic POPC/POPG (75:25 mol/mol) vesicles attract electrostatically the cationic detergent. However, as soon as the membrane charge is compensated the binding isotherm will be bent towards the x-axis because of electrostatic repulsion and K_{app} will become small.

Figure 9 displays the variation of K_{app} with

Figure 9

c_{eq} for POPC/POPG (75:25 mol/mol) bilayers in 0.1 M NaCl, 25 mM Hepes, pH 7.5. Again the experimental data (open symbols) are compared with the theoretical prediction.

Phase Diagram for Membrane Solubilization. Micelle formation and membrane insertion are similar processes. We have shown for a series of non-ionic detergents that an approximately linear relationship exists between the free energies of micellization and membrane insertion [9,19]. This concept was extended to calculate the limiting detergent-to-lipid ratio, X_b^{sat}, which initiates membrane destabilization. For non-ionic detergents X_b^{sat} could be approximated by the relationship [20].

$$X_b^{sat} = K \cdot CMC$$

As an example, dodecyl maltoside has a CMC = 0.17 mM and K = 5000 M^{-1} for POPC bilayers leading to a calculated $X_b^{sat} = 0.85$. The experimental value is $X_b \approx 0.9$ [21]. In this simple form, the above equation cannot be applied to charged detergents as the concentration of detergent near the membrane interface is not the CMC but $c_M = CMC \cdot e^{-zF_0\psi_0/RT}$. Considering DTAC, the detergent mainly discussed in this work, the CMC is 9.01 mM and the binding constant is $K_D^0 = 3500\ M^{-1}$ for POPC/POPG bilayers in buffer (at 25 °C). The surface concentration of detergent can then be calculated as $c_M = 0.33$ mM leading to $X_b^{sat} = 1.16$ which compares well with the experimental value of $X_b^{sat} = 1.42$. Alternatively, as $X_b^{sat} = K_D^0 \cdot c_M = K_D^0 \cdot CMC \cdot \exp(-z\psi_0 F_0/RT) = K_{app} \cdot CMC$ one can equally use K_{app} at the CMC to calculate X_b^{sat}.

The phase boundary for membrane saturation and beginning micellization for DTAC is $c_D^0 = 6.33 + 1.42\ c_L^0$ (POPC/POPG 3:1). About 1.4 molecules of DTAC per 1 phospholipid are required to initiate micellization. The corresponding phase boundary for

SDS is given by $c_D^0 = 2.2 + 0.283\ c_L^0$ (POPC). 0.3 SDS molecules per POPC lipid are already sufficient to disrupt the membrane and SDS must be considered a strong detergent as $R_D^{sat} << 1$. Part of the difference between DTAC and SDS could be caused by the membrane composition. In the POPC/POPG (3:1) system part of the DTAC is needed to neutralize POPG. However, even taking into account neutralization by 0.25 mole DTAC per mole total lipid, 1.17 DTAC molecules per lipid are still needed to start the micellization. The SO_4^- and the $^+N(CH_3)_3$ head groups must have different positions with respect to the plane of the membrane. Deuterium NMR could be used to quantitate these differences.

Concluding Remarks.

In view of the wide-spread use of dodecyltrimethylammonium chloride in commercial applications such as cationic emulsifier, textile fiber softener, antistatic agent or hair conditioner it is surprising that no quantitative data can be found in the literature about the interaction of DTAC with lipid membranes. Hazard identifications of DTAC are, among others, severe skin and eye burns, as DTAC may be absorbed through the skin with possible systemic effects. The present study is a first step for a quantitative understanding of these phenomena. Employing high sensitivity isothermal titration calorimetry the interaction of ionic detergents carrying the $^+N(CH_3)_3$ or SO_4^- polar groups with neutral and charged lipid bilayers was quantitated. Electrostatic attraction/repulsion was corrected for using the Gouy-Chapman theory and the essentially hydrophobic interaction was described over a large range of conditions by a surface partition equilibrium with $X_b = K_D^0\, c_M$. The hydrophobic binding constants were $K_D^0 = 3.5 \times 10^2$ M^{-1} to 3×10^5 M^{-1} for n-alkyl-$^+N(CH_3)_3$ with n = 10 to 16, and $K_D^0 = 2.7 \times 10^3$ to 5×10^5 for n-alkyl-SO_4^- with n = 10 to 14. At a given chain length the SO_4^- detergents bind ~ 10fold better than $^+N(CH_3)_3$ detergents, most likely because of the smaller size of the head group. At room temperature, the reaction enthalpies ΔH_D^0 are all very small and the driving force of the reaction is predominantly the entropy term of the free energy. The molar heat capacity change, ΔC_p^0, of the binding reaction is negative and at 65 °C the

negative reaction enthalpy is the more favorable binding term. The micelle formation of ionic detergents was described in terms of a new aggregation model based on cooperative nucleation and growth. At sufficiently high concentrations detergents will dissolve lipid membranes and form mixed micelles. Using dynamic light scattering and sufficiently long equilibration times the phase boundaries of this process could be determined for DTAC in equilibrium with POPC/POPG (75:25 mol/mol) 100 nm vesicles.

Acknowledgement.

We are grateful to X. Li-Blatter and A. Seelig for making their n-alkyl-$N(CH_3)_3Cl$ data available to us. This work was supported by the Swiss National Science Foundation grant # 3100-107793.

Table 1

Thermodynamic parameters of micelle formation of dodecyl- and decyl-trimethylammonium chloride [a)]

	Temp ^{0}C	micelle size n	cooperativity σ	K^0_{mic} M^{-1}	CMC mM	ΔH^0_{mic} kcal/mol	$\Delta C^0_{p,D}$ (cal/molK)
DTAC	15	60	10^{-4}	103	9.71	1.92	
(C12)	25	60	10^{-4}	111	9.01	0.80	
	35	45	10^{-4}	113	8.85	-0.28	-94.6
	45	45	10^{-4}	116	8.62	-1.33	
	45	45	10^{-4}	110	9.09	-1.27	
	65	45	10^{-4}	97	10.31	-2.77	
DeTAC (C10)	25	40	10^{-4}	13.5	74.1	1.57	

[a)] Measurements in buffer (0.1 M NaCl, 25 mM Hepes, pH 7.5)

Table 2
POPC or POPC/POPG 3:1 (100 nm) vesicles titrated into dodecyl trimethylammonium chloride solution [a)]

Temp. (°C)	c_D^0 (μM)	c_L^0 (mM)	POPC/POPG %	K_D^0 M^{-1}	ΔH_D^0 kcal/mol	ΔG_D^0 kcal/mol	$T\Delta S_D^0$ kcal/mol
25	40	23.86	100/0	3.5×10^3	-0.99	-7.18	6.19
35	20	26.5	100/0	3.3×10^3	-1.48	-7.39	5.91
35	40	26.5	100/0	3.3×10^3	-1.43	-7.39	5.96
45	30	25.19	100/0	3.0×10^3	-2.35	-7.57	5.22
25	50	24.55	75/25	3.6×10^3	-0.96	-7.20	6.24
35	80	26.04	75/25	3.1×10^3	-2.23	-7.35	5.12
45	80	26.26	75/25	2.8×10^3	-2.87	-7.53	4.66
55	80	26.87	75/25	2.4×10^3	-3.53	-7.66	4.13
55	80	26.87	75/25	2.4×10^3	-3.87	-7.66	3.79
55	80	26.21	75/25	2.2×10^3	-3.61	-7.61	4.00
65	80	26.47	75/25	2.1×10^3	-4.21	-7.81	3.60
35	80	26.03	75/25	3.3×10^3	-2.08	-7.39	5.31
45	80	26.3	75/25	3.0×10^3	-3.86	-7.57	3.71
55	80	26.06	75/25	2.4×10^3	-3.94	-7.66	3.72

[a)] Measurements in buffer (0.1 M NaCl, 25 mM Hepes, pH 7.5)

Table 3

Comparison of detergents as a function of chain length

(25 C, 0.1M NaCl,with or without 25 mM HEPES buffer pH 7.5)

		Micelle Formation						**Membrane Partitioning**				
head group	n	CMC mM	ΔG^0_{mic} [a] kcal/mol	ΔH^0_{mic} kcal/mol	$T\Delta S^0_{mic}$ kcal/mol	reference	membrane composition	K^0_D M^{-1}	$\Delta G^0_{D,part}$ [b] kcal/mol	$\Delta H^0_{D,part}$ kcal/mol	$T\Delta S^0_{D,part}$ kcal/mol	reference
thio-glucose	8	9	-5.15	1.44	6.59	[22,23]	PC[c]	240	-5.60	1.0-2.0		[24]
glucose	8	23	-4.60	1.29	5.89	[25,26]	PC	120	-5.19	1.3	6.49	[27]
	10	2.2	-5.98	1.17	7.15	[28]	PC	1600	-6.72	1.2	7.92	[27]
maltose	8	19.5	-4.69	2.39	7.08	[28]	PC	25	-4.27	2.4	6.67	[9]
	10	1.8	-6.10	3.35	9.45	[28]	PC	200	-5.50	3.1	8.60	[9]
	12	0.17	-7.49	0.96	8.45	[28]	PC	5000	-7.40	1.0	8.40	[9]
$^+N(CH_3)_3$	10	74.1	-3.91	1.57	5.48	this work	PC/PG[d] 3:1	355	-5.83	-0.38	5.45	this work
	12	9.01	-5.15	0.80	5.95	this work	PC/PG 3:1	3600	-7.20	-0.96	6.24	this work
	14	0.77	-6.60			[10]	PC/PG 3:1	1.60E+04	-8.08	-2.51	5.57	this work
$^+N(CH_3)_3$	12						PC	3.50E+03	-7.18	-0.99	6.19	this work
	12						PC [e]	5.2E+03	-7.58	-2.1	5.48	(Li-Blatter and Seelig, unpublished)
	14						PC [e]	6.0E+04	-9.22	-1.6	7.62	(Li-Blatter and Seelig, unpublished)
	16						PC [e]	3.0E+05	-10.3	-1.0	9.3	(Li-Blatter and Seelig, unpublished)
$-SO_4^-$	10	13.3	-4.92			this work	PC	2.73E+03	-7.04	-3.84	3.20	this work
	12	1.57	-6.18	-0.80	5.38	[1,25]	PC	3.30E+04	-8.51	-4.23	4.28	this work

	14	PC	5.00E+05	-10.11	-2.69	7.42	this work
$-SO_4^-$	10	PC/PG 3:1	7.00E+03	-7.59	-1.33	6.27	this work
	12	PC/PG 3:1	3.70E+04	-8.58	-3.7	4.88	this work
	14	PC/PG 3:1	6.50E+05	-9.66	-2.42	7.23	this work

[a] calculated according to $\Delta G^0_{mic} = RT \ln (CMC/55.5)$

[b] calculated according to $\Delta G^0_D = -RT \ln 55.5\ K^0_D$

[c] PC: 1-palmitoyl-2-oleoyl-*sn*-glycero-3-phosphocholine

[d] PG: 1-palmitoyl-2-oleoyl-*sn*-glycero-3-phosphoglycerol

[e] 30 nm vesicles, 50 mM Tris, 0.114 M NaCl, 37 °C

Legends to figures

Figure 1 Demicellization Reaction of Dodecyl Trimethylammonium Chloride.

(A) Titration calorimetry of DTAC (c_D^0 = 100 mM) in buffer (0.1 M NaCl, 25 mM Hepes, pH 7.5) into pure buffer of the same composition (at 65 °C). Each peak corresponds to the injection of 10 μL DTAC solution into the calorimeter cell (cell volume 1.4 mL). (B) Heat of demicellization, δh_i, as a function of injection number. Neglecting additional dilution effects, the heat of micelle disintegration is constant for the first 12 injections, but decreases rapidly as the detergent concentration in the calorimeter cell approaches the critical micellar concentration. The solid line is the theoretical prediction calculated with the aggregation model described in the text. The corresponding parameters are K_D^0 = 97 M^{-1} (CMC = $1/K_D^0$ = 10.31 mM), ΔH_D^0 = -2770 cal/mol, $\sigma = 10^{-4}$, n = 45. (C) The fraction of monomers, $\alpha = c_A / c_A^0$ as a function of the total detergent concentration in the calorimeter cell. During the initial injections, the ~100 fold dilution leads to a complete dissolution of micelles and α = 1. The solid line is again the theoretical analysis calculated with the same parameters as above.

Figure 2 Thermodynamics of Micelle Formation of Dodecyl Trimethylammonium Chloride.

(A) Enthalpy of micelle formation as a function of temperature. Linear regression yields ΔH_{mic}^0 (cal/mol) = -94.9 T(°C) + 3156. (B) Critical micellar concentration (CMC) as function of temperature (■) this work; (▲) data of [10]. The solid line is the theoretical prediction using van't Hoff law and the temperature-dependent ΔH_{mic}^0 shown in 2A.

Figure 3 Heat of Dilution of DTAC.

A solution of 7.2 mM DTAC (in buffer) was injected into pure buffer at different temperatures. The DTAC concentration is below the CMC at all temperatures. Each data point corresponds to the injection of 10 μL into the calorimeter cell with a volume of V_{cell}

= 1.4 mL. The molar heat of dilution, ΔH_{Dil}, is plotted vs. the total DTAC concentration, c_D^0, in the measuring cell. Temperatures from top to bottom: 15, 25, 45, 65 °C.

Figure 4 Partition Equilibrium of DTAC with POPC/POPG (3:1) 100 nm Lipid Vesicles.

(A) Lipid-into-DTAC titration. Titration calorimetry of DTAC (c_D^0 = 80 μM) with lipid vesicles (c_L^0 = 26.4 mM) in buffer (0.1 M NaCl, 25 mM Hepes, pH 7.5) at 35 °C. Each peak results from the addition of 10 μL vesicle suspension to the DTAC solution in the calorimeter cell (V_{cell} = 1.4 mL). (B) The reaction heats, δh_i, as a function of the injection number N_{inj}. Experimental results (■) are compared with the theoretical analysis (solid line). (C) Binding isotherm for DTAC partitioning into the outer monolayer of POPC/POPG vesicles. The extent of binding, X_b, is defined as the molar ratio of bound DTAC, n_D^b, total lipid, n_L^0, in the outer monolayer. (■) Experimental results; (solid line) theoretical prediction. The theoretical analysis in B and C is based on a partition constant of $K_D^0 = 3 \times 10^3$ M^{-1} and ΔH_D^0 = -2.65 kcal/mol. In particular, DTAC binding was assumed to follow a surface partition model according to $X_b = K_D^0 c_M$ where c_M is the surface concentration of detergent. It is determined by the electrical surface potential, ψ_0, and related to the DTAC equilibrium concentration, c_{eq}, according to $c_M = c_{eq} \exp(-\psi_0 z F_0/RT)$.

Figure 5 Thermodynamic Parameters of DTAC Partitioning into POPC and POPC/POPG (3:1) 100 nm Vesicles.

(A) Temperature dependence of the binding enthalpy ΔH_D^0. (▲) POPC vesicles (♦) Mixed POPC/POPG vesicles. (B) Temperature dependence of the binding constant K_D^0. The solid line is the theoretical prediction calculated with the van't Hoff equation and the temperature dependence ΔH_D^0 values for POPC/POPG vesicles shown in (A).

Figure 6 Kinetics of Vesicles Dissolution by DTAC.

POPC/POPG vesicles (c_L^0 = 100 μM) were mixed with 80.4 mM DTAC and the optical density was monitored as a function of time and temperature. The temperatures are from right to left: 25, 35, 45 °C.

Figure 7 Saturation and Solubilization of POPC/POPG 100 nm Vesicles by DTAC.

Determination of vesicle size by dynamic light scattering. Measurements in buffer (0.1 M NaCl, 25 mM Hepes, pH 7.5). Lipid and DTAC were mixed in defined concentrations. The mixture was equilibrated at 25 °C for 12 hrs. The average size of the resulting vesicles was then determined by dynamic light scattering. Each data point in the figure corresponds to a separate lipid/DTAC preparation. The polydispersity index (PDI) before saturation was less than 0.2; after solubilization the PDI was < 0.25.

Figure 8 Membrane Partitioning and Micelle Formation as a Function of the Length of the Alkyl Chain.

Comparison of neutral, anionic and cationic detergents. (A) Free energy of micelle formation. (B) Free energy of membrane partitioning. The polar groups are (■) glucose, (♦) maltose, (●,○) SO_4^-, (▲) $^+N(CH_3)_3$. The bilayer is composed of POPC for maltose (♦), glucose (■) and SO_4^- (○). A mixed POPC/POPG bilayer is used for $^+N(CH_3)_3$ (▲) and SO_4^- (●).

Figure 9 Apparent Binding Constant K_{app}.

The binding of DTAC to a lipid membrane follows a surface partition equilibrium according to $X_b = K_D^0 c_M = K_D^0 \cdot c_{eq} \exp(-\psi_0 z F_0 / RT)$. c_M is the surface concentration of DTAC immediately above the plane of binding. The intrinsic binding constant K_D^0 is independent of the DTAC concentration and a plot of X_b vs. c_M is linear. However, c_M cannot be measured directly but must be calculated with the Gouy-Chapman theory. For

practical purposes X_b can be plotted versus c_{eq} and an apparent binding constant, $K_{app} = X_b/c_{eq}$ can be defined. The figure shows the variation of the experimental K_{app} (■) with the equilibrium concentration, c_{eq}. The membrane is composed of POPC/POPG (75:25 mol/mol) and the measurement was performed at 45 °C. The solid line was calculated as $K_{app} = K_D^0 \exp(-\psi_0 z F_0 / RT)$ with K_D^0 = 3000 M^{-1}. At low detergent concentrations $K_{app} \rangle\rangle K_D^0$ as the electrostatic attraction increases the binding affinity. Near the end of the titration experiment electric neutralization is reached and K_{app} approaches K_D^0.

References

(1) Tan, A.; Ziegler, A.; Steinbauer, B.; Seelig, J. Thermodynamics of Sodium Dodecyl Sulfate Partitioning into Lipid Membranes. *Biophys J* **2002**, *83*, 1547-1556.

(2) Hope, M. J.; Bally, M. B.; Webb, G.; Cullis, P. R. Production of Large Unilamellar Vesicles by a Rapid Extrusion Procedure. Characterization of Size Distribution, Trapped Volume and Ability to Maintain a Membrane Potential. *Biochim Biophys Acta - Biomembranes* **1985**, *812*, 55-65.

(3) Mayer, L. D.; Hope, M. J.; Cullis, P. R. Vesicles of Variable Sizes Produced by a Rapid Extrusion Procedure. *Biochim Biophys Acta* **1986**, *858*, 161-168.

(4) Cantor, C. R.; Schimmel, P. R. *Biophysical Chemistry*; Freeman: San Francisco, 1980; Vol. I.

(5) Heyn, M. P.; Bretz, R. The Self-Association of Atp: Thermodynamics and Geometry. *Biophys Chem* **1975**, *3*, 35-45.

(6) Robinson, B. H.; Seelig, A.; Schwarz, G. In *Chemical and Biological Applications of Relaxation Spectrometry*, 1975; pp 481-485.

(7) Seelig, J. Titration Calorimetry of Lipid-Peptide Interactions. *Biochim Biophys Acta* **1997**, *1331*, 103-116.

(8) Seelig, J.; Nebel, S.; Ganz, P.; Bruns, C. Electrostatic and Nonpolar Peptide-Membrane Interactions. Lipid Binding and Functional Properties of Somatostatin Analogues of Charge Z = +1 to Z = +3. *Biochemistry* **1993**, *32*, 9714-9721.

(9) Heerklotz, H.; Seelig, J. Titration Calorimetry of Surfactant-Membrane Partitioning and Membrane Solubilization. *Biochim Biophys Acta* **2000**, *1508*, 69-85.

(10) Beyer, K.; Leine, D.; Blume, A. The Demicellization of Alkyltrimethylammonium Bromides in 0.1 M Sodium Chloride Solution Studied by Isothermal Titration Calorimetry. *Colloids Surf B Biointerfaces* **2006**, *49*, 31-39.

(11) Chakraborty, I.; Moulik, S. P. Self-Aggregation of Ionic C(10) Surfactants Having Different Headgroups with Special Reference to the Behavior of

Decyltrimethylammonium Bromide in Different Salt Environments: A Calorimetric Study with Energetic Analysis. *J Phys Chem B* **2007**, *111*, 3658-3664.

(12) Sarac, B.; Bester-Rogac, M. Temperature and Salt-Induced Micellization of Dodecyltrimethylammonium Chloride in Aqueous Solution: A Thermodynamic Study. *J Colloid Interface Sci* **2009**, *338*, 216-221.

(13) Lichtenberg, D.; Robson, R. J.; Dennis, E. A. Solubilization of Phospholipids by Detergents. Structural and Kinetic Aspects. *Biochim Biophys Acta* **1983**, *737*, 285-304.

(14) Perger, T. M.; Bester-Rogac, M. Thermodynamics of Micelle Formation of Alkyltrimethylammonium Chlorides from High Performance Electric Conductivity Measurements. *J Colloid Interface Sci* **2007**, *313*, 288-295.

(15) Zielinski, R. Effect of Temperature on Micelle Formation in Aqueous NaBr Solutions of Octyltrimethylammonium Bromide. *J Colloid Interface Sci* **2001**, *235*, 201-209.

(16) Tanford, C. *The Hydrophobic Effect. Formation of Micelles and Biological Membranes*; Wiley: New York, 1980.

(17) Salem, L. Attactive Forces between Long Saturated Chains at Short Distances. *J Chem Phys* **1962**, *37*, 2100.

(18) Seelig, A. Local Anesthetics and Pressure: A Comparison of Dibucaine Binding to Lipid Monolayers and Bilayers. *Biochim Biophys Acta* **1987**, *899*, 196-204.

(19) Heerklotz, H.; Seelig, J. Correlation of Membrane/Water Partition Coefficients of Detergents with the Critical Micelle Concentration. *Biophys J* **2000**, *78*, 2435-2440.

(20) Heerklotz, H.; Seelig, J. Detergent-Like Action of the Antibiotic Peptide Surfactin on Lipid Membranes. *Biophys J* **2001**, *81*, 1547-1554.

(21) de la Maza, A.; Parra, J. L. Solubilizing Effects Caused by the Nonionic Surfactant Dodecylmaltoside in Phosphatidylcholine Liposomes. *Biophys J* **1997**, *72*, 1668-1675.

(22) Saito, S.; Tsuchiya, T. Characteristics of N-Octyl Beta-D-Thioglucopyranoside, a New Non-Ionic Detergent Useful for Membrane Biochemistry. *Biochem J* **1984**, *222*, 829-832.

(23) Brackman, J. C.; Vanos, N. M.; Engberts, J. Polymer Nonionic Micelle Complexation - Formation of Poly(Propylene Oxide)-Complexed N-Octyl Thioglucoside Micelles. *Langmuir* **1988**, *4*, 1266-1269.

(24) Wenk, M. R.; Seelig, J. Interaction of Octyl-Beta-Thioglucopyranoside with Lipid Membranes. *Biophys J* **1997**, *73*, 2565-2574.

(25) Paula, S.; Sus, W.; Tuchtenhagen, J.; Blume, A. Thermodynamics of Micelle Formation as a Function of Temperature - a High Sensitivity Titration Calorimetry Study. *J Phys Chem* **1995**, *99*, 11742-11751.

(26) Antonelli, M. L.; Bonicelli, M. G.; Ceccaroni, G.; Lamesa, C.; Sesta, B. Solution Properties of Octyl-Beta-D-Glucoside .2. Thermodynamics of Micelle Formation. *Coll Polym Sci* **1994**, *272*, 704-711.

(27) Wenk, M. R.; Alt, T.; Seelig, A.; Seelig, J. Octyl-Beta-D-Glucopyranoside Partitioning into Lipid Bilayers: Thermodynamics of Binding and Structural Changes of the Bilayer. *Biophys J* **1997**, *72*, 1719-1731.

(28) Anatrace Catalogue.

Figures

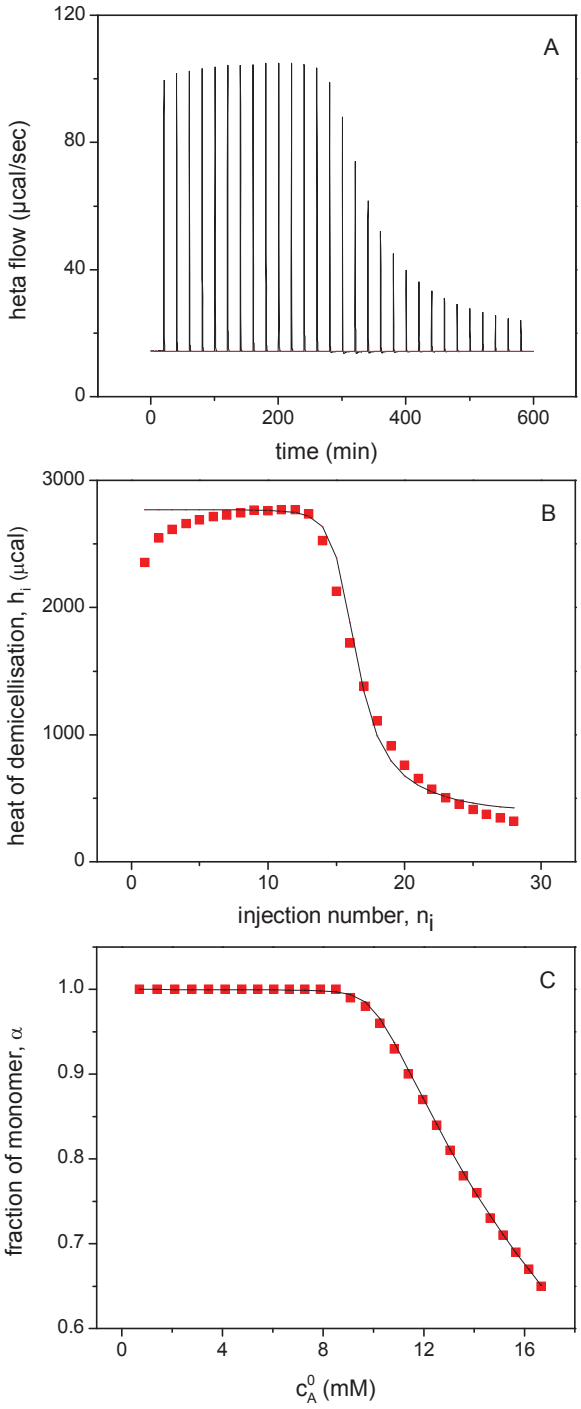

Figure 1

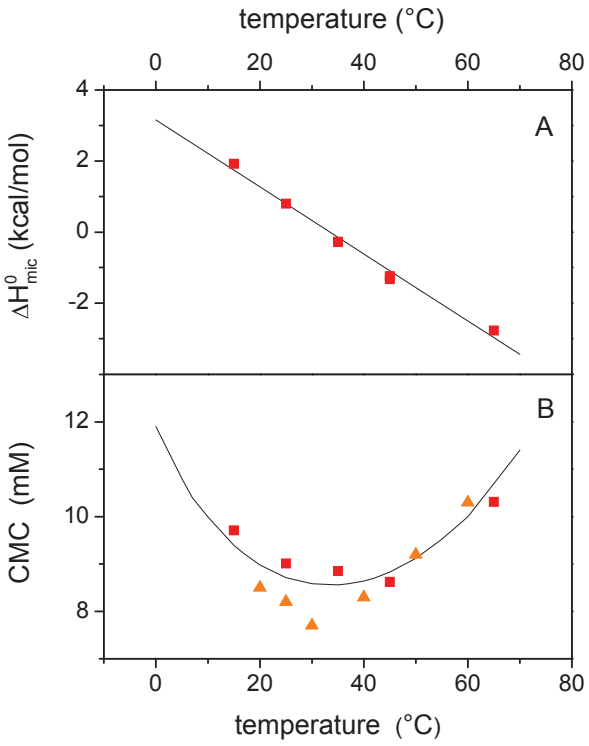
temperature (°C)
0
20
40
60
80
4
2
0
-2
A
ΔH^0_{mic} (kcal/mol)
12
10
8
B
CMC (mM)
0
20
40
60
80
temperature (°C)

Figure 2

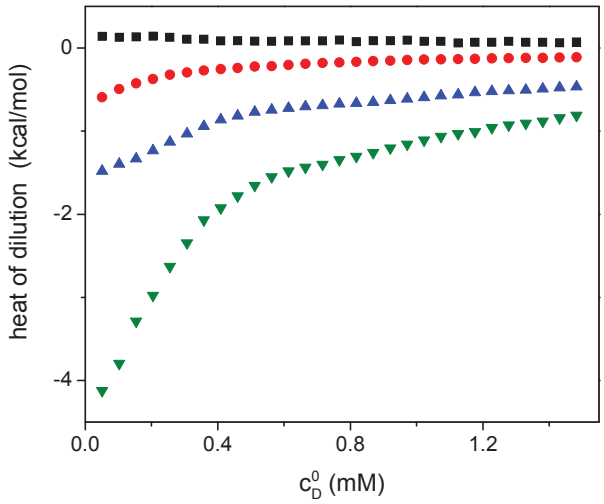

Figure 3

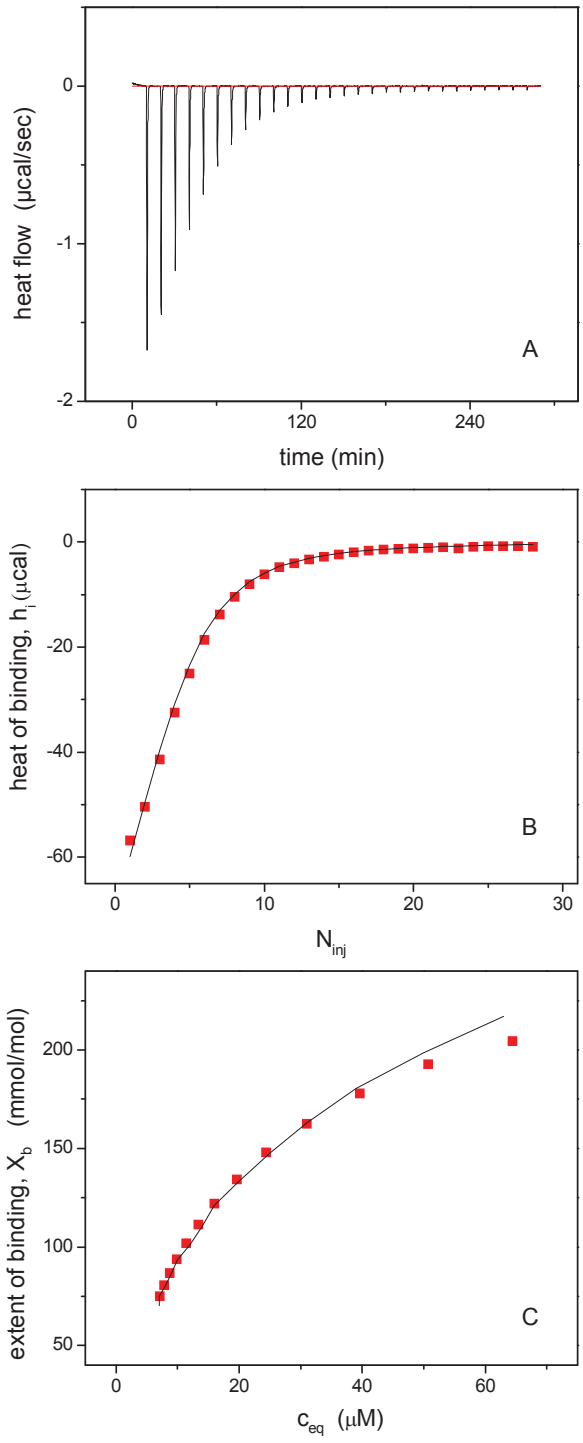
heat flow (µcal/sec)
0
-1
-2
0
120
240
time (min)
A
heat of binding, h_i (µcal)
0
-20
-40
-60
0
10
20
30
N_inj
B
extent of binding, X_b (mmol/mol)
200
150
100
50
0
20
40
60
c_eq (µM)
C

Figure 4

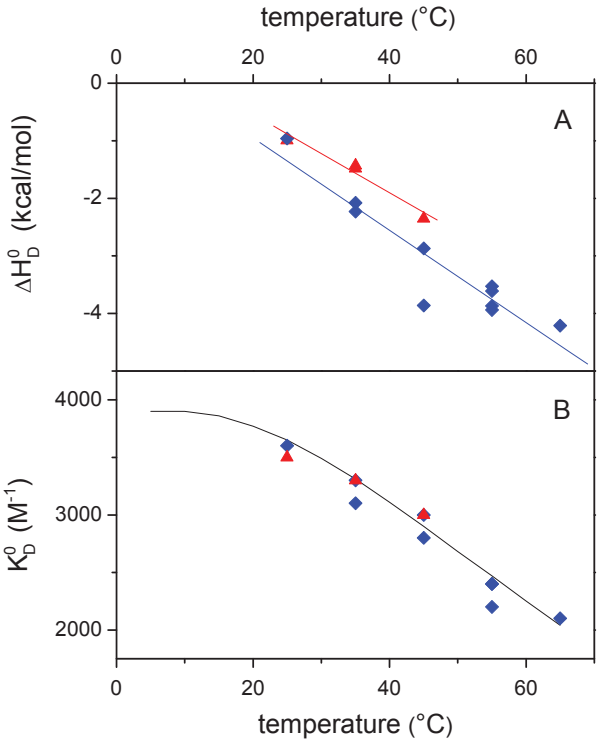
temperature (°C)
0
20
40
60
0
-2
-4
A
ΔH^0_D (kcal/mol)
4000
3000
2000
B
K^0_D (M^{-1})
0
20
40
60
temperature (°C)

Figure 5

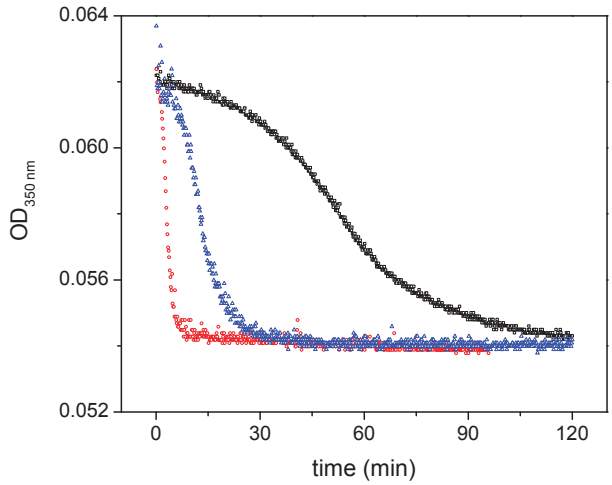

Figure 6

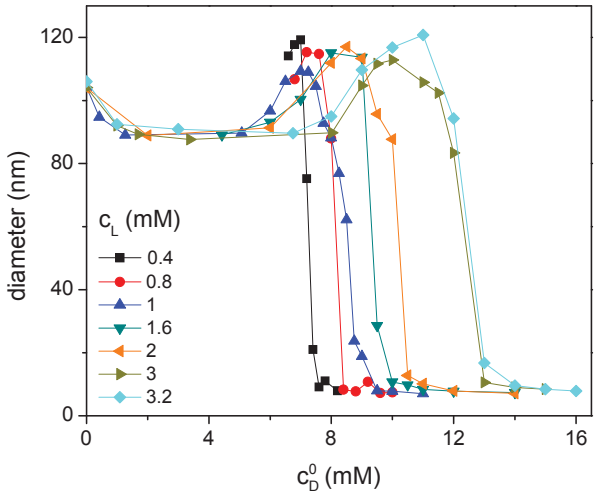

Figure 7

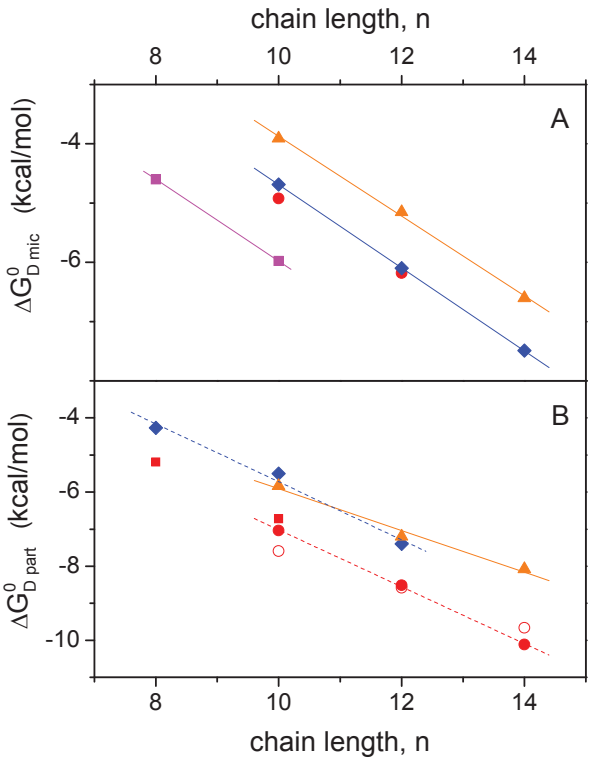
chain length, n
8
10
12
14
A
-4
-6
$\Delta G^0_{D\,mic}$ (kcal/mol)
B
-4
-6
-8
-10
$\Delta G^0_{D\,part}$ (kcal/mol)
8
10
12
14
chain length, n

Figure 8

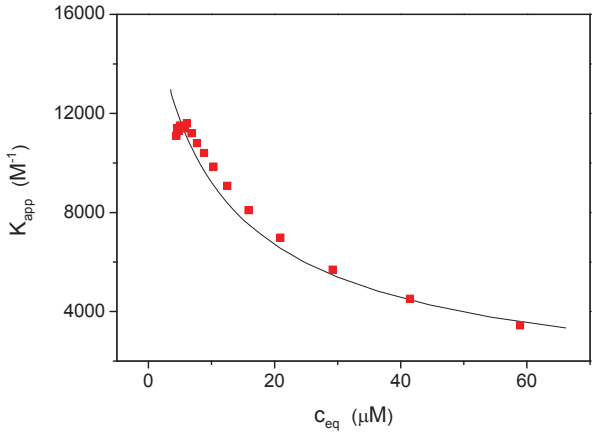

Figure 9

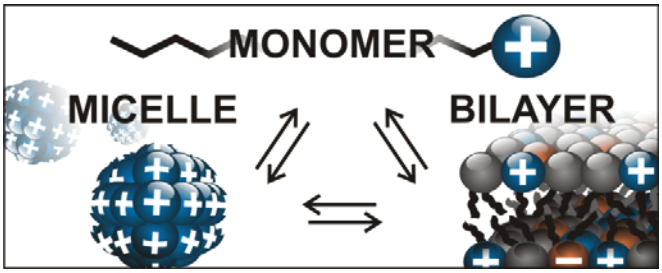

TOC

6.3 Appendix

6.3.1 Determination of apparent binding constant by a model free approach

Materials

1-palmitoyl-2-oleoyl-*sn*-glycero-3-phosphocholine (POPC) and 1-palmitoyl-2-oleoyl-*sn*-glycero-3-phosphoglycerol (POPG), dissolved in chloroform, were from Avanti Polar Lipids (Birmingham, AL). The detergent dodecyl trimethylammonium chloride (DTAC) was obtained from Anatrace (Alabaster, AL). All chemicals used were of analytical grade quality and were used without further purification. The composition of the lipid mixture was 75 % POPC to 25 % POPG (mol %). Chloroform was evaporated under a gentle stream of nitrogen. Solvent residuals were removed under vacuum for at least 8h. Samples of the dried lipids were then weighed and re-suspended in dichloromethane at the desired ratios. After a further evaporation step the dry lipid was suspended in 100 mM NaCl and 25 mM Hepes buffer pH 7.5 by vortexing rigorously. In order to obtain multilamellar vesicles (MLVs) five freeze/thaw cycles were applied. Large unilamellar vesicles (LUVs, 100 nm) were prepared by 15 extrusion steps through a nucleopore polycarbonate filter at 23°C in a Lipex extruder (Northern Lipids, Vancouver, Canada). All steps were performed under an argon atmosphere in order to reduce exposure of the lipids to air.

Methods

ITC experiments were performed with a VP-ITC calorimeter from MicroCal (Northampton, MA).

Model free partition experiments were conducted according to Rowe et al. (Zhang and Rowe 1992). Lipid vesicles were mixed with an appropriate amount of detergents below the CMC. After five freeze/thaw cycles the vesiceles were extruded trough 100 nm polycarbonate filters. Every step was performed under argon atmosphere in order to

reduce exposure to air. The preloaded vesicles were put into the syringe and injected into solutions with different DTAC concentrations.

Light scattering measurements were performed on a Zetasizer ZS90 instrument (ZEN3690) (Malvern Inst., Worcestershire, UK). The device was equipped with a 4 mW HeNe laser generating a wavelength of 633 nm. Because of the principle of non-invasive back scattering the scattering angle was 173°. Prior to use the buffer was filtered with a regenerated, 0.2 µm pore size cellulose filter (Infochroma AG, Zug, CH). The data were analysed using DTS-software provided by Malvern.

Results

The apparent binding coefficient (K_{app}) of DTAC with bulk aqueous phase and lipid membranes (POPC : POPG 3:1 mol%) was measured with a model free protocol according to Rowe (Zhang and Rowe 1992). The apparent partition coefficients were compared with the partition coefficients found by a commonly used ITC-binding protocol which is described in chapter 6.2 in detail. A vesicular suspension preloaded with a subsaturated concentration of DTAC was prepared as follows: A dry lipid film (see Materials and Methods) at the desired molar ratio of POPC:POPG (3:1 mol%) was resuspended in buffer (25 mM Hepes, 100 mM NaCl, pH 7.5 at 25 °C). The solution was subjected to five freeze/thaw cycles and 12 extrusion steps through a 100 nm pore size extruder in order to obtain 100 nm LUVs. DTAC was added to reach a final concentration of 1, 3 or 9 mM. The lipid concentration was kept constant at 10 mM. Thereafter again five freeze/thaw cycles and 12 extrusion steps were performed in order to ensure a homogeneous distribution of DTAC molecules across the lipid bilayer. Vesicle diameter was measured with DLS. Figure 1 shows a typical volume-weighted size distribution plot of the preloaded vesicles. The average of three measurements for each preparation is shown.

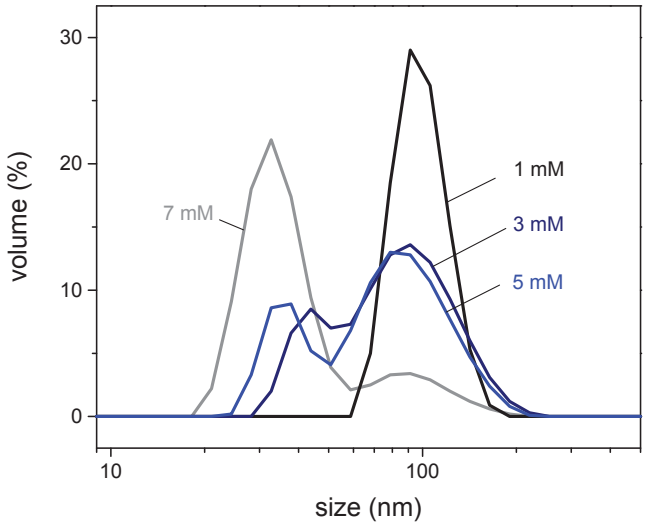

Figure 1 *Vesicles preloaded with DTAC after 12 extrusion runs.* Volume-weighted size distribution plot of vesicles (C_L = 10 mM) prepared in solutions with different DTAC concentrations after applying 5 freeze/thaw cycles and 12 extrusion runs. The concentration indicated is the amount of DTAC present in the suspension. Measurements were taken at 25°C in 25 mM Hepes, 100 mM NaCl at pH 7.5 and were evaluated using DTS-software provided by Malvern.

A gradual shift towards smaller sizes is observed upon increasing the concentration of DTAC in the suspension. This observation can be explained in structural terms as follows. The cone shaped structure of certain detergent molecules favor highly bent structures like micelles, for review (Heerklotz 2008). In contrast, the lipids have so-called inverted cone shaped structures which favor less bent aggregates, like for example vesicles.

In the vesicle preparation above the detergent will be distributed between the lipid bilayer (concentration $C_{D,b}$) and the aqueous phase ($C_{D,eq}$). The purpose of the following experiment is to determine $C_{D,eq}$. The syringe was loaded with the vesicles containing DTAC and the suspension was injected into different DTAC concentrations. The upper panel in Figure 2 shows typical titration peaks obtained for 10 mM POPC:POPG (3:1 mol%) vesicles preloaded with DTAC injected into different DTAC concentrations (typically from 0 to 2 mM, concentrations of DTAC are indicated). The integrated heat peaks were plotted against the detergent concentration in the cell (Fig. 2 lower panel). The zero value (no heat is released or absorbed) corresponds to the free detergent concentration in the cell plus heat of dilution of the vesicles. The titration experiment in Figure 2C shows no endothermic heat flow at all. 10 mM vesicles preloaded with 1mM

DTAC was injected into different amounts of DTAC. No release of DTAC molecules leads to the conclusion that all molecules are bound. Therefore K_{app} is infinitely high at the used conditions.

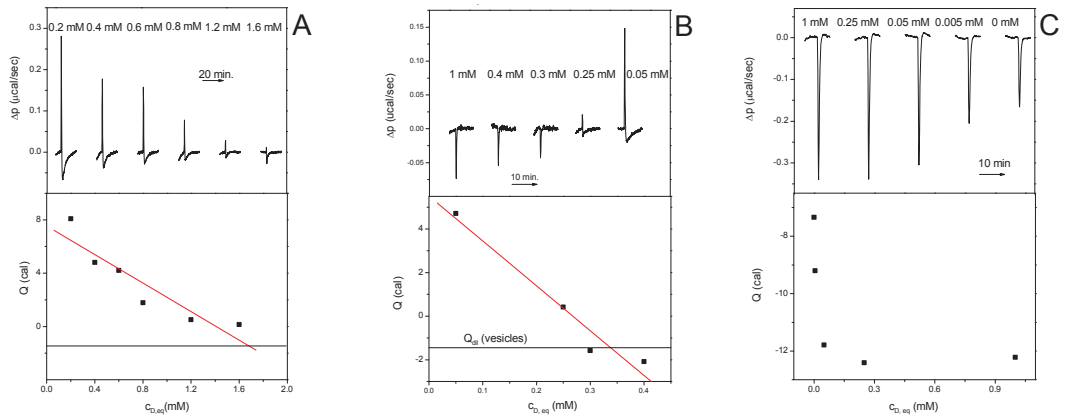

Figure 2. *Experiment according to Rowe.* (A) 10 mM PC:PG (3:1) preloaded with 9 mM DTAC, (B) 10 mM vesicles preloaded with 3 mM DTAC and in C they were preloaded with 1 mM DTAC. All suspensions were injected into different amount of DTAC (usually from 0 to 2 mM). The DTAC concentrations in the cell are shown in the upper panel above each titration peak. The lower figure shows the integrated titration peaks plotted vs. the detergent concentration in the cell.

The heat of dilution of the vesicles alone was determined by injecting a vesicular suspension of 10 mM POPC:POPG (3:1 mol%) into matched buffer (Fig. 3). The heat of dilution was determined by averaging the heat of injection of the titration peaks 2 – 29. The heat of dilution was found to be -1.45 µcal/injection (each injection a 10 µl).

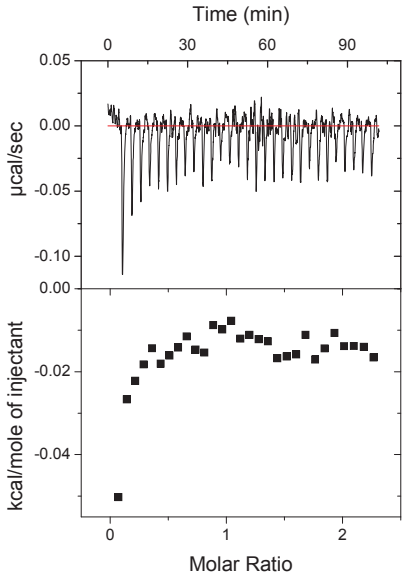

Figure 3. *Heat of dilution.* 10 mM POPC:POPG (3:1 mol%) vesicles were injected into matched buffer at 25°C. Heat of dilution was calculated by averaging the titration peaks 2-29 and was found to be -1.45 µcal/injection (injection volume 10 ml).

The concentration in the syringe, $C_{D,0}$, as well as the lipid concentration, C_L, is known. The measurement allowed the determination of the free concentration of detergent molecules, $C_{D,eq}$, in the syringe. These three parameters allow the determination of K_{app} according to

$X_b = K_{app} / C_{D,eq}$

where X_b is the membrane bound mole fraction of detergent molecules. The bound, $C_{D,b}$, and the free concentration, $C_{D,eq}$, in sum, is the total concentration, $C_{D,0}$ according to $C_{D,0} = C_{D,eq} + C_{D,b}$.

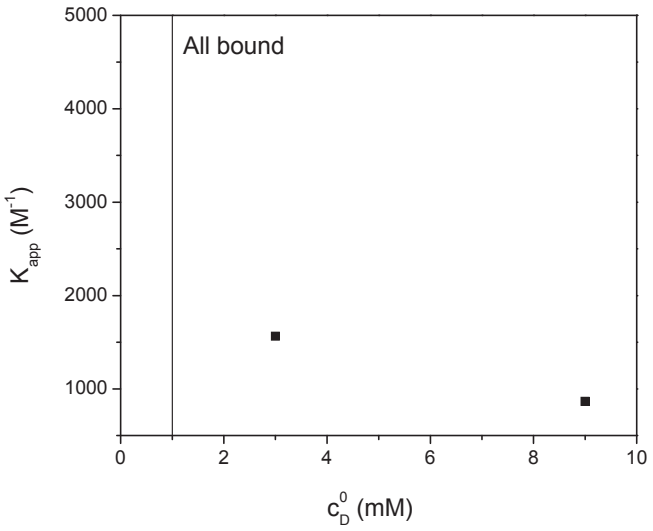

Figure 4. *Apparent partition coefficients.* Apparent partition coefficients determined by the Rowe protocol are shown. The y-axis depicts the binding constant, K_{app}, whereas the x-axis shows the preloaded detergent concentration. The lipid concentration was always 10 mM.

The lipid concentration used for the evaluation was 5 mM as the detergents molecules cannot flip in the studied time scale and at the investigated temperature (Tan and others 2002). Figure 4 displays the binding constants plotted *vs.* the detergent concentration, $C_{D,0}$. All the concentrations and partition coefficients are summarized in Table 1.

C_L Experiment	C_L Calculation	$C_{D,0}$	$C_{D,eq}$	$C_{D,b}$	X_b	K_{app}
mM	mM	mM	mM	mM	mol/mol	M^{-1}
10	5	1	-	-	-	-
10	5	3	0.34	2.66	0.53	1600
10	5	9	1.7	7.3	1.46	700

Table 1 *Parameters derived from Rowe protocol*.

References

Heerklotz H. 2008. Interactions of surfactants with lipid membranes. Q Rev Biophys 41(3-4):205-64.

Tan A, Ziegler A, Steinbauer B, Seelig J. 2002. Thermodynamics of sodium dodecyl sulfate partitioning into lipid membranes. Biophys J 83(3):1547-56.

Zhang F, Rowe ES. 1992. Titration calorimetric and differential scanning calorimetric studies of the interactions of n-butanol with several phases of dipalmitoylphosphatidylcholine. Biochemistry 31(7):2005-2011.

6.3.2 SDS and DTAC Interacting with POPC. A ^{2}H-NMR study.

Introduction

Quantitative studies of charged detergents interacting with lipid membranes are rare. We have quantified the incorporation and the solubilization behavior of dodecyltrimethylammonium chloride (DTAC) with neutral and negatively charged lipid model membranes (POPC and POPC:POPG (3:1 mol %), respectively). The interaction of sodium dodecyl sulfate (SDS) with model membranes was investigated previously (Tan and others 2002). SDS and DTAC exhibit an oppositively charged headgroup with the same chain length. However SDS incorporates 10 – 15 times better than DTAC into neutral model membranes after correction for electrostatic contribution. SDS has a smaller head group than DTAC and therefore can incorporate more easily into lipid membranes. The lateral membrane packing density counteracts the incorporation behavior. A bigger head group of DTAC should disturb the bilayer more than the smaller SDS head group. However we found that SDS solubilizes the membrane at lower critical bound detergent to lipid molar ratio (R_b^{sat}) than DTAC.

^{2}H-NMR measurements were performed in order to detect the motional changes of the cholin moiety of DOPC upon incorporation of the detergents molecules. Deuterated DOPC was mixed in a 1:4 weight ratio with undeutarated POPC. The headgroup of POPC lies in a 30° angle relative to the bilayer surface (Scherer and Seelig 1989). Upon incorporation of cationic molecules the lipid headgroup moves toward the water phase as the cationic choline moiety is repelled by the cationic molecule incorporated in the membrane (Beyer 1986). Incorporation of anionic detergents molecules leads in contrast to a movement of the headgoup towards the plane of the membrane. The aim of the investigation was the determination of the motional change of the choline headgroup upon incorporation of oppositly charged detergents in order to give insight into the different solubilization properties.

The headgoup of DOPC was selectively deuterated at position C_α and C_β. Motions occurring at rates in the 10^6-10^9 Hz range modulate the quadrupole lineshape (Spiess

HW, 1981). The motion of the headgroup is gradually shifted upon incorporation of DTAC or SDS as a function of the bound detergents per lipid molecules.

Materials and Methods

SDS was obtained from Sigma Aldrich and DTAC from Anatrace (Maumee, Ohio, USA). Both substances were used without further purification. The head group of DOPC was selectively deuterated at position C_α and C_β and mixed with undeuterated POPC in a 1:4 weight ratio. Both lipids were obtained from Avanti polar lipids (Alabaster, Alabama, USA). Deuterium depleted water was obtained from ISOTEC (Ohio, USA). The dry lipid film was hydrated in water (^{2}H-depeleted) to a final volume of 300 µl. 10 µl of DATC or SDS, respectively, stock solutions were added consecutively. After applying five freeze/thaw cycles the sample was measured at 35°C.

Solid state NMR experiments were performed on a Bruker Advance 400MHz spectrometer (Bruker AXS, Karlsruhe, Germany). Solid state deuterium NMR experiments were recorded at 61MHz using the quadrupole echo technique. The excitation pulse had a length of 5.5 µs. 8 K FIDs were accumulated.

Results and Discussion

Figure 1 displays the raw ^{2}H-NMR data of DOPC, deuterated at C_α and C_β position at the choline moiety, with different amount of (A) DTAC or (B) SDS, respectively, present in suspension.

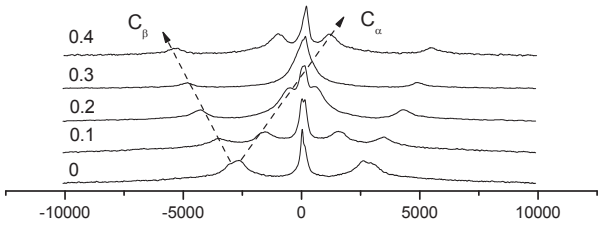

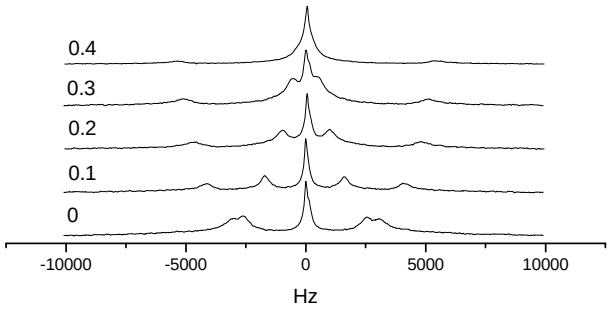

Figure 1A, B. *Raw ^{2}H-NMR measurements*. Figure 1 shows the raw ^{2}H NMR spectra recorded at 35°C in deuterium depleted water where the choline moiety was selectively deuterated at position C_α and C_β. Upon incorporation of a positively charged detergent (DTAC) (A) and a negatively charged detergent (SDS) (B), respectively, the C_α and C_β move in opposite direction. The bound detergents per total lipid molar ratios, X_b, are given to the left. The two dashed arrows indicate the movement of C_α and C_β position upon incorporation of the detergents.

Experiments were performed at 35°C in deuterium depleted water. The X_b values (mol detergent bound per mol total lipid) were determined from the apparent binding constant found by ITC measuements (see chapter 6) and are indicated to the left. The orientation of the choline headgroup is dependent on the membrane surface charge density. Upon incorporation of positively charged compounds the choline headgroup moves towards the water phase (Beyer 1986). On the other hand upon incorporation of a negatively charge molecule the choline headgroup moves towards the membrane. This change is recorded by quadrupole splitting measurements. The slope of the splitting is larger for positively charged compounds than for negatively charged compounds (Scherer and Seelig 1989). For the positively charged compound DTAC the quadrupole splitting is linear with the X_b. The slope of the quadrupol splitting for the negatively charge compound SDS shows deviation from linearity within X_b. However the change in the quadrupole splitting is for positively charged detergents bigger than for negatively charge detergents at the same amount of bound detergents per lipid (X_b). The slope of the straight line for the change in the quadrupole splitting of the C_α as a function of X_b is for cationic detergents m = -18000 (R = 0.997), whereas for the C_β m = 12000 (R = 0.99). On the other hand the change in the quadrupole splitting of the C_α as a function of Xb for anionic detergents is m = 11000 (R = 0.96), whereas for the C_β m = 12000 (R = 0.98) All data derived from figure 1 are summarized in table 1.

Detergents mM	POPC mM	Volume ml	Xb mol/mol	Splitting Hz		DSplitting Hz
DTAC				C_β	C_α	
0	47	0.3	0	6073	5195	878
4	46	0.304	0.1	6991	3106	3885
8	45	0.308	0.2	8585	1026	7559
12	44	0.312	0.3	9727	0	9727
16	42	0.316	0.4	10790	-2139	12929
SDS						
0	36	0.3	0	5720	5020	700
3	35	0.31	0.1	7900	3190	4710
6	33	0.32	0.2	9050	1735	7315
9	32	0.33	0.3	9640	780	8860
12	31	0.34	0.4	10330	0	10330

Table 1. *Quadrupole Splitting.* Table 1 shows all ^{2}HNMR- parameters derived from Figure 2.

We found that the change in the quadrupole splitting of the C_α is larger for positively than for negatively charged detergents. Both detergents upon incorporation drive the headgroup in different directions however not with the same intensity. The C_β segement in contrast moves to the same amount for both detergents however again in the opposite directions as observed for C_α.

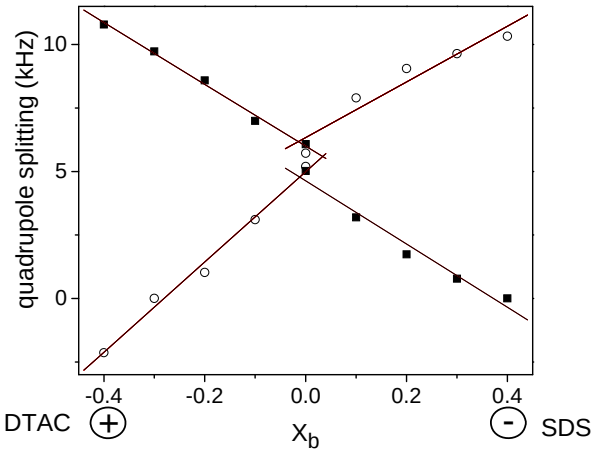

Figure 2. *Quadrupol splitting of deuterated cholin moiety of DOPC.* The open circles represent the movement of the C_α position and the black squares the movement of the C_β position. The solid line shows the linear fit.

We conclude that due to charge effects of the detergents molecules upon incorporation into the lipid bilayer, the headgroup of DOPC moves either towards the water or towards the membrane depending on the sign of the charge on the detergent molecule. The oppositely charged detergents have fundamentally different effects on the headgroup. The explanation of the solubilization behaviour only in structural terms (size of the headgroup and of the tail) seems not to be sufficient. Additional charge effects have to be taken into account.

References

Beyer K. 1986. A 31P- and 2H-NMR study on the structural perturbations induced by charged detergents in the headgroup region of phosphatidylcholine bilayers. Biochimica et Biophysica Acta (BBA) - Biomembranes 855(3):365-374.

Scherer PG, Seelig J. 1989. Electric charge effects on phospholipid headgroups. Phosphatidylcholine in mixtures with cationic and anionic amphiphiles. Biochemistry 28(19):7720-8.

Tan A, Ziegler A, Steinbauer B, Seelig J. 2002. Thermodynamics of sodium dodecyl sulfate partitioning into lipid membranes. Biophys J 83(3):1547-56.

7 Interaction of c-di-GMP with TipF wt, 581NS and 593NS

7.1 Summary

The second messenger cyclic-di-guanosine monophosphate (c-di-GMP) has raised attention in biological research fields as it is involved in controlling multiple aspects of bacterial growth and development. Generally high levels of c-di-GMP promote multi-cellular lifestyles (e.g. biofilm formation) whereas low levels promote single cell lifestyle. Cellular levels of c-di-GMP are regulated by the activites of two antagonistic enzymes, the dyguanylate cyclases that condense two GTP molecules into c-di-GMP and phosphodiesterases that break the phosphodiester bond.

The bacterium *Caulobacter crescentus* undergoes an asymmetric cell division that produces two cell types, the non-motile stalk bearing cell and the planktonic swarmer cell that is equipped with a single polar flagellum. Recently two proteins were identified that are involved in the construction of the polar flagellum, TipF and TipN, respectively (Huitema 2006). *In vivo* studies showed that c-di-GMP binds to TipF. The binding constant was however unknown. We have characterized the binding of c-di-GMP to TipF by means of isothermal titration calorimetry (ITC). All titration experiements showed sigmoidal enthalpy curves. We found that c-di-GMP binds TipF with high affinity (K_d = 0.4 (+/- 0.2 μM)). The stochiometry of TipF/c-di-GMP formation (n ~ 0.35) suggested a complex signaling transduction or partially inactive protein in the calorimeter cell.

7.2 Memo

Materials and Methods

Proteins (TipF wt, 581NS and 593NS) and cdiGMP were prepared by Yaniv Cohen from Prof. Jenals lab (Biozentrum), and were used without further purification.

Isothermal titration calorimetry. The interaction of TipF with cyclic-di-GMP was measured with a VP-ITC (isothermal titration calorimeter) from MicroCal (Northampton, MA), with TipF (32.5 μM) in the calorimeter cell and c-di-GMP (118 μM) in the injection syringe (buffer: 50 mM Tris/HCl, 50 mM NaCl, pH 8.0 at 25°C). All solutions were degassed and equilibrated at desired temperature (25°C or 35°C) before using. The delay between the injections was set to 5 min to ensure re-equilibration between injections. Data were evaluated using Origin software (OriginLab) provided by Microcal (Northampton, MA) and fitted to model describing one type of binding site.

Results

Figure 1A shows the raw ITC-titration pattern for 10 μL injections of a buffered (50 mM Tris/HCl, 50 mM NaCl, pH 8.0 at 25°C) c-di-GMP solution (118 μM) titrated into TipF (32.5 μM) at 25°C.

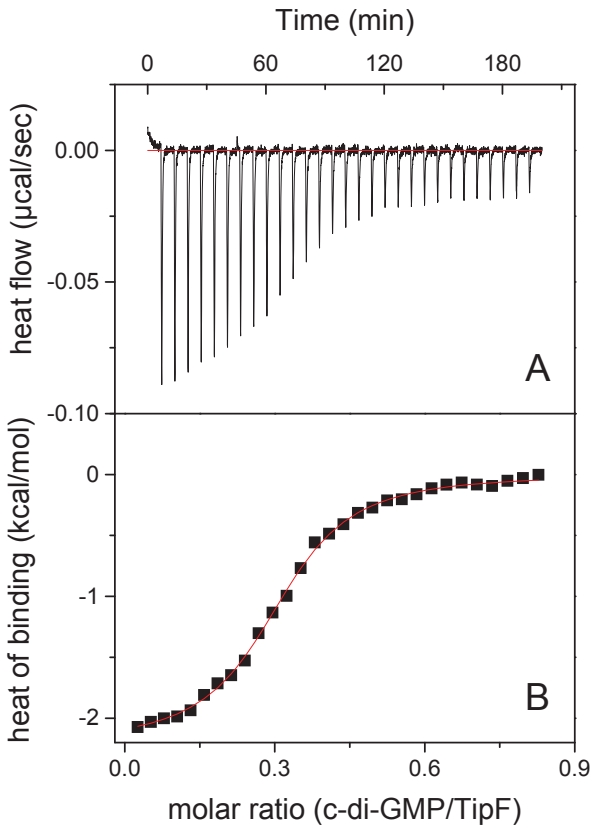

Figure 1A, B. *Cyclic di-GMP binding to TipF*. (A) Raw ITC-titration pattern of TipF (32.5 µM) titrated with cyclic di-GMP (118 µM) in 10 µL injection steps. (B) shows the integrated titration peaks (squares) fitted to a model describing one type of binding sites (solid line). Note that the heat of dilution was subtracted.

Figure 1B shows the integrated titration peaks (squares) fitted to a model describing one type of binding sites (solid line). Four different experiments were performed with three different protein batches measured under the same conditions (50 mM Tris/HCl, 50 mM NaCl, pH 8.0 at 25°C). All integrated titration peaks produced sigmoidal enthalpy curves for the interaction between TipF and cyclic di-GMP. The average dissociation constant, K_D, was 0.4 (+/- 0.2 µM), the stochiometry of binding, n, was 0.35 (+/- 0.1) and the enthalpy of reaction, ΔH^0 was -2.1 (+/- 0.3 kcal/mol). Note that the error indicated of the binding constant (as well as the enthaply of reaction) is somewhat larger than expected. A possible explanation is the fact that c-di-GMP was once produced in the lab (Prof. Schirmer, Biozentrum) by a protein and once bought as synthesized version. C-di-GMP has multiple conformations what makes the determination of the exact concentration difficult due to different absorption intensities of the various species (Zhang and others

2006). Two experiment were performed at 35°C (buffer was not adjusted to temperature). At 35°C the average dissociation constant, K_D, was 0.3 (+/- 0.1 μM), the stoichiometry of binding, n, was 0.3 (+/- 0.02) and the enthalpy of binding, ΔH^0, was -4.75 (+/- 0.25) kcal/mol (all thermodynamic parameters are summarized in table 1). The slope of the line obtained when the enthalpy is plotted versus the temperature provides the change in molar heat capacity ($\Delta C_P^0 = \Delta H^0/\Delta T$) upon formation of the TipF - cyclic di-GMP complex. The heat capacity was fitted as -270 (cal/molK^{-1}) (data not shown). The negative ΔC_P^0 suggests hydrophobic interaction upon cyclic di-GMP/TipF binding.
Surprisingly the stochiometry of binding implies that two (or even three) proteins (TipF) form a complex with one molecule cyclic di-GMP what is in contrast to the prediction of a 1:1 binding. A more complex signalling behaviour of TipF including e.g. dimerization (or protein-association of higher order, respectively) or partially inactive TipF in the calorimeter cell could not be ruled out.

Temperature °C	K_D M	n	ΔH^0 kcal/mol
25	3.1E-7	0.26	-1.78
25	2.81E-7	0.43	-2.04
25	6.37E-7	0.31	-2.21
25	1.33E-7	0.39	-2.45
35	4.33E-7	0.28	-5.01
35	3.18E-7	0.32	-4.5

Table 1. Thermodynamic parameters of cdiGMP interacting with TipF (wt) in 50 mM Tris/HCl, 50 mM NaCl, pH 8.0 at 25°C.

The two point mutants of TipF, 593NS and 581NS, respectively, were measured at the same conditions as TipF (wt) (figure 2).

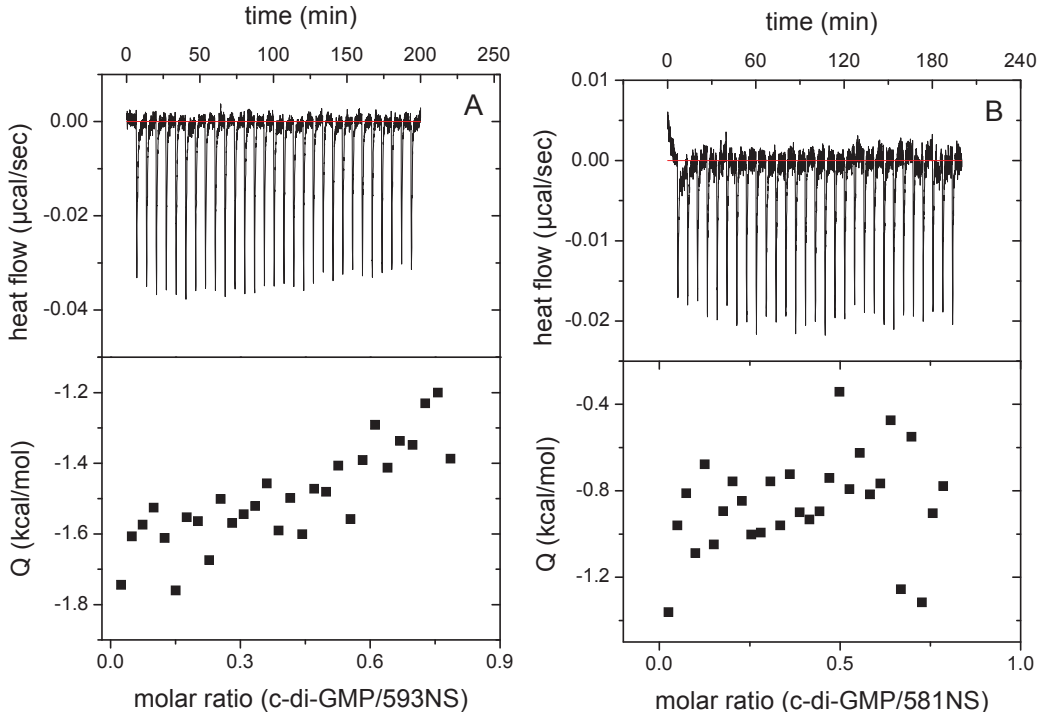

Figure 2. (A) dciGMP solution (100 µM) was injected into a 581NS protein solution (29 µM) at 25°C . No interaction was found in investigated concentration range. (B) dciGMP solution (100 µM) was injected into 593NS protein solution (29 µM) at 25°C. Also here no interaction was observed in the studied concentration range.

No interaction was found in the same concentration range (protein (29 µM) and cyclic di-GMP (100 µM)) as investigated above. The ITC-titration pattern and the intergarted titration peaks of the interaction of c-di-GMP with the point mutant 593NS is shown in figure 2 (A), whereas (B) shows the equivalent for the measurement of the point mutant 581NS.

References

Huitema E, Pritchard S, Matteson D, Radhakrishnan SK, Viollier PH. 2006. Bacterial Birth Scar Proteins Mark Future Flagellum Assembly Site. Cell 124(5):1025-1037.

Zhang Z, Kim S, Gaffney BL, Jones RA. 2006. Polymorphism of the Signaling Molecule c-di-GMP. Journal of the American Chemical Society 128(21):7015-7024.

8 Summary

This thesis aimed at revealing the substrate specificity of the bacterial ABC-transporter, Sav1866. For this purpose the ABC-transporter was reconstituted into model membranes and characterized in terms of basal and drug induced ATPase activity, respectively. The results were compared with analogous data from the well characterized human ABC-transporter P-glycoprotein which is a close structural homologue of Sav1866. Sav1866 is able to transport structurally very diverse substrates as P-gp, binds them however with a different affinity.

Moreover we found that the ATPase activity of Sav1866 was not only stimulated by drugs, but also by an intrinsic cationic lipid, lysyl-DPPG. Our results indicated that Sav1866 may be involved in the transport of the cationic lipid to the outer leaflet of the membrane.

Beside the characterization of the ATPase activity of Sav1866 the reconstitution process was investigated. Reconstitution of membrane proteins is a semi-empirical task due to the lack of quantitative analysis of the process. Model membrane vesicles were therefore solubilized with a non-ionic detergent ($C_{12}E_8$). The detergent was removed with the help of Bio-Beads SM2 from Biorad. The vesicle size during the reconstitution process was directly measured by means of dynamic light scattering. Isothermal titrations calorimetry was used to quantify the degree of detergents removal. We found that still 9 mol% detergents per lipid were left after treatment.

Moreover the effect of a positively charged compound, dodecyltrimethylammonium chloride (DTAC), on neutral and negatively charged membranes was investigated in detail. The thermodynamic properties of DTAC were compared with the negatively charged counterpart sodium dodecyl sulphate (SDS). After correction for electrostatic contribution we found that SDS incorporates 10-15 times better into a membrane than DTAC, what is explained by the smaller headgroup of SDS. However SDS solubilizes the membrane at much lower critical ratios than DTAC. We revealed the movement of the POPC headgroup upon incorporation of the positively or the negatively charged detergent molecule by means of ^{2}H-NMR. We found that upon incorproration of the cationic detergent the choline moiety of the lipid moves toward the plane of the bilayer,

and vice versa for the anionic molecule. We conclude that the solubilization behaviour of the lipid membranes by charged detergnets is not only dependent on the structural properties of the detergents but also on the effective charge of the detergent molecule.

As a last point we investigated the critical role of TipF in assembly of the flagellum in *Caulobacter crescentus*. ITC experiemnts were performed to give insight into the binding properties of c-di-GMP with TipF. C-di-GMP is a second messenger involved in controlling growth and developpement in bacteriae. *In vivo* studies showed that TipF binds c-di-GMP, the binding constant was however unknown. We showed that c-di-GMP binds TipF with high affinity (K_d = 0.4 μM).

9 Acknowledgement

This work was carried out from the Mai 2007 until June 2010 in the laboratories of Prof. Dr. Anna Seelig and Prof. Dr. Joachim Seelig in the Department of Biophysical Chemistry at the Biozentrum of University of Basel, Switzerland.

I would like to sincerely express my thanks and gratidue to Professor Anna Seelig who shed light into the complicated story of ABC-transporters. Moreover Anna gave me insight into the pharamceutical research which is sometimes very difficult to combine with basic biological research. She manages to close this gap very sophisticatedly. Further I want to express my deep gratitude to Professor Joachim Seelig who despite of his great knowledge and his impressive analytical skils gave me a very intense view into a scientific life which is sometimes more politically than scientifically orientated. I want to thank Professor Dagmar Klostermeier for reading and evaluating this thesis.

Certainly Päivi Äänismaa has to be mention at this point as she introduced my practically as well as theoretically into measurements with ABC-transporter. Her very warm character was always very helpful in the cold and loud research environment. Thanks Päivi.

Thanks go to André Ziegler who was always open for fruitful discussions even though he was most of the time very busy. Reto Sauder is a coworker and friend who made the scientific life much easier than it was supposed to be. Moreover I would like to thank Mark Finlayson for keeping always a smile during rainy days.

At this point I offer my regards and blessings to the research groups of both laboratories Seelig and Seelig for being patient and nice. It was really nice to work in a noncompetitive environment.

Acknowledgement

In the end I give many thanks to my girlfriend, Sandra Jaggi, my brother, Thomas Beck, and my parents, Ruth and Reinhard Beck. Without their love and support this thesis would not have been possible.